

ARCHITECTURE OF THE SILURIAN SEDIMENTARY COVER SEQUENCE IN  
THE CADIA PORPHYRY AU-CU DISTRICT, NSW, AUSTRALIA: IMPLICATIONS  
FOR POST-MINERAL DEFORMATION

by

MALISSA WASHBURN

B.S. University of Maine, 2006

A THESIS SUBMITTED IN PARTIAL FULFILMENT OF  
THE REQUIREMENTS FOR THE DEGREE OF  
MASTER OF SCIENCE

in

THE FACULTY OF GRADUATE STUDIES  
(Geologic Sciences)

UNIVERSITY OF BRITISH COLUMBIA  
(Vancouver)

July, 2008

© Malissa Washburn, 2008

## **Abstract**

Alkalic porphyry style Au-Cu deposits of the Cadia district are associated with Late-Ordovician monzonite intrusions, which were emplaced during the final phase of Macquarie Arc magmatism at the end of the Benambran Orogeny. N-striking faults, including the curvilinear, northerly striking, moderately west-dipping basement thrust faults of the Cadiangullong system, developed early in the district history. NE-striking faults formed during rifting in the late Silurian. Subsequent E-W directed Siluro-Devonian extension followed by regional E-W shortening during the Devonian Tabberabberan Orogeny dismembered these intrusions, thereby superposing different levels porphyry Au-Cu systems as well as the host stratigraphy.

During the late Silurian, the partially exhumed porphyry systems were buried beneath the Waugoola Group sedimentary cover sequence, which is generally preserved in the footwall of the Cadiangullong thrust fault system. The Waugoola Group is a typical rift-sag sequence, deposited initially in local fault-bounded basins which then transitioned to a gradually shallowing marine environment as local topography was overwhelmed. Basin geometry was controlled by pre-existing basement structures, which were subsequently inverted during the Devonian Tabberabberan Orogeny, offsetting the unconformity by up to 300m vertically. In the Waugoola Group cover, this shortening was accommodated via a complex network of minor detachments that strike parallel to major underlying basement faults. For this reason, faults and folds measured at the surface in the sedimentary cover can be used as a predictive tool to infer basement structures at depth.

## Table of Contents

<b>Abstract .....</b>	<b>ii</b>
<b>Table of Contents .....</b>	<b>iii</b>
<b>List of Tables .....</b>	<b>vi</b>
<b>List of Figures .....</b>	<b>vii</b>
<b>Acknowledgements .....</b>	<b>xii</b>
<b>Dedication .....</b>	<b>xiv</b>
<b>Chapter One: Introduction .....</b>	<b>1</b>
<b>THESIS OVERVIEW .....</b>	<b>3</b>
<b>Methodology .....</b>	<b>4</b>
<b>REGIONAL GEOLOGY .....</b>	<b>5</b>
<b>The Tasmanides and the Lachlan Tectonic Cycle .....</b>	<b>6</b>
<b>The Lachlan Fold Belt .....</b>	<b>11</b>
<b>The Macquarie Arc .....</b>	<b>14</b>
<b>THE CADIA DISTRICT .....</b>	<b>17</b>
<b>Chapter Two: Stratigraphic Framework .....</b>	<b>19</b>
<b>INTRODUCTION .....</b>	<b>19</b>
<b>ORDOVICIAN BASEMENT .....</b>	<b>22</b>
<b>Weemalla Formation .....</b>	<b>22</b>
<b>Forest Reefs Volcanics .....</b>	<b>22</b>
<b>Cadia Intrusive Complex .....</b>	<b>24</b>

<b>SILURIAN COVER.....</b>	<b>24</b>
<b>Basal Units .....</b>	<b>26</b>
LIMESTONE.....	29
BOULDER CONGLOMERATE.....	31
RED SILTSTONE .....	31
<b>Lower Siltstone-Dominant Succession .....</b>	<b>34</b>
<b>Upper Sandstone-Dominant Succession .....</b>	<b>37</b>
<b>INTERPRETATIONS .....</b>	<b>39</b>
<b>Paleogeography and Basin Evolution.....</b>	<b>39</b>
<b>Regional Correlations .....</b>	<b>47</b>
<b>IMPLICATIONS .....</b>	<b>50</b>
 <b>Chapter Three: Structural Relationships in the</b>	
 <b>Cadia District .....</b>	<b>55</b>
<b>INTRODUCTION.....</b>	<b>55</b>
<b>REGIONAL AND DISTRICT SCALE STRUCTURE.....</b>	<b>56</b>
<b>Regional Structure .....</b>	<b>56</b>
<b>District-Scale Structural Trends .....</b>	<b>59</b>
N-STRIKING FAULTS.....	65
NE-STRIKING FAULTS .....	66
<b>STRUCTURES IN THE SILURIAN WAUGOOLA GROUP .....</b>	<b>67</b>
<b>Intra-cover Deformation .....</b>	<b>83</b>
<b>FAULT REACTIVATION HISTORY .....</b>	<b>90</b>
<b>Boulder Conglomerate.....</b>	<b>92</b>



<b>Sharps Ridge</b> .....	92
<b>Waugoola Group Geometry</b> .....	94
<b>SUMMARY AND CONCLUSIONS</b> .....	96
<b>Hierarchy of Faults</b> .....	96
<b>Basement-Cover Interaction</b> .....	101
<b>Basin Inversion</b> .....	101
<b>Chapter Four: Conclusions</b> .....	104
<b>INTRODUCTION</b> .....	104
<b>CONCLUSIONS</b> .....	105
<b>IMPLICATIONS</b> .....	108
<b>Post-mineral Deformation and</b>	
<b>Using Structure in the Cover Sequence to</b>	
<b>Understand the Basement</b> .....	109
<b>FUTURE WORK</b> .....	111
<b>References</b> .....	113
<b>Appendices</b> .....	126
<b>APPENDIX I: Bedding Measurements</b> .....	126
<b>APPENDIX II: Fault Measurements</b> .....	147
<b>APPENDIX III: Drillcore Logs</b> .....	157

## List of Tables

1.1	The Lachlan Tectonic Cycle .....	9
3.1	Basement Fault Fabrics in the Cadia District .....	62

## List of Figures

1.1	Map of the Tasmanides .....	7
1.2	Map of the Lachlan Fold Belt .....	12
1.3	Map of the Macquarie Arc .....	16
2.1	Simplified map and stratigraphic column of the Cadia District .....	21
2.2	Photographic plate of macrofossils from the sedimentary cover rocks .....	25
2.3	Waugoola Group stratigraphy and surface map.....	27
2.4	Basal unit distribution map .....	28
2.5	Photographs of limestone and calcirudite .....	30
2.6	Photographs of boulder conglomerate .....	32
2.7	Photographs of red siltstone.....	33

2.8	Photographs of siltstone .....	35
2.9	Photographs of arkose .....	36
2.10	Photographs of sandstone .....	38
2.11	Interpretive stratigraphic cross-sections of the Waugoola Group on Sharps Ridge .....	41
2.12	Interpretive depiction of stratigraphic relationships in the Waugoola Group on the southern wall of the Cadia Hill pit .....	42
2.13	Cross-section and paleogeographic interpretation of the Waugoola Group across Cadia Hill and Cadia East .....	44
2.14	Diagram showing idealized rift-sag sequence features.....	46
2.15	Regional tectonic controls of evolution of the Cadia District.....	51
2.16	Map showing the stratigraphic position of the Forest Reefs Volcanics at the unconformity with overlying Waugoola Group sedimentary rocks.....	52

3.1	Regional geologic map .....	58
3.2	Generalized geology map of the Cadia District.....	61
3.3	Cross-section across mineral deposits in the Cadia District .....	63
3.4	Annotated aerial photograph of Cadia Hill and Cadia East.....	64
3.5	Structural domain map of Cadia Hill and Cadia East.....	68
3.6	Map of the Waugoola Group with bedding orientations .....	70
3.7	Reference map for locations of photographs used in chapter three figures.....	72
3.8	Panoramic photograph of the southern wall of Cadia Hill pit showing relationships between basement and cover faults .....	73
3.9	Photographs of unconformity features on the southern wall of Cadia Hill pit .....	75

3.10	Panoramic photograph of the eastern wall of Cadia Hill pit showing structural relationships on Sharps Ridge .....	76
3.11	Photographs of faults from the eastern wall of Cadia Hill pit .....	77
3.12	Faults and folds at the unconformity on the southern slope of Sharps Ridge .....	79
3.13	Detailed field sketch and photograph showing faults and folds related to the Cat Fault .....	81
3.14	Photographs of open folds related to the Copper Gully Fault .....	82
3.15	Photographs illustrating bedding plane parallel slip .....	84
3.16	Detailed field sketches and panoramic photographs of folds and thrust faults in sandstone .....	85
3.17	Photographs and stereonet of tight fault-related folds in siltstone related to the Gibb Fault .....	87
3.18	Photographs and stereonet of fault related folds in Cadia East .....	88



## Acknowledgements

This thesis would not have been possible without the intellectual, logistical, and emotional support of many people. First and foremost, I would like to thank my primary advisor, Dick Tosdal for setting up this project, traveling back and forth from Vancouver to Australia to make sure I was on track, and making many valuable suggestions both in the field and during the editing process. Thanks to Dick's input, I have had the opportunity to grow as a geologist, and as a writer. Ken Hickey and Lori Kennedy, my other committee members, also offered valuable criticism at my defence that has enabled me to improve the presentation of my research, and for that I am grateful.

Anthony Harris from CODES at the University of Tasmania has also provided invaluable insight into the district-scale geology of the Cadia Valley and where this project fits in to the bigger picture. Even at the beginning when no one else thought the unaltered and unmineralized rocks at the surface mattered, Anthony supplied logistical support and scientific encouragement to an often confused student very far from home.

Many Thanks to John Holliday, Ian Tedder, Dean Collett, Paul Dunham, Colin MacMillan, Matt Hatzl, Mark Aheimer, Robyn Ransley, Lal Mendis, Adam Marcinek, and Dougal Munro, all with Newcrest Mining LTD. for making mapping possible and safe, helping with the database and other technical support issues, moving core boxes, and asking lots of insightful questions. Thanks especially to Caroline Hassal and her parents, Rosemary and Frank, for providing lodging, transportation, and entertainment in Spring Hill, and introducing me to cordial, pavlova, and Braford's.

Thanks to Dave Cooke from CODES for discussions in Hobart about regional tectonics, and to Ian Percival, for his amazing knowledge of fossils. Arne Toma and Ken



Hickey at MDRU deserve a great deal of appreciation for technical support with Map Publisher, the plotter, and countless other computer-related inquiries. Thanks to the SEG Canada Foundation Award for funding transportation to and from Australia for my second field season. I would also like to thank my professors from the University of Maine for getting me started in Geology, instilling in me a healthy dose of skepticism, and preparing me, as best they could, for grad school. In particular, Scott Johnson, Peter Koons, and Marty Yates were instrumental in guiding me toward this point in my career.

Personally, if it hadn't been for the emotional support of my Dad, and my friends Liz, Sara, Shawn, and Bobby, I might have broken down a long time ago, and would have never realized my potential as a geologist and a human being. Thanks for being there for me despite the growing physical distance between us. Thanks also to my fellow grad students at UBC for conversation, companionship, and countless wine-tastings in the basement. Last, but certainly not least, much gratitude to my husband Wes Groome, for comforting me through the difficult parts, laughing with me through the fun parts and inspiring me to ride the rollercoaster to the end. If it weren't for Wes' advice, as a geologist, editor, and friend, I wouldn't have been able to come this far in such a short time.

## **Dedication**

*To my mother*

## **Chapter One: Introduction**

To better guide resource development, from exploration to mining, in regions with complex geologic histories, it is important to understand the nature of pre-, syn-, and post-mineralization tectonism. Ground preparation prior to mineralization may enable transport and localization of ore-forming fluids via several mechanisms, including the juxtaposition of thermally, chemically, or rheologically disparate materials, the formation of interconnected fracture networks that act as fluid flow pathways, and the development of permeability barriers (e.g. Bierlein et al., 2002; Jaques et al., 2002). During mineralization, active deformation may assist the movement of fluids through the system and concentrate ore in locally dilatant sites as the transient permeability structure of the host rock changes (Tosdal and Richards, 2001). Syn-mineral deformation may also result in active fluid transport along structures via seismogenic fault-valve action (seismic pumping) due to regional changes in the stress regime (e.g. Jaques et al., 2002). Post-mineral deformation can dismember the orebody or provide new pathways for subsequent remobilization of ore fluids (e.g. Dilles et al., 1991; Willis and Tosdal, 1992). In relation to porphyry systems, which form at relatively shallow depths (1-3 km), post-mineral uplift and erosion may remove part or all of the orebody (Camus, 2003; Cooke et al., 2005). However, a transition to an extensional regime following mineralization may result in burial of the deposit and enhance the possibility of preservation (Sillitoe, 2000).

Australia is an important producer of copper and gold worldwide, including multi-million ounce porphyry Au-Cu deposits within the Paleozoic Tasman Orogenic system (Jaques et al., 2002; Cooke et al., 2007). In the Lachlan Orogen, a subset of the

Tasmanides, porphyry and related epithermal and skarn deposits formed during the late Ordovician to early Silurian in subduction-related volcanic arc and arc-associated host rocks that were localized by long-lived, large-scale crustal structures active during the Benambran Orogeny (e.g. Cooke et al., 2007; Glen et al., 2007c). Major mineral districts in the eastern part of the Lachlan Orogen include Cadia (the focus of this study), Cowal, Copper Hill, Goonumbla, Peak Hill and Gidginbung, all of which formed during Ordovician to Early Silurian Macquarie Arc magmatism. Multiple episodes of subsequent tectonic activity resulted in polydeformation and complex structural relationships. Not only is placing these major mineral deposits into a tectonic context important for regional exploration, comparative district- and deposit-scale studies enable more complete tectonic models to be constructed for the evolution and growth of the Australian continent.

Alkalic porphyry deposits and skarns of the Cadia District have been a significant source of Cu, Au, and Fe for Australia since the 1850's (Holliday et al., 2002). Currently, the Cadia District is one of the largest alkalic porphyry deposits worldwide in terms of contained gold (Wilson et al., 2004; Cooke et al., 2004; Cooke et al., 2007). Pre-mine resources of the Cadia district were estimated at 585 t Au and 2.35 Mt Cu (Holliday et al., 2002). The intrusive history, fluid evolution, and alteration systems of the district have been studied extensively, and are well understood to date (Holliday et al., 2002; Wilson et al., 2003; Forster et al., 2004; Cooke et al., 2006b; Wilson et al., 2007a; Wilson et al., 2007b; Squire and Crawford, 2007). Such ore processes occur over timescales that are relatively short (10s to 100s of thousands of years) compared to regional tectonic processes (millions of years).

On a global scale, giant porphyry deposits have been recognized to cluster in orogen-scale mineral provinces, which suggests that they are localized by orogen-scale geodynamic processes (e.g. Clark, 1995; Cooke et al, 2005). In older orogens, such as the late Ordovician-early Silurian Benambran Orogeny, the preservation potential of porphyry deposits is directly related to the post-mineral history of uplift, erosion, and orogenesis (Cooke et al., 2005). Therefore, it is critical to put the mineralizing system in a temporal and spatial context in order to develop a complete, holistic model to explain present day ore distribution.

## **THESIS OVERVIEW**

The aims of this thesis are to describe the Silurian Waugoola Group sedimentary cover sequence in the Cadia District and characterize the post-mineral deformation. This structural analysis is then incorporated into district-scale tectonic models for the history of orebody formation and dismemberment. Furthermore, reconstruction of the Silurian succession and recognition of the hierarchy of faults is essential to the on-going project attempting to reconstruct the syn-mineralization Ordovician architecture of the district. This project is part of the larger ‘district-to-deposit-scale structural and geochemical study of the Cadia porphyry Au-Cu deposits’ managed by CODES ARC Centre of Excellence in Ore Deposits.

Like other porphyry deposits of the Macquarie Arc, mineralization in the Cadia district occurred at the end of the Benambran Orogeny (~443-438 Ma). At least three subsequent deformation events have been regionally recognized in the Lachlan Fold Belt;

these include the Bindian (Late Silurian), Tabberabberan (Early Devonian), and Kanimblan (Early Carboniferous) Orogenies. Because the Waugoola Group was deposited in the middle Silurian (~424-426 Ma), after ore formation and the cessation of Benambran deformation, but prior to later tectonic events, it preserves a record of post-mineral deformation. This can then be used to geometrically constrain district-scale reconstructions. Greater understanding of these structural relationships will also be crucial for developing exploration models in and around the Cadia East deposit, and also for constructing geotechnical and hydrologic models as development and production commences.

The remainder of Chapter One is a discussion of regional geology. In Chapter two of this thesis, a stratigraphic succession for the Waugoola Group at Cadia East is presented in order to form a basis for structural analysis in Chapter Three. Finally, the regional significance of deformation recorded in the Waugoola cover sequence, and the implications of orebody dismemberment will be discussed in light of the current models for the tectonic history of the Cadia District in Chapter Four.

## **Methodology**

Mapping of the sedimentary cover sequence at Cadia East was undertaken from August to October, 2006, and May to August, 2007, in order to constrain the character and scale of faulting and folding in different geographic areas and stratigraphic horizons. Detailed field sketches of outcrops along the Cadia Hill Access Road, in Copper Gully, and from the southern and eastern walls of Cadia Hill pit were used to understand

structural relationships at the 1:200 scale. Strike and dip measurements of bedding and faults were taken using a Brunton compass and geographically referenced with a GPS for compilation into a 1:5,000 map of the sedimentary cover rocks at Cadia East and the surrounding areas. Due to safety restrictions in Cadia Hill Pit, measurements from pit walls were estimated from a distance of at least 5m. Surface and pit wall mapping covered an area of roughly 4km<sup>2</sup>.

Lithological data was also gathered by producing graphic logs of the cover rocks in drillcore. Because drillcore was not oriented, structures were noted but not measured. Magnitude of fault offsets in drillcore is also poorly constrained. In combination with surface measurements, drillcore data was used in producing interpretive cross-sections through the sedimentary cover rocks. This was combined with pre-existing datasets for faults in the Ordovician basement rocks provided by Newcrest Mining Ltd, constrained by drillcore and geotechnical mapping in Cadia Hill Pit. Spatial information was organized in MapInfo, and was subsequently exported to Adobe Illustrator using Map Publisher for editing.

## **REGIONAL GEOLOGY**

Southeastern Australia has experienced multiple orogenic events from the Late Proterozoic to the late Mesozoic (Glen, 2005; Cawood, 2005; Gray et al., 2006). In this region, multiple cycles of compression and extension associated with the growth of the Australian continent have been identified, resulting in a complex regional geologic history. The Cadia District is located in the Macquarie Arc, a late Ordovician volcanic

island arc in the eastern Lachlan Fold Belt. Mineralization occurred ~440 Ma, and the age of the unconformably overlying Waugoola Group sedimentary cover sequence is ~425 Ma. Regional variations in lithology and older structural fabrics have locally influenced deformation at the district-scale. In order to understand the effect of these events on the Cadia District and the resulting associations between structure and ore distribution, it is necessary to review the regional tectonic history, from continent- to district-scale.

### **The Tasmanides and the Lachlan Tectonic Cycle**

The Tasmanides are a long-lived, composite orogenic belt that formed through episodic accretion to the Gondwanan margin of eastern Australia, commencing in the early Paleozoic with the breakup of Rodinia and concluding in the Early Mesozoic with the cratonization of the western portions of the New England Orogen (Figure 1.1; Gray and Foster, 2004). The eastern margin of the Australian Craton approximately follows the Tasman Line, an irregular north-south “zig-zag” line that bisects Australia, and marks the eastern margin of the Precambrian basement (e.g. Hill, 1951; Li and Powell, 2001; Direen and Crawford, 2003).

The Tasmanides have been divided into six major structural belts. The Delamerian Orogen to the southwest, the Lachlan Fold Belt to the southeast, the Thompson Fold Belt to the northwest, and to the northeast, the Hodgkinson-Broken River Fold Belt, are all separated from the New England Fold Belt by the Sydney-Bowen Basin



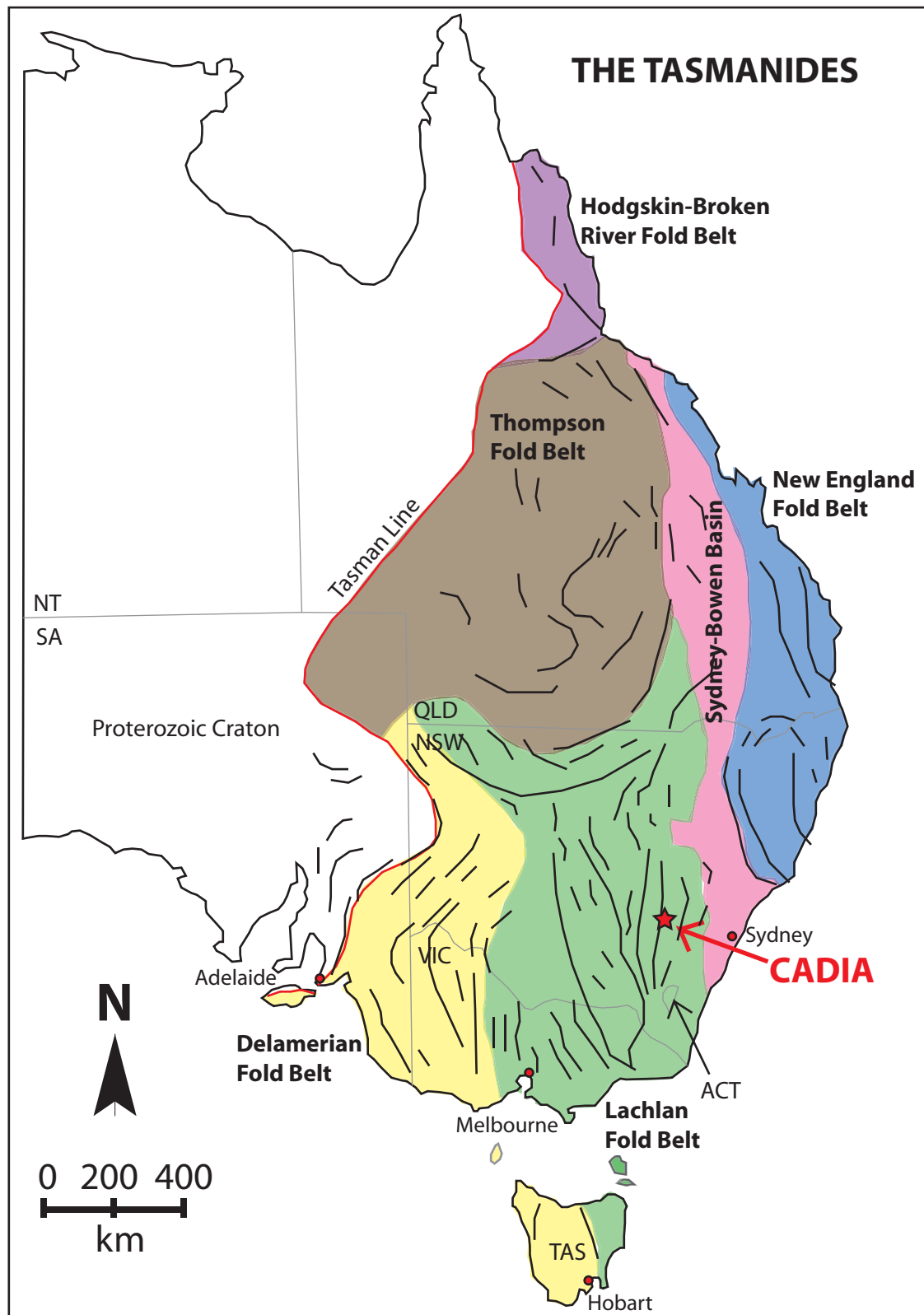


**Figure 1.1:** The Tasmanides are a long-lived composite orogenic belt that composes much of eastern Australia. Cadia is located in the Lachlan Fold Belt. Map of the Tasmanides modified from Scheibner and Basden, 1996; structural form lines after Gray and Foster, 2004.

(Scheibner and Veevers, 2000). These orogenic zones generally young toward the east, and represent separate episodes of orogenesis (Gray and Foster, 2004; Glen, 2005).

The timing and geometry of terrane assembly in the Tasmanides has been described by Glen (2005) in terms of three major tectonic cycles: the Delamerian Cycle (830-490 Ma), the Lachlan Cycle (490-320 Ma), and the Hunter-Bowen Cycle (320-230 Ma). The Lachlan Cycle is further subdivided into the Benambran (~443-430 Ma), Bindian (~420 Ma), Tabberabberan (~380 Ma), and Kanimblan Orogenies (~340) (Glen, 2005). The Lachlan tectonic cycle had the greatest effect on the Cadia region, and will be discussed in greater detail below (Table 1.1).

Convergence associated with the early phase of the Benambran Orogeny marks the beginning of the Lachlan Tectonic Cycle and coincides with the end of the Delamerian Cycle (Glen, 2005). The collisional stage of the Benambran Orogeny in the Lachlan Fold Belt occurred in two distinct phases. The first at ~443 Ma resulted in folds, thrusts, cleavage formation and some strike-slip faults deforming Ordovician turbidites and black shale due to E-W shortening (Glen, 2005). By this time, magmatism in the Macquarie Arc had ceased and arc rocks were thrust over and accreted onto backarc turbidites (Glen, 2005). This compressional phase was followed by a period of extension and basin formation in the earliest Silurian (Glen et al., 2004). The second collisional phase of the Benambran Orogeny lasted from ~433-430 Ma (Glen, 2005). During this phase, oblique thrusting in the Central Lachlan and translation of the Macquarie Arc to the southwest was accompanied by uplift and thrusting of turbidites as well as portions of the arc itself (VandenBerg, 1999; Glen, 2005). Emplacement of syn-tectonic granites also occurred at this time (VandenBerg, 1999).

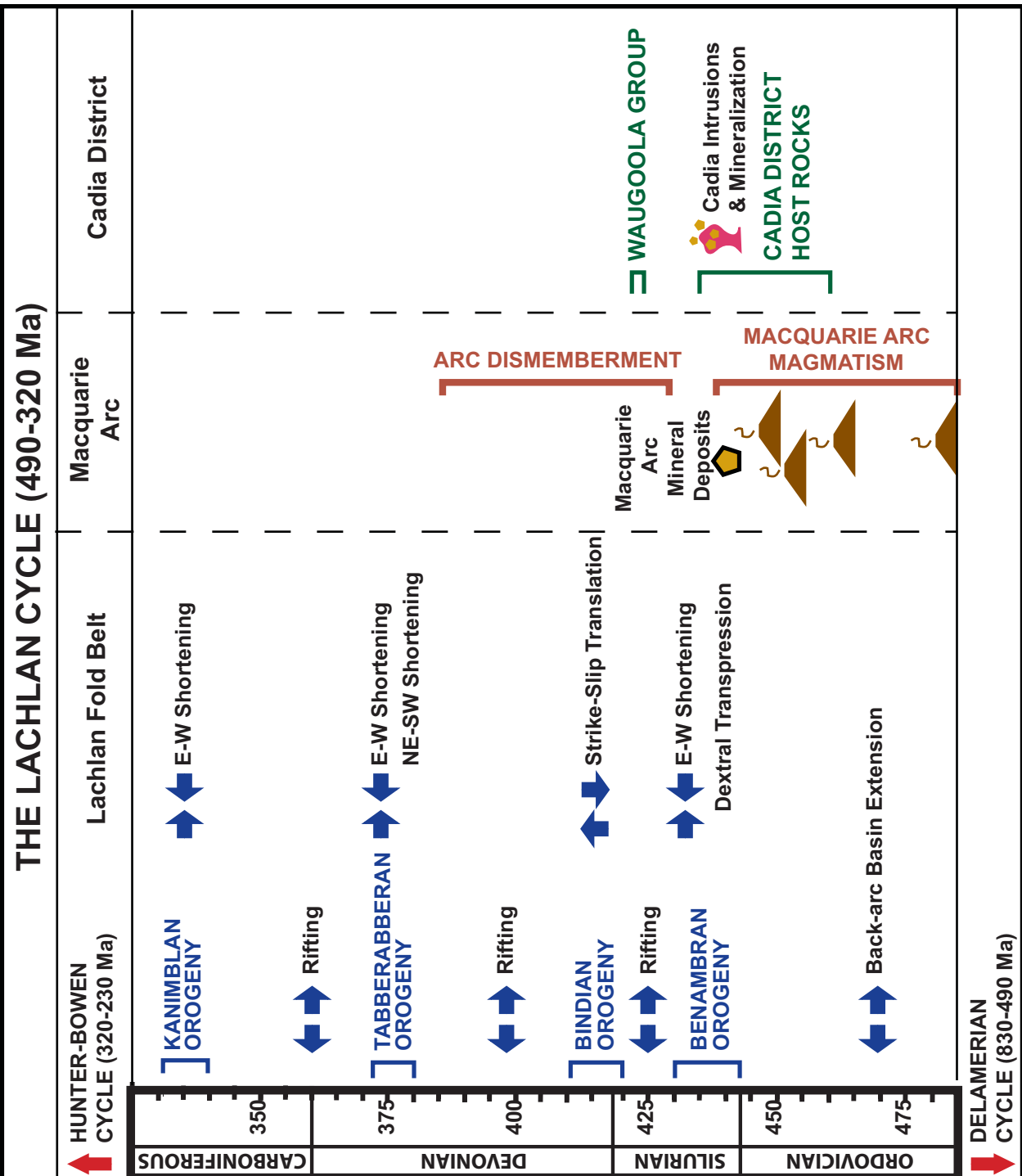


**Table 1.1:** Timing of tectonic events in the Lachlan Cycle, the Macquarie Arc and mineralization in the Cadia District. Ages compiled from Glen et al., 2007; Harris, in prep, Percival and Glen, 2007; Rickards et al., 2001; Pogson and Watkins, 1998; Glen, 2005, and references therein.

The Bindian Orogeny (~420-410 Ma) resulted in translation and thrusting of the central Lachlan Orogen to the south-southeast (Willman et al., 2002). This translation was facilitated along major bounding fault systems that separate the central Lachlan from the western and eastern subprovinces. Throughout the Tasmanides, Bindian orogenesis marked a major period of strike-slip deformation.

Late Silurian to Late Devonian arc magmatism related to a west-dipping subduction zone formed as a result of Tabberabberan convergence in the New England Orogen (Offler and Gamble, 2002). The Lachlan Orogen, in the backarc setting during convergence of the Tabberabberan Cycle, experienced rift or transtensional basin formation and granite emplacement (Reed et al., 2002; Spaggiari et al., 2004). Tabberabberan deformation was caused by collision of the intra-oceanic arc generated during the previous convergent phase and accretion to the continental margin in the Northern New England Orogen. Inversion of basins in the Lachlan Orogen during the middle Devonian characterizes the deformation (Hood and Durney, 2002; Willman et al., 2002). In the eastern Lachlan Orogen, shortening at ~380 Ma was NE-SW directed (Miller et al., 2001; Watson and Gray, 2001). The final stage of Tabberabberan contraction formed conjugate NE- and NW-trending brittle faults that offset major plutons in order to partition E-W shortening around resistant plugs of newly cooled granites (Glen, 1992).

The Kanimblan Cycle began with rifting in the Early to Middle Devonian. At ~340Ma, Kanimblan Orogenesis commenced, and was the last major deformation to affect the Lachlan Fold Belt. Shortening was predominantly E-W, with minor strike-slip separation occurring locally (Glen, 2005). In the eastern Lachlan Orogen, N- striking

faults were reactivated and accompanied by folds and cleavage development as the basins were inverted (Glen, 2005).

### **The Lachlan Fold Belt**

The Lachlan Fold Belt extends from southern Queensland to southeastern Tasmania, and underlies most of New South Wales and Victoria. In general, the Lachlan Fold Belt is thought to have formed during episodic accretion of deformed oceanic sequences, volcanic arcs and arc-related rocks, and microcontinents to the Gondwana margin during the Lachlan Tectonic Cycle as described above (e.g. Bierlein et al., 2002; Gray and Foster, 2004; Glen, 2005). In general, the Lachlan Fold Belt is composed of low-metamorphic-grade turbidites that were deposited in a back-arc environment and deformed in three separate thrust systems. Local high-T/low-P metamorphic complexes and island arcs are also present (Figure 1.2; Gray et al., 2006).

Turbidites are the dominant rock type across the orogen, suggesting an oceanic setting for the whole of the Lachlan Fold Belt (Gray and Foster, 2004). This turbidite package, along with associated accreted rocks (including the Ordovician Macquarie Arc), was repeatedly thickened by folding and thrusting, dismembered by strike-slip faulting, thinned by extensional faulting, intruded by plutons, and eventually merged through stepwise accretion (Coney, 1992). The crustal architecture of the Lachlan Orogen includes both thin-skinned (multiple detachments producing a leading imbricate fan system) and thick-skinned (major faults extending to the Moho) features, with a transition

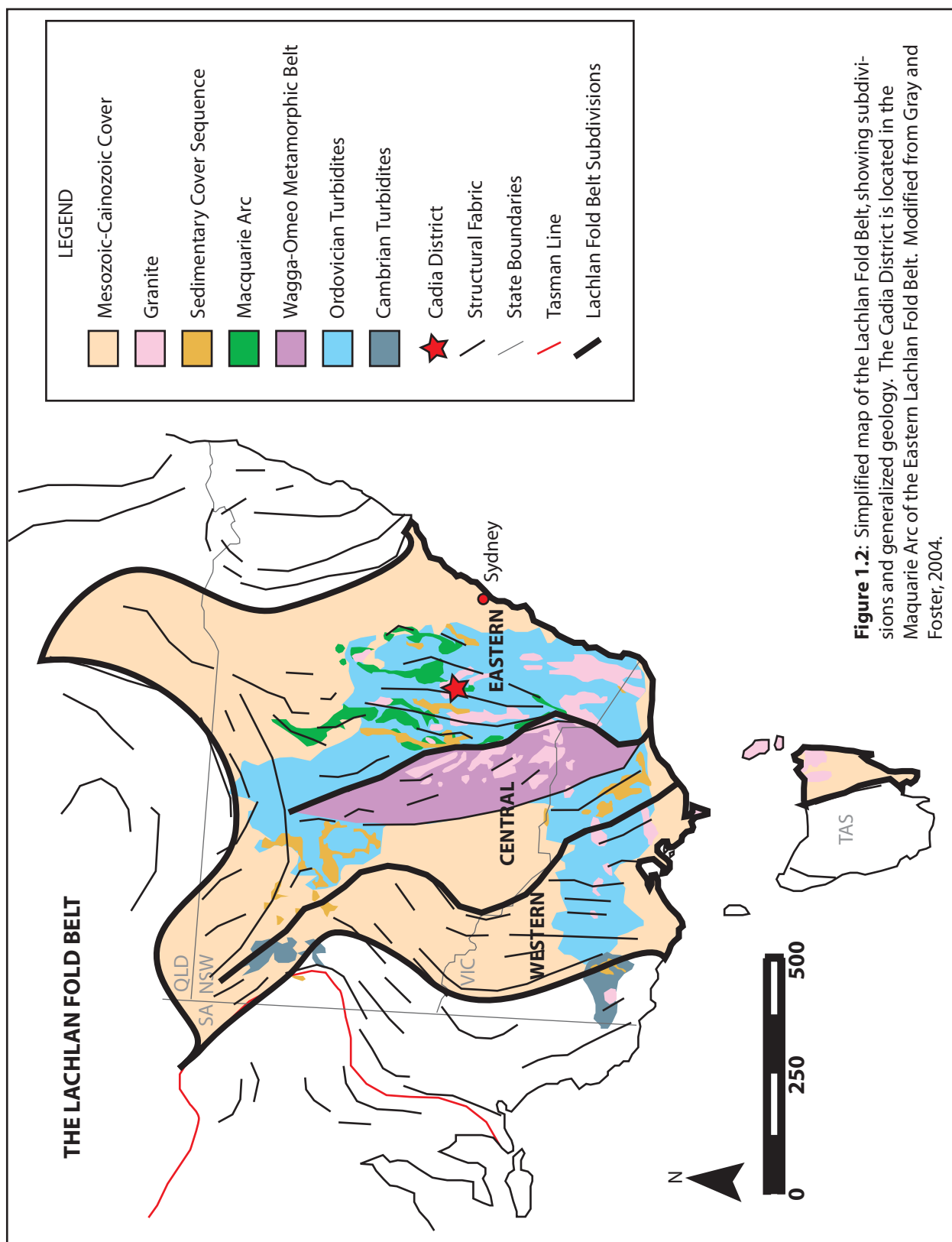


**Figure 1.2:** Simplified map of the Lachlan Fold Belt, showing subdivisions and generalized geology. The Cadia District is located in the Macquarie Arc of the Eastern Lachlan Fold Belt. Modified from Gray and Foster, 2004.

from western thin-skinned tectonism to eastern thick-skinned tectonism (Gray et al., 2006).

The Lachlan Fold Belt, assembled from west to east via roughly N-striking regional structures, can be subdivided into three structural zones: the western, central, and eastern subprovinces (Figure 1.2). The distinction between these zones has been defined based on geochronology of deformation and major structural breaks (Gray and Foster, 2004; Glen, 2005; Gray et al., 2006). In general, the western subprovince consists of tightly folded turbidites and low grade metamorphosed ophiolites, the central subprovince is dominated by a high-grade metamorphic core complex and an accretionary complex, and the eastern subprovince is a folded and faulted turbidite package and an Ordovician island arc system (Gray and Cull, 1992). Early Carboniferous sedimentary rocks are found in localized basins throughout the Lachlan Fold Belt, and Siluro-Devonian granites are also present in all zones of the Lachlan Fold Belt (Suppel et al., 1998; Coney, 1992).

Metallogenically, the western Lachlan is rich in orogenic lode gold deposits, whereas the central Lachlan contains a more diverse range of mineral deposit types, including intrusive-hosted, volcanogenic massive sulphide, and epigenetic sediment-hosted gold and base metal deposits (Bierlein et al., 2002). Porphyry-style mineralization in the Lachlan Orogen is restricted to the eastern portion, particularly the Ordovician Macquarie Arc, although volcanic-hosted massive sulphides, sediment-hosted base metals, and some orogenic lode gold deposits are also present in the eastern Lachlan (Bierlein et al., 2002). These deposits are thought to be related to slab rollback following seamount collision at ~455 Ma (Squire and Miller, 2003).

Deformation in the western subprovince commenced at ~455 Ma, characterized by mostly west-dipping thrust faults and west vergent chevron folds (Gray and Foster, 1998; Foster et al., 1998; Squire and Miller, 2003; Gray and Foster, 2004). Deformation migrated to the east at ~440 Ma and continued throughout the Lachlan Belt into the Silurian, with east-west shortening, sinistral wrenching, and south-east directed thrusting in the western subprovince, and east-west shortening, south-directed thrusting, and strike-slip faulting in the central and eastern subprovinces (Foster et al., 1999; Miller et al., 2001). In the central and eastern subprovinces, deformation was accompanied by the largest and final outpouring of shoshonitic magma in the Macquarie Arc at ~440 Ma (Perkins et al., 1995; Squire and Miller, 2003; Glen et al., 2007a; Glen et al., 2007b). Much of the mineralized centers in the Lachlan Orogen formed at this time (Squire, 2001; Miller and Wilson, 2002).

### **The Macquarie Arc**

The Macquarie Arc is a long-lived Ordovician volcanic arc composed of predominantly subaqueous volcanic rocks and associated shallow-level intrusions with a calc-alkalic to shoshonitic affinity (e.g. Cooke et al., 2007). Magmatic activity in the Macquarie Arc commenced in the Early Ordovician at the boundary between the Australian and the proto-Pacific plates (Glen et al., 1998; Glen et al., 2007b; Meffre et al., 2007). Episodic evolution of the arc continued for ~50 Ma until magmatism ceased in the early Silurian (Glen et al., 2007b). The Macquarie Arc formed over a west-dipping subducting slab that underwent slab rollback, resulting in eastward migration of the



magmatic center preserved as a general east-younging of the arc rocks (Percival and Glen, 2007). Turbidites and other arc-related sedimentary rocks are intercalated with the volcanic rocks (Squire and McPhie, 2007).

The Macquarie Arc is separated into three distinct structural belts, although it is probable that these three belts formed together as part of one arc and were subsequently disrupted during rifting in the Silurian and Devonian (Figure 1.3; Percival and Glen, 2007). From west to east, and generally youngest to oldest, these belts are the Junee-Narromine Volcanic Belt, the Molong Volcanic Belt, and the Rockley-Gulgong Volcanic Belt. The Kiandra Volcanic Belt is a fourth structural division of the Macquarie Arc that occurs to the south near the Victoria-New South Wales border, and may represent a portion of the Junee-Narromine belt that was dismembered during strike-slip faulting (Glen et al., 2007b; Percival and Glen, 2007).

A number of Au and Cu deposits are associated with Macquarie Arc magmatism. Porphyry deposits of the Macquarie Arc are aligned along a northwest striking trend, known as the Lachlan Transverse Zone (LTZ). The intersection of this regional- to deposit-scale fabric with N-trending, arc-parallel faults may have localized mineralization (Glen and Walshe, 1999; Finlayson et al., 2002). Seismic imaging has shown that these lineaments are zones of weakness in the lithosphere that may have been long-lived zones of reactivation (Glen and Walshe, 1999; Finlayson et al., 2002).

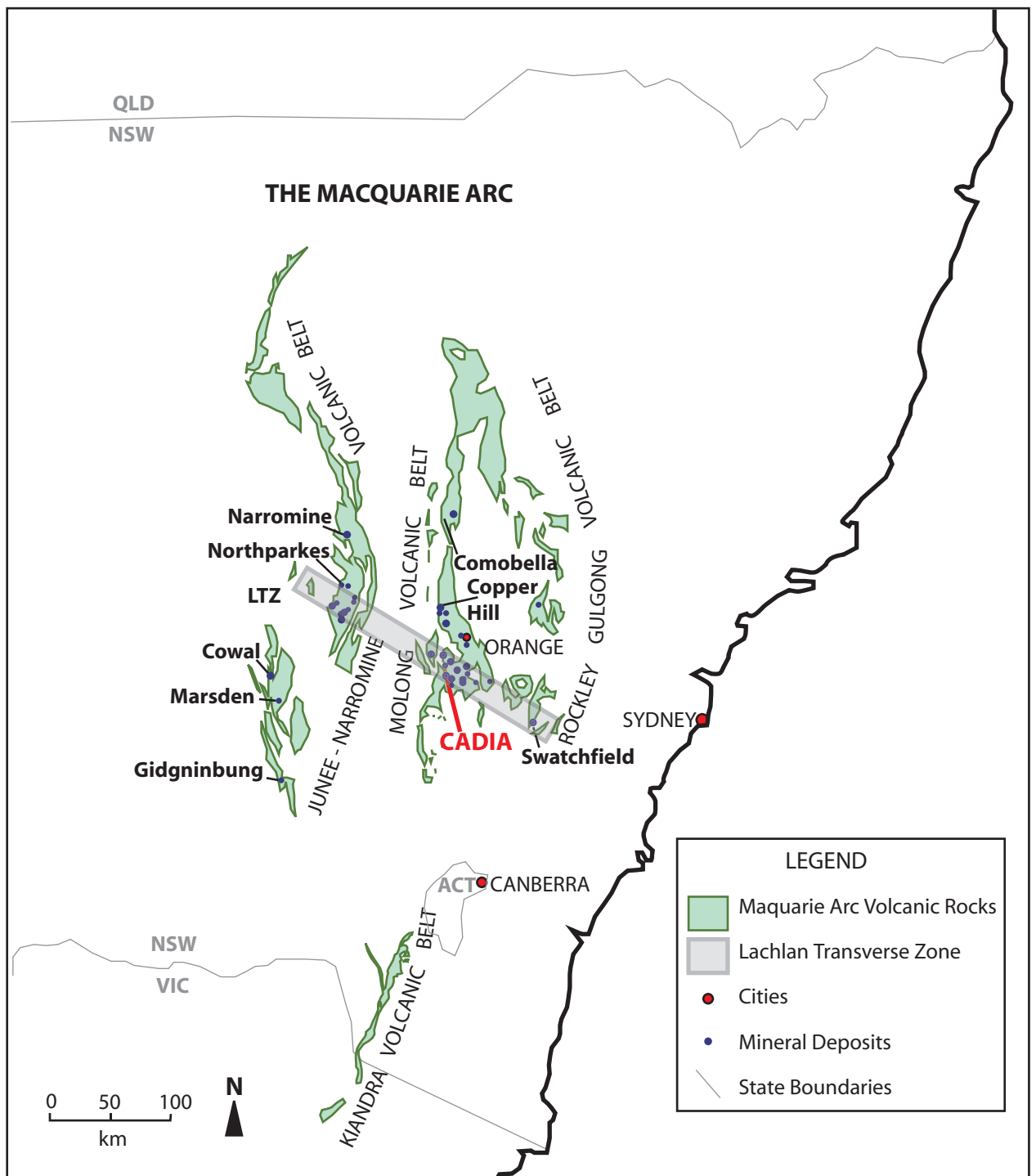


**Figure 1.3:** Mineral deposits and structural belts of the Macquarie Arc. Volcanic rocks associated with arc volcanism during the late Ordovician to early Silurian were accreted to the proto-Australian margin during the Benambran Orogeny and subsequently dismembered during rifting. The Cadia District is located in the Molong Volcanic Belt, and occurs on the Lachlan Transverse Zone (LTZ). Modified from Holliday et al., 2002 and Glen et al., 2007.

## THE CADIA DISTRICT

Copper was first discovered in the Cadia District in 1851. By the mid 1860's mining was underway at the West Cadia and White Engine deposits, and Cadia Village became a major settlement in New South Wales. Gold was discovered in the early 1870's. During the world wars, the Cadia district saw a period of increased mining activity, as it became an important source of iron ore. Newcrest Mining Ltd. acquired the property in 1991, and porphyry-style copper-gold mineralization in sheeted vein complexes was discovered at the Cadia Hill deposit in 1992 (Holliday et al., 2002; Wilson et al., 2003). Mineralization at Cadia East and Cadia Far East (currently included in Cadia East) was discovered in 1994 and 1996 respectively. The high-grade Ridgeway deposit was found in 1996. Total *in-situ* resource for the Cadia District has been estimated at 32 Moz Au at 0.7g/t and 4700 kt Cu at 0.36% (Newcrest Mining Ltd., annual report, 2006). With ore zones extending over 1km across along a 6 km long northwest-striking trend, the Cadia district is the largest porphyry district in Australia.

Mineralization is associated with late Ordovician alkalic monzodiorite, monzonite, and quartz-monzonite intrusions of the Cadia Intrusive Complex. Mineralization is typically hosted in stockwork and sheeted vein complexes within the intrusions and the surrounding Forest Reefs Volcanics. Mineralized porphyries occur typically as dikes and plugs, related to a batholith at depth (Holliday et al., 2002).

Intrusions at Ridgeway are dated at ~443 Ma and are monzodioritic to monzonitic in composition (Harris, 2007b; Wilson et al., 2007b). High-grade ore at Ridgeway occurs in stockworks and is associated with abundant magnetite (Wilson et al., 2003). Ore in

Cadia Hill and Cadia Quarry is concentrated in sheeted veins associated with a composite quartz monzonite stock (Holliday et al., 2002). Mineralization at Cadia East is primarily hosted in volcaniclastic rocks of the Forest Reefs Volcanics (Holliday et al., 2002; Wilson et al., 2003). The Big Cadia and Little Cadia skarns occur in a calcareous sandstone unit near the top of the Forest Reefs Volcanics stratigraphy (Forster et al., 2004). All deposits in the Cadia district display zoned alteration and sulphide distribution characteristic of alkalic porphyry systems (Cooke et al., 2006b; Wilson et al., 2007a).

## **Chapter Two: Stratigraphic Framework**

### **INTRODUCTION**

The stratigraphy in the Cadia District preserves a complex history of evolution from a foreland setting to an active volcanic arc complex in the Late Ordovician, to an extensional basin setting in the Silurian. Structural dismemberment has occurred post-Silurian during numerous overprinting brittle deformation events. In order to better constrain the effects of this brittle deformation, stratigraphic relationships of both the Ordovician and Silurian is needed to provide a spatial and temporal framework. To produce structural reconstructions of the district, as discussed in the following chapter, depositional (pre-deformation) lithological distribution and basin geometry must be understood.

The uppermost preserved Paleozoic succession in the Cadia district is the Waugoola Group sedimentary cover sequence. A refined stratigraphy for the Waugoola Group in the Cadia district has helped to constrain the effects of post-mineral deformation in two ways. First, lithological and rheological differences influenced fold and fault geometry. Second, distribution of facies, particularly of the basal unit, provides evidence for fault-related topographic controls on deposition of the Waugoola Group. While the focus of this study is the Silurian sedimentary cover succession, a review of older stratigraphic units in the district is necessary to place the Silurian sedimentary cover sequence into context.

The stratigraphy of the Cadia district can be subdivided into Ordovician basement and the Silurian cover. The Ordovician basement is divided further into the Weemalla Formation, the Forest Reefs Volcanics, and intrusive rocks of the Cadia Intrusive Complex (Figure 2.1). For the sake of simplicity, earliest Silurian strata at the top of the Forest Reefs Volcanics will be grouped with Ordovician basement, as the majority of the Forest Reefs succession is Ordovician in age. Basement rocks are distinguished from Silurian sedimentary rocks due to differences in alteration. The Silurian cover rocks are unaltered, whereas Ordovician to early Silurian basement rocks are variably altered by chlorite-hematite and feldspathic alteration (e.g. Holliday et al., 2002; Wilson et al., 2003).

Ordovician basement is separated from the Silurian cover by an unconformity. The unconformity between the Ordovician basement, including the Cadia Intrusive Complex and the enclosing Forest Reefs Volcanics, and the Waugoola Group represents unroofing of the intrusions during the early Silurian (Wilson et al., 2007b). The relative elevation of the unconformity varies across the district, as does the stratigraphic level of the Ordovician basement rocks below. For this reason, understanding the subjacent Ordovician stratigraphy is critical for understanding the paleogeography and pre-Silurian basinal architecture.

**RIDGEWAY**

**BIG CADIA**

**CADIA QUARRY**

**WHITE ENGINE**

**CADIA HILL**

**SHARPS RIDGE**

**COPPEL GULLY**

**LITTLE CADIA**

**CADIA EAST**

**GIBB**

**CADIAN GULLONG**

0 0.5 1 1.5 2 km

**N** ↑

Projection/Datum:  
Australian Map Grid  
AGD 66

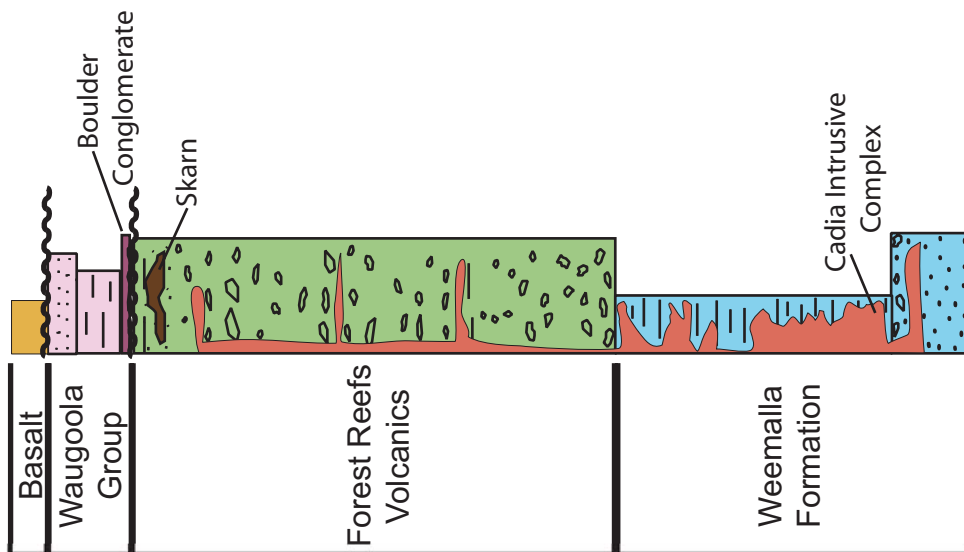


**Figure 2.1:** Simplified map and stratigraphic column of the Cadia District. Cadia Hill pit outline is shown with a dashed line. Major faults are labeled in blue. Topographic contours are 10m. Stratigraphy modified from Harris, 2007; unpublished report to Newcrest Mining, Ltd.

## **ORDOVICIAN BASEMENT**

### **Weemalla Formation**

The oldest unit in the Cadia District is the mid to late Ordovician Weemalla Formation (~460-450 Ma) (Packham et al., 1999; Holliday et al., 2002). It is composed of fine grained, thinly laminated feldspar-rich siltstone and sandstone, and includes minor interbedded carbonate and arenaceous volcanoclastic layers (Holliday et al., 2002). The depositional environment for the Weemalla Formation was a broad, unconfined deep-water fan of volcanic detritus shed off a partially emergent volcanic edifice (Pogson and Watkins, 1998; Packham et al., 1999).

In the western parts of the Cadia district, the Weemalla Formation is at least 2000m thick and hosts part of the Ridgeway deposit (Wilson et al., 2007b). Here, the Weemalla Formation generally dips gently to the northeast (343/12; strike/dip in AMG, AGD66; Wilson, 2003) and is conformably overlain by the Forest Reefs Volcanics, with a gradational contact (Holliday et al., 2002; Wilson et al., 2003). The Weemalla Formation has not yet been intersected in drillcore at Cadia East.

### **Forest Reefs Volcanics**

Regionally, the Forest Reefs Volcanics form a major part of the Molong Volcanic Belt and represent the main phase of the late Ordovician-early Silurian Macquarie Arc volcanism in the Cadia district (e.g. Cooke et al., 2007; Wilson et al., 2007a). The Forest



Reefs Volcanics consist of coherent and clastic volcanic and volcanoclastic rocks. In the Cadia district, the Forest Reefs Volcanics also include minor limestone and calcareous sandstone, and are intruded by hypabyssal intrusives (Holliday et al., 2002; Wilson, 2003; Wilson et al., 2007b). Wilson (2003) has recognized stratigraphic thickness and facies variations in the Forest Reefs Volcanics across the Cadiangullong Fault. To the east of the Cadiangullong fault, the Forest Reefs Volcanics generally dips gently to the southeast (052/12; strike/dip in AMG, AGD66; Wilson, 2003). In the Cadia District, the Forest Reefs Volcanics are up to 2000m thick (Holliday et al., 2002).

The Forest Reefs Volcanics was deposited in a shallow submarine basin from extra- and intra- basinal intermediate to mafic volcanism, occurring as a multiple-vent, locally emergent volcanic complex (Squire and McPhie, 2007; Harris, 2007a; Harris 2007b). Paleofaunal assemblages found in calcareous horizons have yielded a middle Late Orovician age of Forest Reefs Volcanics deposition, roughly from ~460 to ~450 Ma (late Eastonian; Packham et al., 1999), although conodonts and a brachiopod occurrence from the uppermost strata in the Forest Reefs Volcanics suggest an Early Silurian (448 Ma) age (Llandovery-Wenlock; Harris, 2007b.). This unit hosts gold- and-copper bearing magnetite skarn deposits at Little Cadia and Big Cadia, as well as the Junction Reefs Deposit ~20km south of the Cadia District (Gray et al., 1995; Green, 1999; Packham et al, 1999; Foster et al., 2004).

## **Cadia Intrusive Complex**

The Cadia Intrusive Complex intrudes the Weemalla Formation and the Forest Reefs Volcanics, and is unconformably overlain by the Silurian Waugoola Group (Pogson and Watkins, 1998). Late Ordovician composite intrusions of the Cadia Intrusive Complex range in composition from monzodiorite, diorite, and minor gabbro, to quartz monzonite, and have mineralogic and geochemical shoshonitic affinities (Holliday et al., 2002). Texture varies from porphyritic to equigranular (Pogson and Watkins, 1998). Intrusions at Ridgeway are dated ~442 Ma, those at Cadia Hill are dated at ~437 Ma (Wilson et al., 2007b; Harris, 2007b).

## **SILURIAN COVER**

Sedimentary rocks of the Silurian cover succession are temporally correlative on a regional scale with the Waugoola Group, and unconformably overlie the Forest Reefs Volcanics and the Cadia Intrusive Complex (Rickards et al., 2001). Altogether, the Silurian cover sequence in the Cadia district is less than 200m thick, although true thickness is uncertain due to erosion.

Macrofossils recognized in the siltstone include orthid brachiopods and graptolites (e.g. *testograptus testis*) that constrain the age of the Waugoola Group in the Cadia District to the Late Wenlock (426-424 Ma) (Figure 2.2; Rickards et al., 2001; Percival, pers. comm.). Other paleofauna reported in Rickards et al. (2001) have been identified in the Waugoola Group in the Cadia District, and support this age of

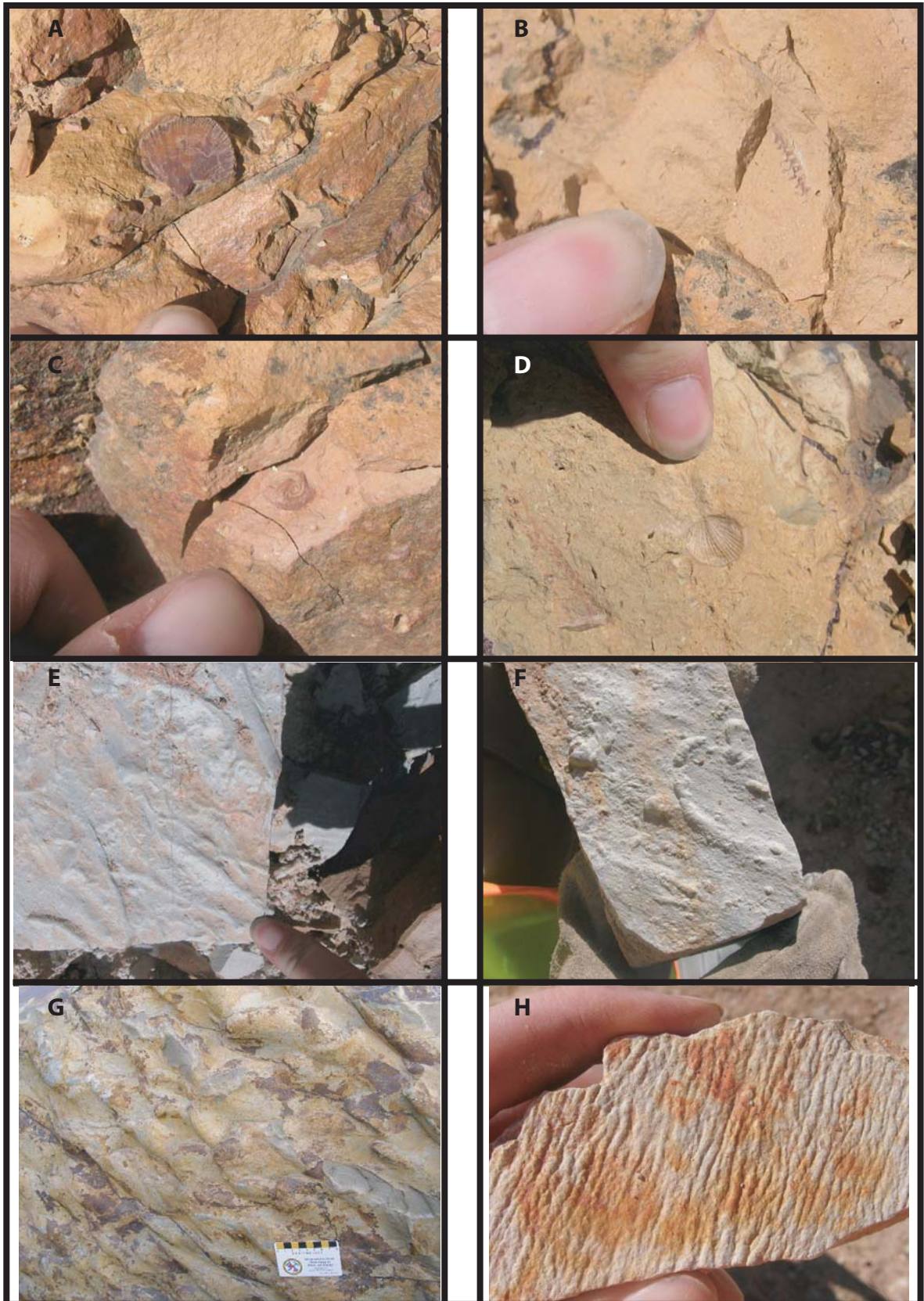


**Figure 2.2:** Macrofossils collected from the Cadia Hill Access Road and trace fossils from the Waugoola Group sedimentary cover sequence. A: brachiopod (orthid). B: graptolite (*testograptus testis*). C: brachiopod (*a. australis*). D: brachiopod (orthid). E and F: flute casts in siltstone collected from Cadia East. G: ripple casts in sandstone collected from Sharps Ridge. H: ripples in sandstone collected from Cadia East (same location as flute casts).

deposition. Ripples and flute casts are also preserved in the siltstone and sandstone across the district.

In the Cadia District, the Waugoola Group is divided into a basal unit, a lower siltstone-dominant succession, and an upper sandstone-dominant succession (Figure 2.3). The sandstone-dominant upper unit is divided into interbedded siltstone and sandstone, of varying proportions (siltstone- or sandstone- dominant) and overlying massive sandstone. The basal unit varies across the district (Figure 2.4). Locally boulder conglomerate, calcirudite limestone, or redbeds occur at the unconformity.

### **Basal Units**

Different packages at the base of the Silurian sedimentary cover sequence in the Cadia district reflect different depositional environments at the onset of Waugoola Group sedimentation. Changes in the basal unit across the district provide insight into post-mineral uplift and erosion, and the resultant paleogeography. Interpreting these facies variations is therefore critical to understanding the basin geometry that controlled Waugoola Group deposition and reconstructing both pre- and post- depositional deformation.

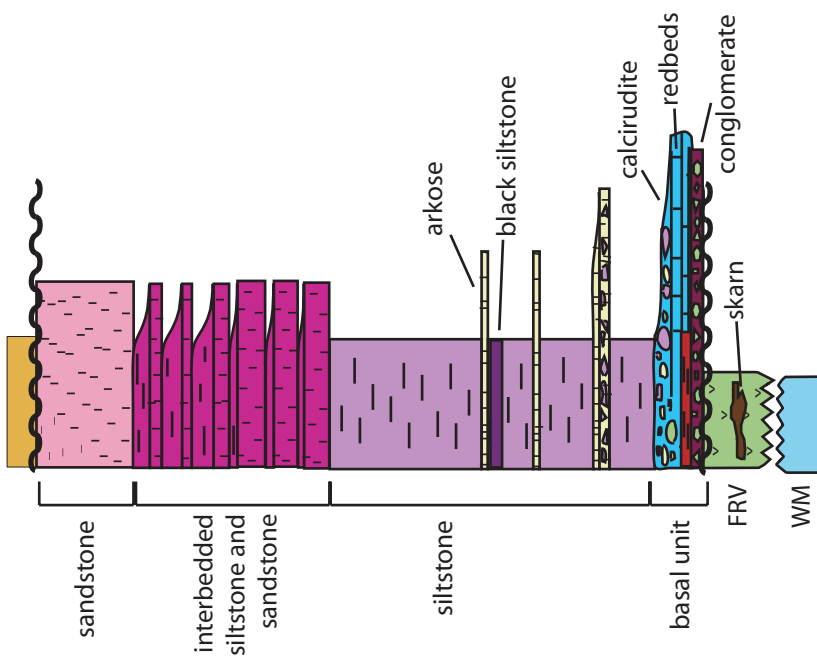
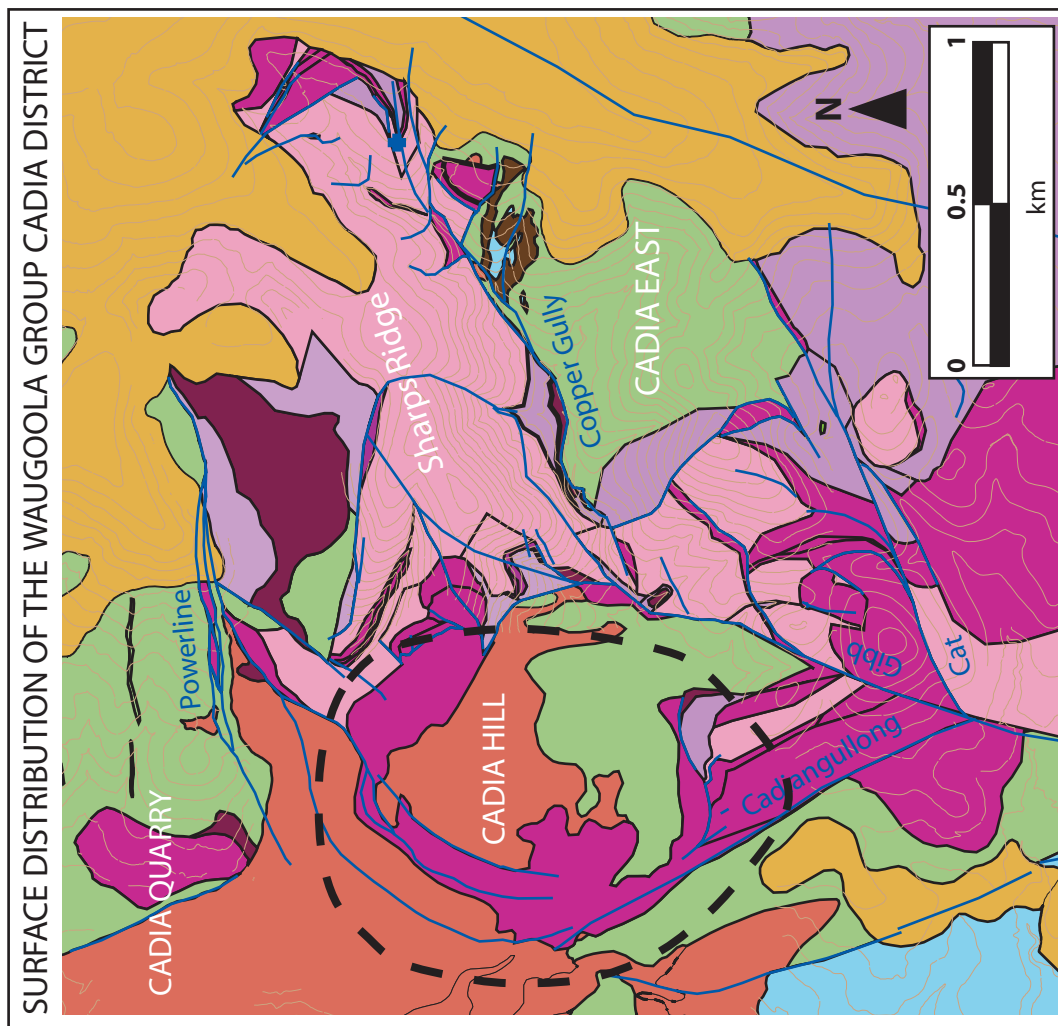


**Figure 2.3:** Generalized Waugoola Group stratigraphy and surface distribution (map). Basal unit varies across the district, and redbeds, limestone, and conglomerate do not typically appear together. Relative thicknesses shown on the stratigraphic column are based on average values for Cadia East. FRV = Forest Reefs Volcanics; WM = Weemalla Formation. Cadia Hill pit outline shown as a black dashed line.



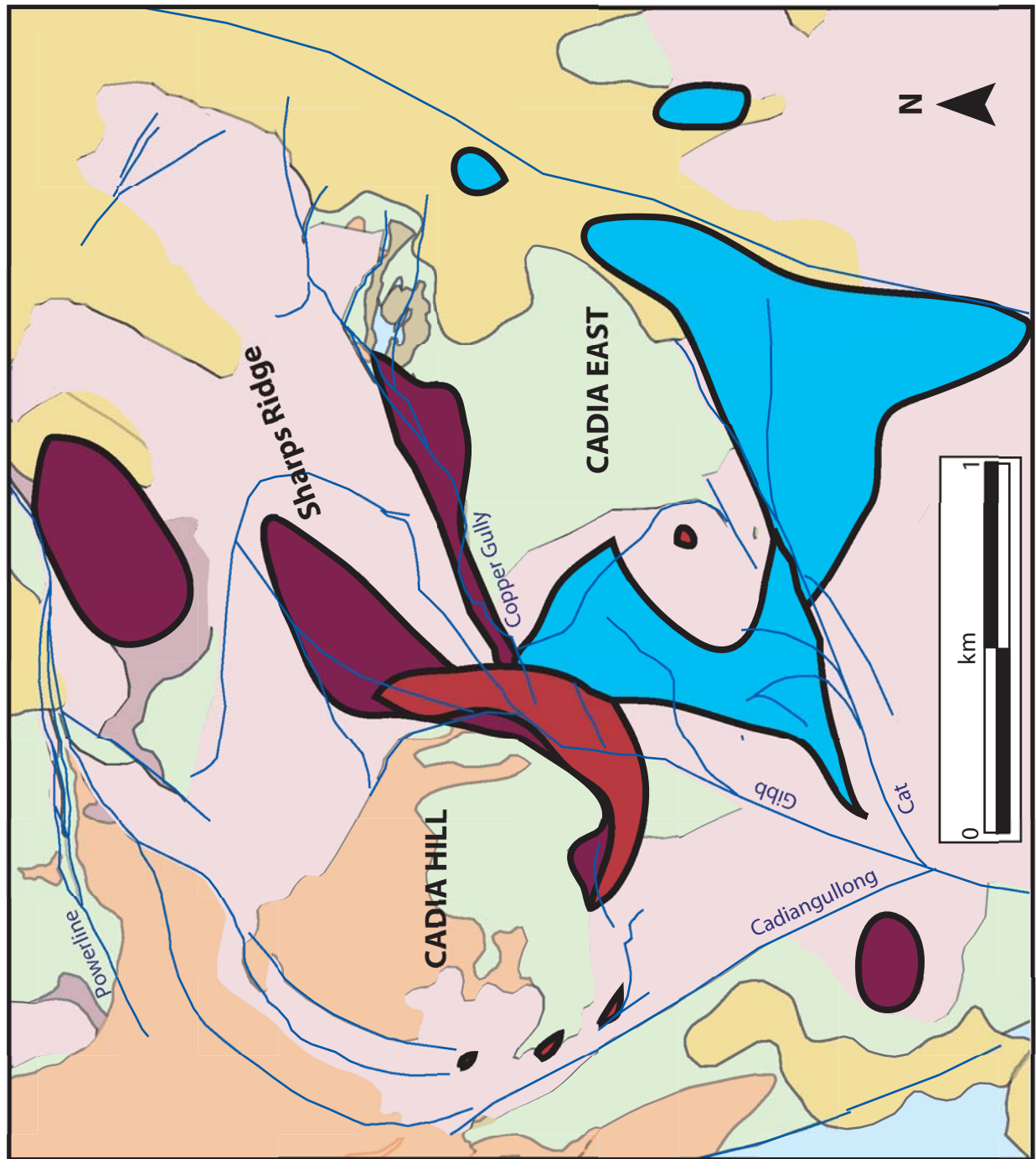
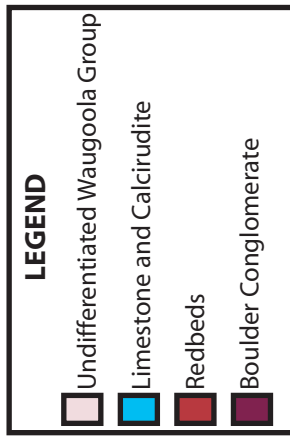


**Figure 2.4:** Map showing basal distribution of different basal units for the Silurian Waugoola Group including surface and subsurface occurrences constrained by drillcore data. Areas where the Waugoola Group is undifferentiated reflect uncertainty in interpreting drillcore data or sparse coverage. General district geology and faults are included for reference.

## LIMESTONE

The basal unit for much of the Waugoola Group at Cadia East is a pink, red, white, grey or green biolitic, variably recrystallized limestone and fossiliferous calc-rudite (Figure 2.5). Rounded limestone and biolitic coral clasts vary in size between the centimeter to the meter scale. Rare clasts of Forest Reefs Volcanics are also present. Infill varies between gritty micaceous arkose, red, green, or grey siltstone, and calcareous sand or mud. Some areas of the basal limestone unit are recrystallized and stylolitized, and appear massive and grey in drillcore. A conformable, gradational contact with overlying siltstone and/or arkose is common. The base of the limestone at the unconformity with the Forest Reefs Volcanics or the Cadia Intrusive Complex may be brecciated, with altered volcanic-derived clasts and unaltered siltstone clasts set in calcite-rich sedimentary matrix.

The basal limestone varies in thickness across the district, but is typically ~10m. At Cadia Quarry, it is up to 50m thick, and to the north, it locally exceeds vertical thicknesses of 100m; this may in part represent structural thickening, rather than depositional control. Only one surface outcrop of the basal limestone unit is present in Cadia East (686,432 E, 6,295,830 N). The basal limestone is absent from pit wall exposures at Cadia Hill, to the west of the Gibb fault and on Sharps Ridge. It thins and is absent from the section along the Cat fault in Cadia East, as well as other un-named faults recognized in the sedimentary cover sequence (see chapter 3).



**Figure 2.5:** Limestone and Calcirudite from the base of the Waugoola Group at Cadia East. A: clastic limestone outcrop in Copper Gully Creek. B: massive limestone from CE046. C: grey recrystallized clastic limestone with some stylolites. D: fine-grained clastic calcirudite. E: rounded pebble conglomerate with carbonate matrix near the base of the limestone. F: carbonate matrix conglomeratic limestone. G: coarse grained calcirudite.



## BOULDER CONGLOMERATE

Where the basal limestone is absent in the footwall of major basement faults, the basal unit of the Waugoola Group is a matrix-supported, polymict conglomerate (Figure 2.6). Pebble to boulder sized clasts include altered volcanic rock, intrusive rock, and massive magnetite-pyrite skarn, as well as minor local unaltered siltstone, arkose, and limestone. Unaltered sandstone clasts are uncommon. Most clasts are subangular and poorly sorted set in a grey, green or red siltstone and/or feldspathic fine-grained sandstone. Clasts at the base of the boulder conglomerate appear locally derived from the Forest Reefs Volcanics or Cadia Intrusive Complex. By contrast, unaltered clasts of other Waugoola Group rocks appear toward the top of the boulder conglomerate. Thickness of the basal conglomerate varies between ~20-120m, with the thickest sections adjacent to faults. Where observed, a conformable gradational contact exists between the boulder conglomerate and overlying siltstone packages.

## RED SILTSTONE

In the Cadia Hill open pit, a ~20m thick package of red siltstone is present. This unit is not laterally extensive, and is mostly restricted to a ~0.15 km<sup>2</sup> area near the intersection of the Copper Gully and Gibb faults (Figure 2.7). Isolated outliers of red siltstone also occur in Cadia East. Where this unit does not occur directly on the unconformity, it conformably overlies the boulder conglomerate. Red siltstones are massive to laminated with interbedded conglomeratic zones (with clasts of locally

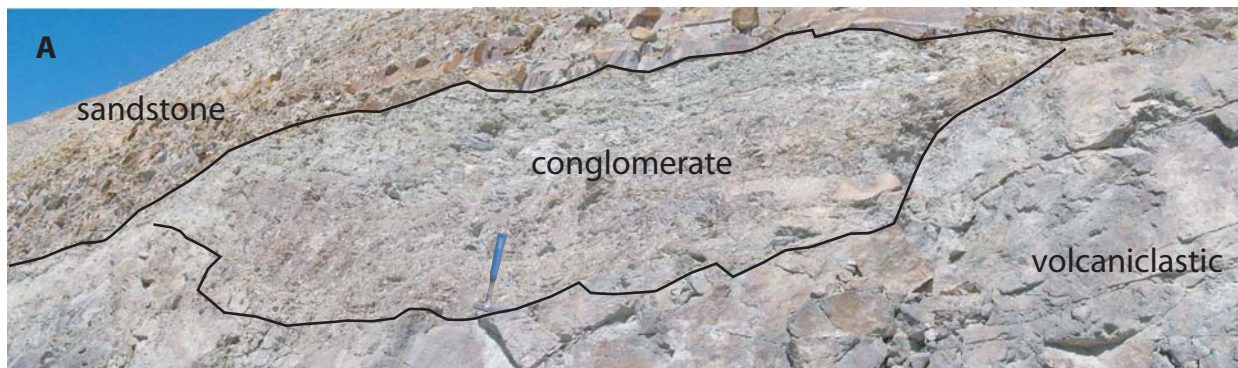


**Figure 2.6:** Boulder conglomerate at the base of the Waugoola Group. A: basal conglomerate in local lows along the unconformity from the southern wall of Cadia Hill pit. B: close-up of conglomerate from A. C: boulder conglomerate from the haul road near the southern wall of Cadia Hill pit with locally derived angular clasts of the Forest Reefs Volcanics. D: boulder conglomerate in Copper Gully Creek with locally derived skarn clasts. E: boulder conglomerate from Copper Gully Creek with clasts of Waugoola Group limestone, arkose, and siltstone. F: conglomerate from drillcore with hematite-rich matrix and locally derived volcanic clasts.



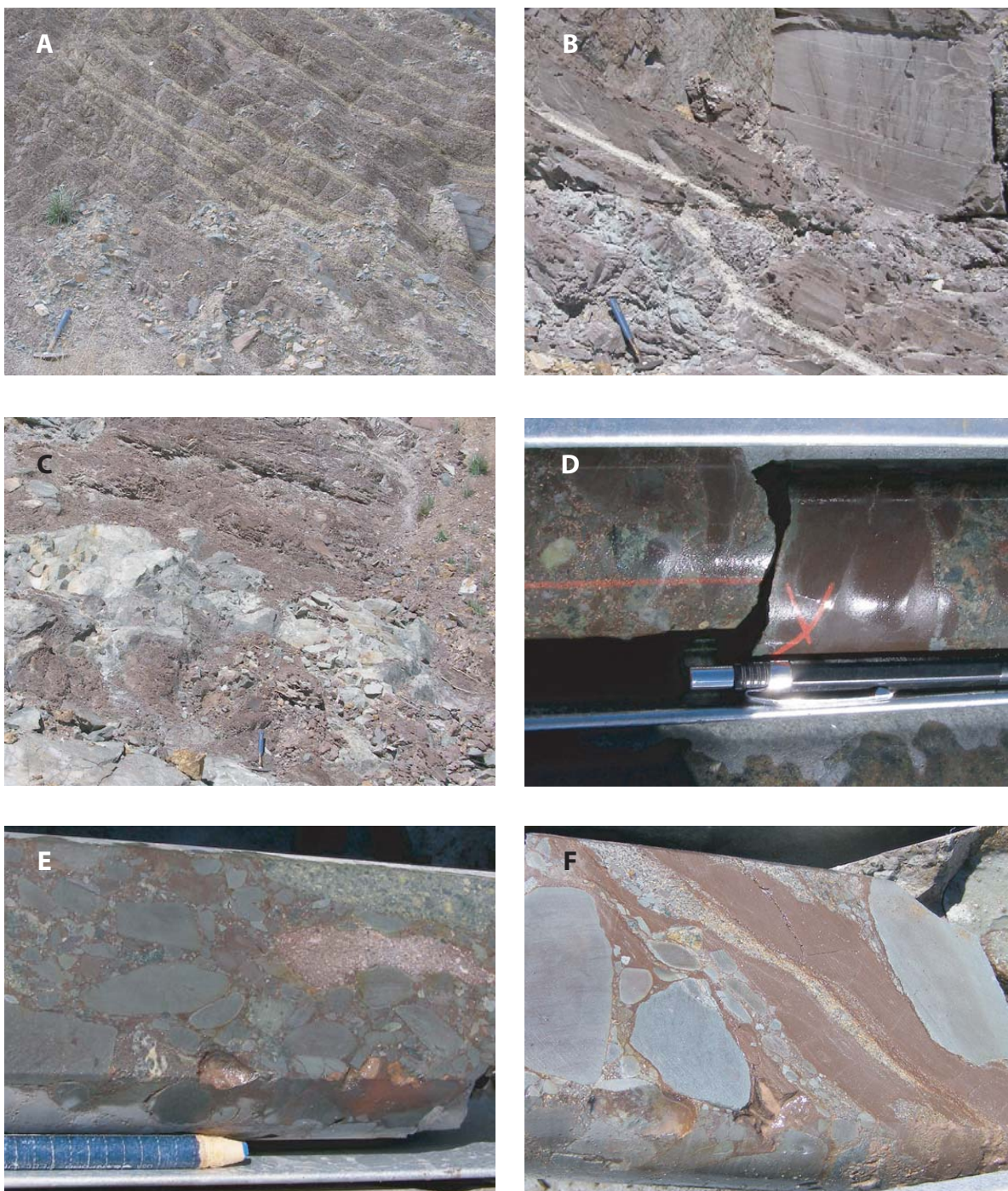


**Figure 2.7:** Photographs of hematite-rich siltstone redbeds. A: massive to laminated red siltstone from the southern wall of Cadia Hill pit. B: massive to laminated red siltstone with thin arkosic horizon. C: angular boulders of locally derived Forest Reefs Volcanics in red siltstone from the southern wall of the Cadia Hill pit. D: pebbles of Forest Reefs Volcanics in red siltstone and arkosic matrix. E and F: pebbles of hematite-poor siltstone in arkosic redbeds.

derived Forest Reefs Volcanics or unaltered Waugoola Group siltstone) and rarer arkosic beds. The upper contact with green or gray siltstone is poorly preserved, but appears gradational. The distinctive red color is more likely a result of deposition in oxidizing subaerial conditions rather than a product of hematitic hydrothermal alteration as this reddened appearance is spatially restricted to the more massive siltstones that are relatively impermeable. This unit is therefore a locally developed, intra-basinal redbed sequence. It is uncertain whether this unit is time correlative with the basal limestone seen elsewhere in the Cadia district.

### **Lower Siltstone-Dominant Succession**

The basal unit is conformably overlain by laminated to massive grey, green, or brown siltstone with rare fossiliferous, bioturbated, and calcareous horizons (Figure 2.8). Millimeter-scale ripple marks and rare trace fossils occur. Total thickness of siltstone package varies between ~50 and 200m (averaging 70m), and generally thickens towards the east. The siltstone package is locally absent (e.g., Sharps Ridge), inferred to be related to areas of higher elevation. Despite this, this siltstone package is laterally extensive and the most volumetrically significant unit in the Waugoola Group sedimentary cover.

Medium-to coarse-grained sandstone interbeds (0.1 to 0.3m, up to 3m thick) are abundant in the siltstone (Figure 2.9). Degree of consolidation varies between moderately well-indurated and poorly indurated gritty textures. Color varies between white, green, and tan. The mineralogy of these beds is dominantly feldspathic, with



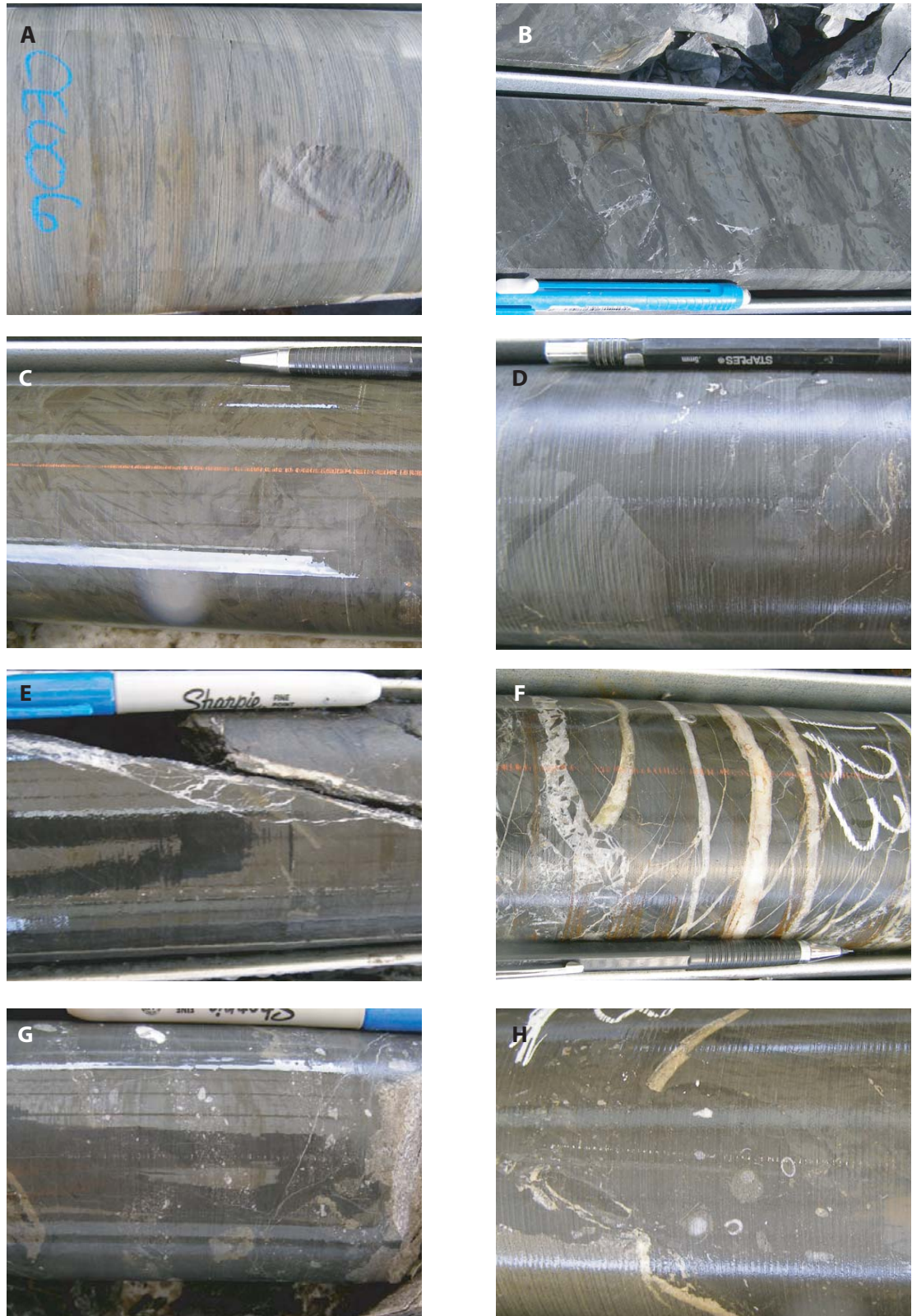


**Figure 2.8:** Photographs of Waugoola Group siltstone from drillcore. A: laminated siltstone with faint wispy flaser bedding. B: irregular flaser bedding in siltstone. C: clast supported breccia in flaser bedded siltstone with rotated angular clasts; flaser bedding is disrupted and chaotic. D: siltstone matrix supported breccia with angular clasts of flaser bedded siltstone. E: carbonate veins in massive black shale. F: dense carbonate veins in flaser bedded siltstone with minor angular siltstone clast breccia. G: fossiliferous zone in massive black shale marginal to arkose horizon. H: fossiliferous zone in massive muddy siltstone .



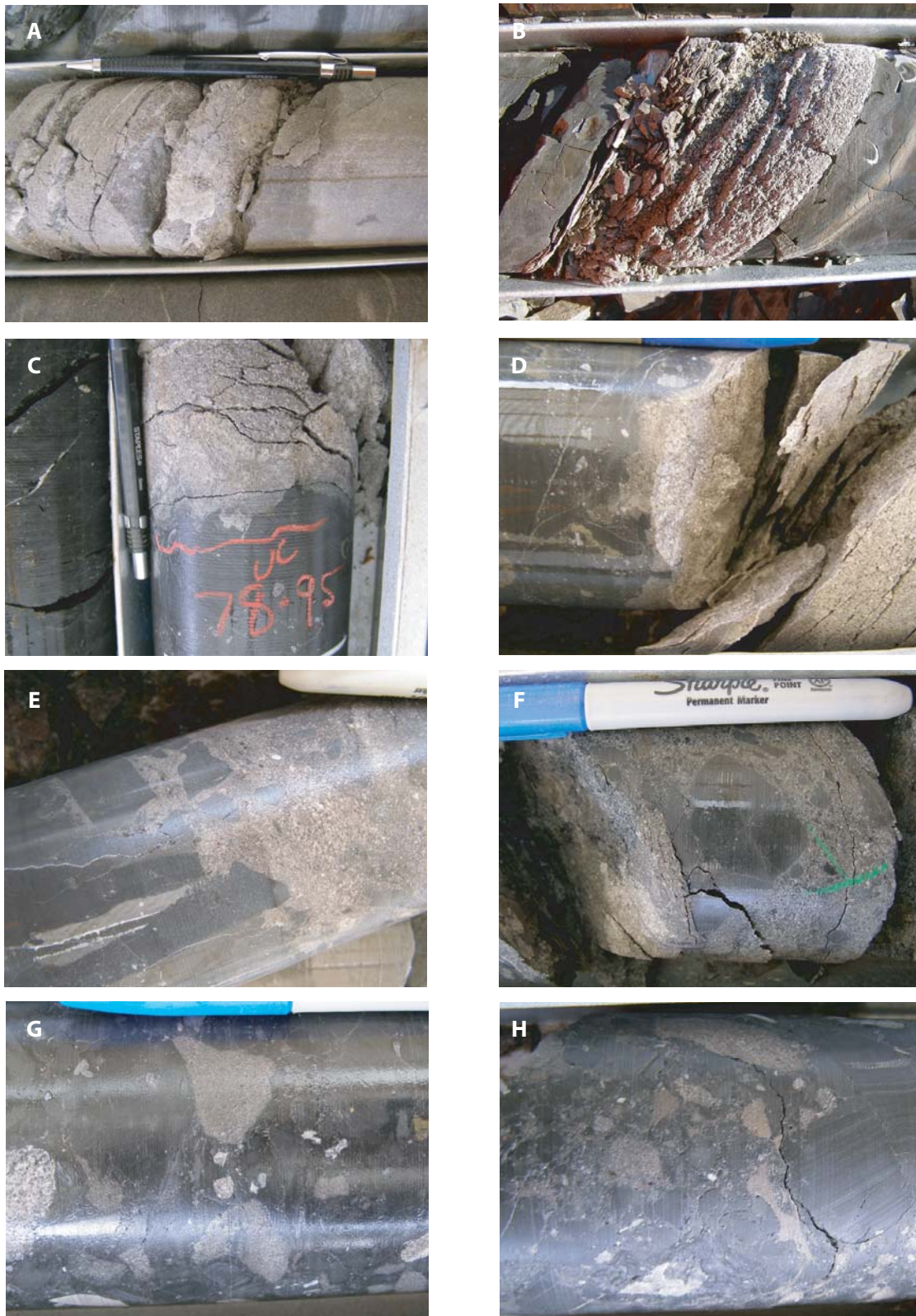


**Figure 2.9:** Coarse grained arkosic horizons in the siltstone package. A: thick arkose horizon with mica and carbonate. B: thin horizon of gritty micaceous arkose with bedding parallel fabric. C: irregular contact between arkose and enclosing siltstone. D: irregular contact between arkose and fossiliferous black shale. E: angular siltstone clasts incorporated at the margin of arkosic horizon. F: arkose matrix supported siltstone clast breccia. G: arkose clasts in siltstone pebble conglomerate. H: arkose clasts and matrix in siltstone pebble conglomerate.

minor lithic clasts and quartz. Many of these coarse arkosic beds contain abundant mica, with some being more carbonate rich. Irregular and wispy contacts with the enclosing siltstone are also present, indicative of soft-sediment deformation. Rip-ups of angular siltstone clasts also occur.

Flaser bedding, defined by fine wisps of carbonaceous mud, is common in the grey and green siltstone, and may display regular or extremely chaotic bedding orientations. Where flaser bedding is most disrupted, clast supported breccias of siltstone are present. Angular clasts of flaser bedded siltstone are also present in the boulder conglomerate and locally developed conglomeratic zones in the siltstone package. Flaser bedding is associated with deposition in a distal fan environment, where changes in current are frequent.

Black shale associated with calcareous and fossiliferous material is also present locally in the lower siltstone-dominant succession. This unit does not appear to be laterally extensive and does not exceed 20m in bed thickness. Local conglomeratic interbeds contain sub-rounded, pebble sized clasts of siltstone and arkose in a siltstone matrix.

### **Upper Sandstone-Dominant Succession**

At Cadia, interbedded and graded sandstone and siltstone (the upper sandstone-dominated succession) conformably overlies the siltstone-dominant lower portion of the Waugoola Group (Figure 2.10). The proportion of siltstone to sandstone varies continuously between siltstone-dominated (up to 90 % siltstone) and sandstone-





**Figure 2.10:** Sandstone-dominant upper stratigraphic units of the Waugoola Group in the Cadia District, including interbedded siltstone and sandstone and massive to thick-bedded quartz sandstone. A: siltstone-dominant turbidites from the high wall in Cadia Hill pit (Sharps Ridge). B: interbedded siltstone and sandstone of roughly equal proportions, from the southern wall of the Cadia Hill pit. C: drillcore from sandstone-dominant turbidite with bedding-parallel fabric in the siltstone bed; graded bedding is evident. D: graded bedding in sandstone-dominated turbidite. E: thick bedded to massive quartz sandstone from the southern wall of Cadia Hill pit. F: massive sandstone from drillcore.



dominated (up to 90% sandstone) horizons. Relative proportions of siltstone- and sandstone-dominated units vary over the district, as does stratigraphic position relative to each other. Thickness of individual graded beds commonly varies on the centimeter scale, although some beds may exceed 2 meters in the interbedded siltstone and sandstones. Total thickness of the upper sandstone-dominant succession is up to 40m.

The uppermost outcropping unit in the Waugoola Group consists of fine- to medium-grained massive to thick-bedded (1-4m) buff-colored or grey quartz sandstone. Thickness varies between 10 and 40m, but commonly occurs as 20m beds of massive to thick-bedded sandstone. True thickness of this unit is unknown due to erosion.

## **INTERPRETATIONS**

### **Paleogeography and Basin Evolution**

After magmatism ceased in the earliest Silurian, erosional unroofing of the mineralized intrusions of the Cadia Intrusive Complex and the altered enclosing Forrest Reefs Volcanics strata took place. Volcanic, intrusive, and skarn clasts in the basal conglomerate and at the base of the calc-rudite provide evidence of uplift and erosion of Ordovician basement rocks prior to deposition of Waugoola siltstones and sandstones. Some of the eroded material was deposited locally in areas of relatively low elevation as boulder conglomerate.

The boulder conglomerate at the base of the sedimentary cover sequence appears spatially related to major faults that penetrate the Ordovician basement. Thick debris

flows such as these are present on either side of Sharps Ridge, between the Powerline fault and the Copper Gully fault, and also in the footwall of the Gibb fault (Figure 2.11). The boulder conglomerate contains locally sourced clasts and was deposited in a high energy environment, which reflects local topography prior to and during earliest Waugoola Group deposition. Because the conglomerate is localized along faults, it was probably deposited in local lows associated with fault scarps, such as half-graben basins that formed during rifting. Clasts of Waugoola Group rocks in upper portions of the boulder conglomerate fault scarp deposits indicate syn-depositional faulting was important in maintaining topography.

Redbeds were deposited in a localized area at the intersection of the Gibb fault with the Copper Gully fault, and are exposed on the southern wall of Cadia Hill pit (Figure 2.12). Redbeds provide evidence that part of the district underwent subaerial sedimentation during the early stages of rifting and associated Waugoola Group deposition in the Cadia District. As subsidence continued, ephemeral lakes in which redbeds were deposited dropped below sea level, and deposition of oxidized sediments gave way to deposition of fine-grained marine sedimentary rocks. However, it is uncertain if submarine deposition of other basal units, i.e. the limestone, was taking place elsewhere in the district at this time, or if continued subsidence following redbed deposition produced the depocenter for carbonate sediments.

Continued subsidence led to deposition of carbonate sediments in relative basinal lows. Clasts of limestone in the boulder conglomerate provide evidence for the persistence of significant local topography and continued conglomerate deposition during carbonate sedimentation. Concomitant with conglomerate deposition, carbonate detritus,

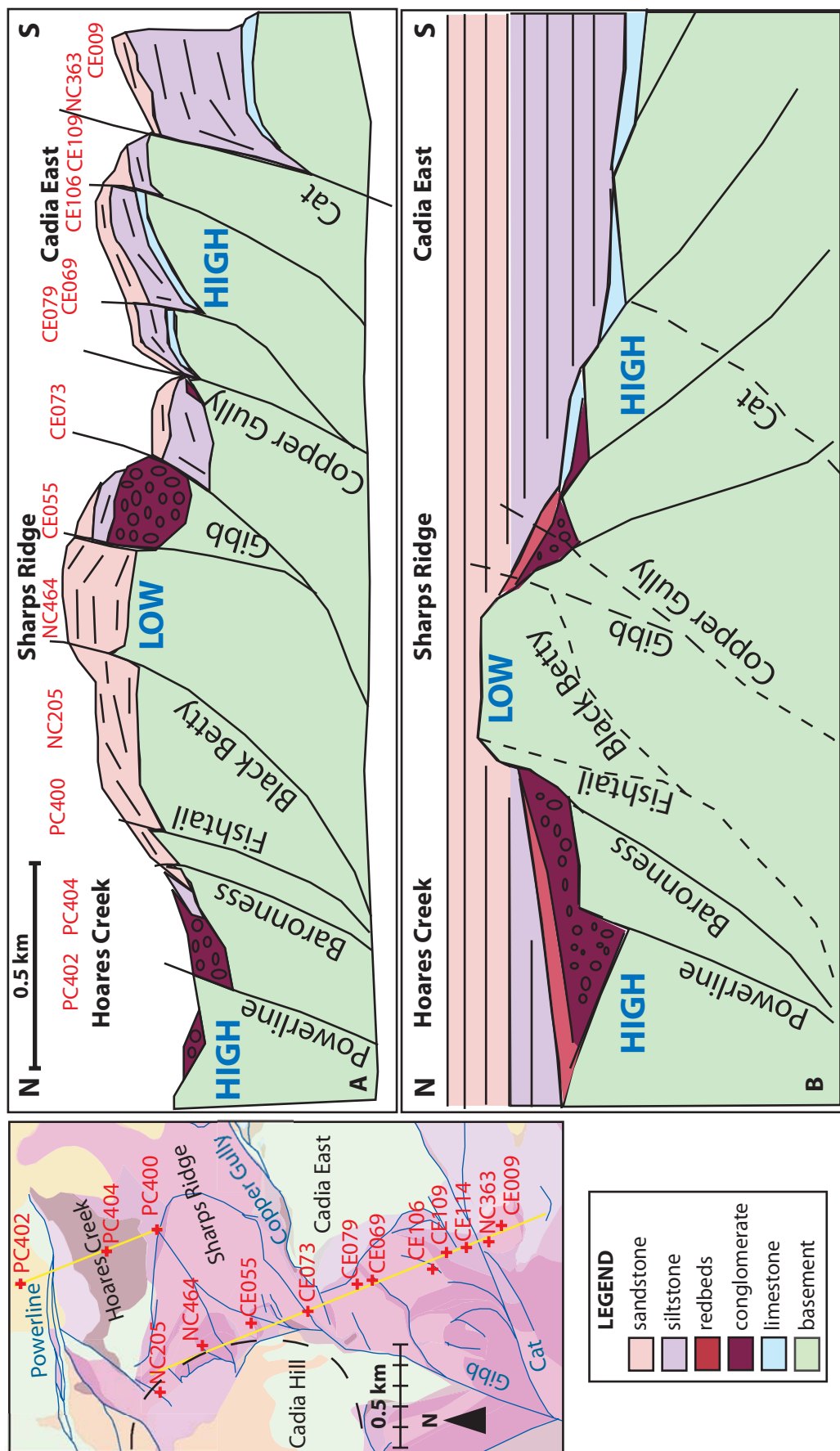


**Figure 2.11:** Interpretive sections showing stratigraphic variations in the Waugoola Group across Sharps Ridge and Cadia East. Blue "high" and "low" indicate relative stratigraphic position of the Forest Reefs Volcanics preserved at the unconformity. A: cross section constrained by drillcore and surface mapping shows variations in the basal unit. Reference map below shows section line in yellow and drillcore collar locations in red; see appendix 3. B: interpretation of Sharps Ridge depositional environment during Waugoola Group deposition. Variations in basal lithology reflect local fault-related topography. Dashed lines represent present-day fault configuration, and are provided for reference. These faults were not necessarily active at this stage.



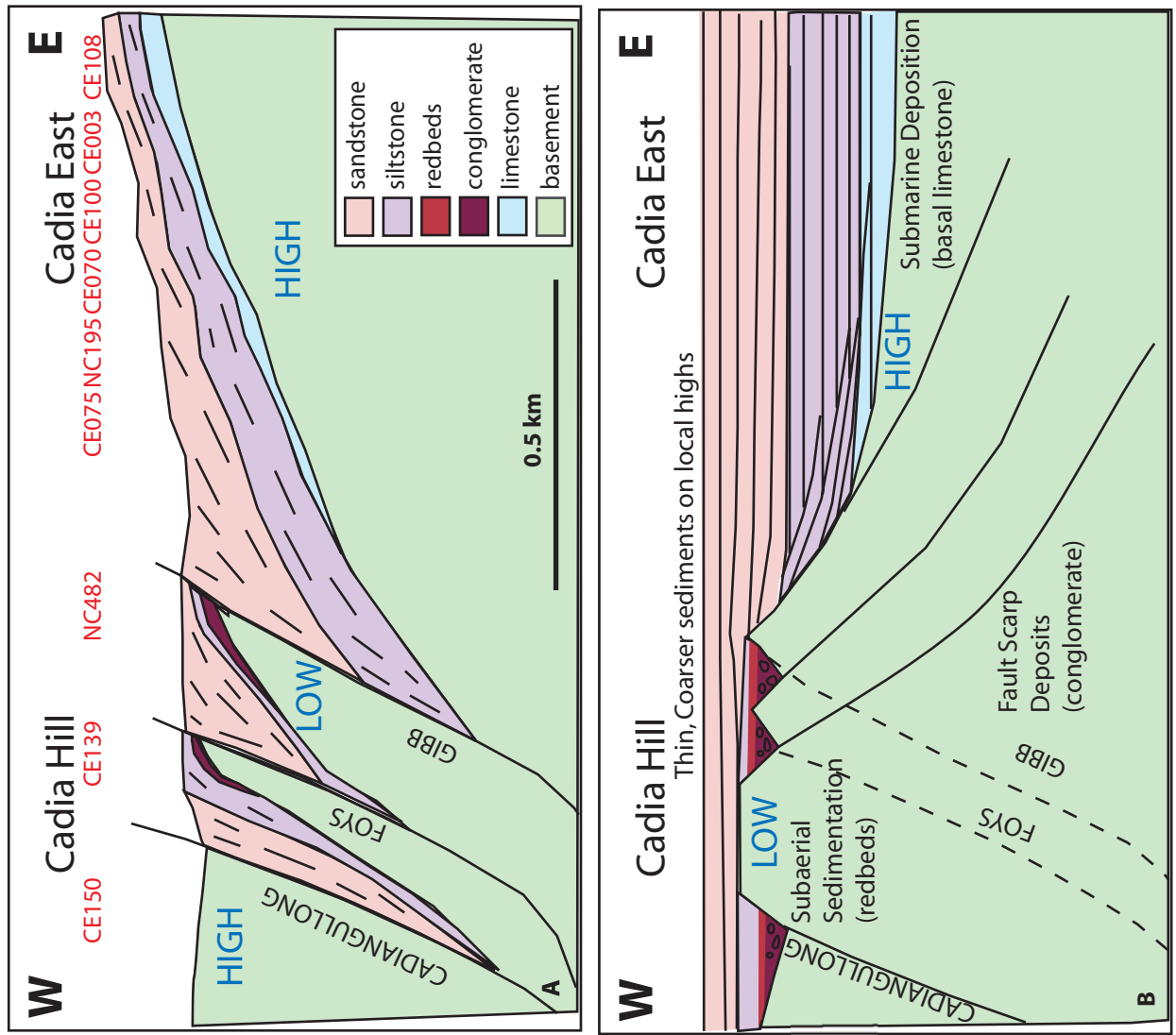
**Figure 2.12:** Observed geology and interpreted depositional environment from the southern wall of Cadia Hill pit. A: Panoramic photograph of the Waugoola Group sedimentary cover sequence with stratigraphy superimposed. B: Interpretive reconstruction of undeformed sequence. Locally derived angular clasts were shed off of fault scarps into local half-graben basins. Redbeds were deposited in ephemeral lakes localized by faults. As subsidence continued, sediments filled in topography and eventually covered local highs. Subsequent shortening tilted and faulted the entire package.

including fragments of corals, began shedding into developing basins. Laterally continuous limestone horizons at the base of the Waugoola Group imply a dominantly submarine depositional setting (Figure 2.13). The absence of limestone north of the Copper Gully fault on Sharps Ridge and west of the Gibb Fault may suggest that these areas were relative topographic highs and Cadia East was an area of relatively low relief. Additionally, thinning of limestone approaching the Cat fault and other faults in Cadia East may reflect that these faults controlled basin geometry. The basal limestone in the Cadia District probably does not represent *in-situ* reefs, but transported carbonate material derived from reefs that formed on regionally significant palaeo-highs. The fragmental nature, lateral continuity and fairly constant thickness of basal limestone supports this interpretation.

The siltstone package was deposited in a low energy marine environment. Local highs in the Cadia District persisted during this stage, as evidenced by the lack of significant siltstone on Sharps Ridge. The geometry and mineralogy of arkose horizons suggests intermittent sediment input from an intermediate igneous source. Future palaeocurrent studies, detrital zircon dating, and thorough mineralogical analysis may clarify the provenance of these horizons.

As rates of sedimentation overtook rates of subsidence, filling of basins reduced local topography and a fine-grained marine succession was deposited. The interbedded siltstone and sandstone unit is interpreted as a turbidite package, which is commonly deposited at slope-breaks as a result of mass wasting. Thick- to- massive sandstone beds that compose the uppermost unit suggest abundant sediment supply and fast sedimentation rates. As active extension associated with rifting ceased, isostatic sagging

**Figure 2.13:** Cross-section and paleogeographic interpretation for Cadia Hill and Cadia East. Blue "high" and "low" indicates the relative stratigraphic level of the Forest Reefs Volcanics preserved at the unconformity. A: Stratigraphic cross section constrained by drillcore and surface mapping. Drillcore collars are shown on reference map below; see appendix 3. Limestone is present east of the Gibb fault, and the siltstone and sandstone packages are thick. West of the Gibb fault, the sandstone packages are thin, the siltstone and sandstone package is thin, and the basal unit is boulder conglomerate and red siltstone. B: Interpretation of depositional environment based on section A. Dashed lines represent present-day fault positions for reference; faults in this configuration are not necessarily present at this stage. Fault scarp deposits and subaerial sedimentation in ephemeral lakes west of the Gibb Fault. Continued subsidence drops the lakes below sea level. Limestone is deposited in a submarine basin to the east of the Gibb Fault, and continued basin-filling results in a thick siltstone and sandstone package.



of the rift basin resulted in widespread deposition of marine sedimentary rocks across the regional rift basin. At this stage, local topographic controls on sedimentary facies may have persisted, but were probably less important, as small, isolated basins were overwhelmed by finer-grained marine sedimentation.

The evolution of basins in the Cadia district as recorded in the Waugoola Group, preserves a transition from deposition of clastic and carbonate rift sediments to a fine-grained marine succession during the early late Silurian. Equivalent successions are regionally extensive across central New South Wales (being Siluro-Devonian in age). Where preserved, such successions are globally recognized as a rift-sag sequence (Figure 2.14). Rift-sag sequences are deposited when extension and subsidence driven by tectonic processes give way to the effects of thermal relaxation of the lithosphere following rifting (e.g. Blake and Stewart, 1992; O'Dea et al., 1997). When this occurs, isolated basins separated by topographic highs are filled in, and are overlain by regionally extensive transgressive marine successions (e.g. Betts and Lister, 2001). In the Cadia district, clastic sedimentation into locally developed, fault related basins is preserved in variations in the spatial distribution of basal units and represents the rift phase of the rift-sag sequence. As subsidence continues entering the sag phase, these isolated basins are overwhelmed by marine sedimentation, represented in the Cadia district by the siltstone and sandstone packages.

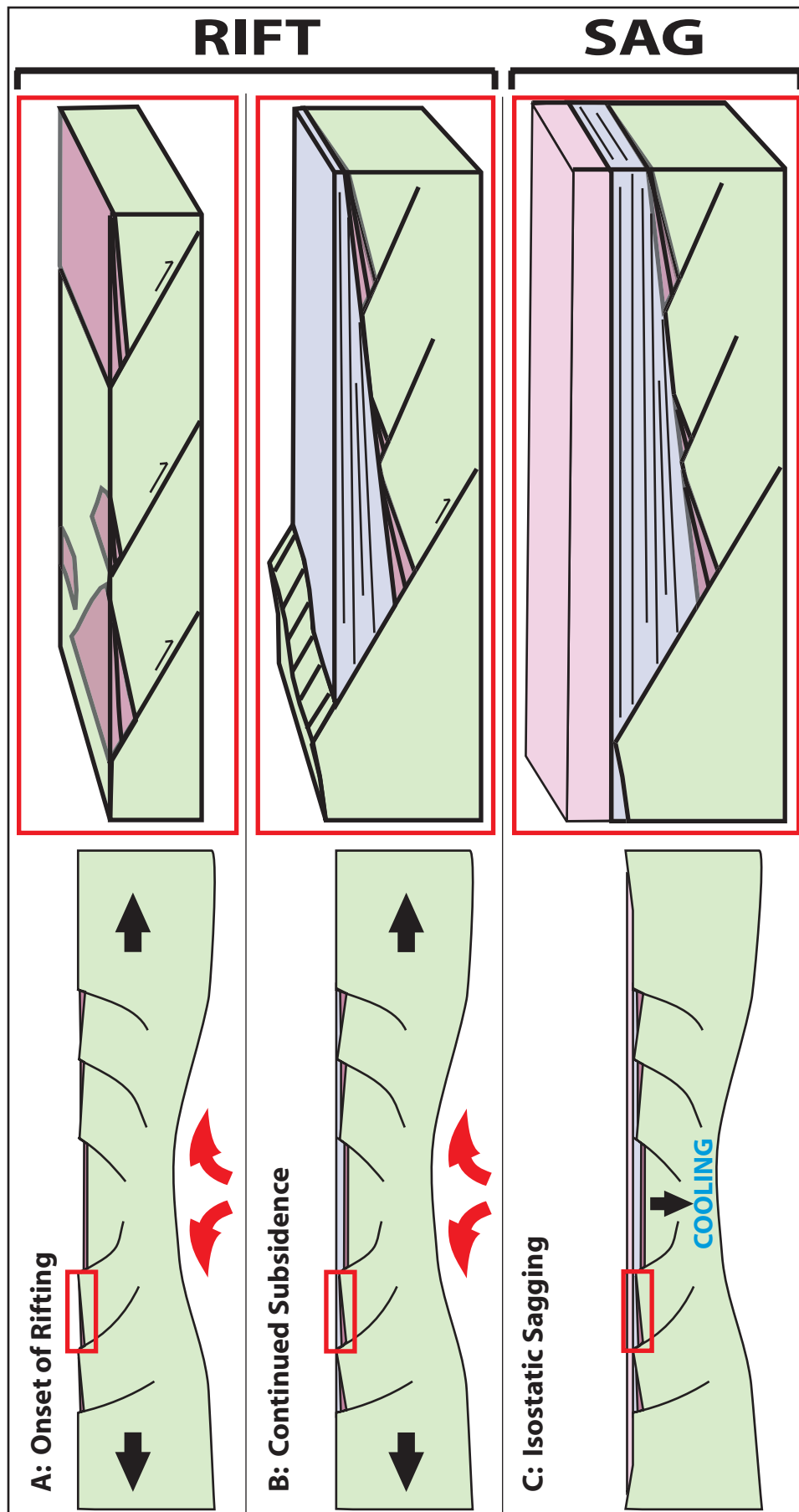


**Figure 2.14:** Generalized tectonic model for rift-sag sequence deposition. A rift sag sequence occurs when isolated half-graben basins form at the onset of rifting and are filled with locally derived clastic material (A). If rifting and basin subsidence continues, the basin grows outward and continues to fill, but the thickness of sedimentary rocks being deposited at this time is still influenced by half-graben geometry (B). Once active extension associated with rifting ceases, the extended crust begins to cool, and as it is loaded with sediments, it begins to isostatically sag (C). As the rate of sediment supply overwhelms the rate of extension, local topographic barriers are removed as basins fill with finer grained marine sediments. This process is reflected regionally and in the Cadia District by the Waugoola Group. Modified from Olsen, 1997 and Schlische et al., 2000.



## **Regional Correlations**

In general, the Waugoola Group is regionally interpreted as a transgressive marine sequence, beginning with shallow water carbonates and evolving to deeper water conditions (Jenkins, 1978; Pogson and Watkins, 1998). Lithic sandstone and conglomerate at the base of the Waugoola Group grade upward into the Cobblers Creek Limestone (Jenkins, 1978; Pogson and Watkins, 1998). The Cobblers Creek Limestone consists of coarse feldspathic and conglomeratic sandstone and cobble to boulder conglomerate with a gradational upper contact into thinly bedded calcirudite (containing rounded pebbles of corals in a calcareous matrix) and calcarenite containing fragments of corals, limestone clasts and rare volcanic detritus (Jenkins, 1978; Pogson and Watkins, 1998). This study lithologically correlates the Cobblers Creek Limestone with the basal limestone at Cadia East, in agreement with fossil ages reported in Rickards et al. (2001).

Regionally, carbonates of the Cobblers Creek Limestone are conformably overlain by siliceous siltstones and shales of the Glendalough Formation, which also contains minor coarse calcareous quartzofeldspathic sandstones (Burly Jacky Sandstone Member), black shales and dolomitic limestones (Ashleigh Member), and locally developed redbeds (Chaucer Red Bed Member) (Jenkins, 1978; Bischoff, 1986). Based on the refined stratigraphy presented in this study, the siltstone package in the Cadia district probably correlates regionally with the Glendalough Formation.

The Burly Jacky Sandstone Member recognized regionally consists of coarse grained calcareous quartzofeldspathic sandstones and varies in thickness from ~10 m to ~45 m (Jenkins, 1978; Pogson and Watkins, 1998). It locally contains volcanic clasts of

the Angullong formation and transported corals, as well as fossiliferous sandstone and limestone with brachiopods and corals (Jenkins, 1978; Pogson and Watkins, 1998).

Micaceous arkose horizons in the siltstone package described in this study appear to have similar lithological characteristics to the Burly Jacky Sandstone Member of the Glendalough Formation.

In other regional localities where the Waugoola Group is preserved, the Ashleigh Member overlies the Burly Jacky Member and consists of black shale containing abundant graptolites locally interfingered with silty dolomitic limestone and varies in thickness from 20-30m (Jenkins, 1978; Pogson and Watkins, 1998). Black shale and associated locally fossiliferous zones within the lower siltstone-dominant portions of the sedimentary cover sequence identified in drillcore from the Cadia district may correlate regionally with the Ashleigh Member of the Glendalough Formation.

The Chaucer Redbed Member is regionally described as massive to laminated red siltstone and red siltstone matrix conglomerate containing locally derived clasts (Jenkins, 1978). The redbeds are locally developed and thin relative to the enclosing Glendalough Formation siltstone package. In the Cadia District, locally developed redbeds and pebble conglomerates with red siltstone infill described in this study may be broadly correlative with the Chaucer Redbed Member. However, the Chaucer Redbed Member occurs relatively high in the regional Glendalough Formation stratigraphy, whereas in Cadia, it appears near the base of the Waugoola Group. This suggests that the redbeds and associated conglomerate at the base of the sedimentary cover rocks in the Cadia District may represent an older package

Interbedded siltstone and sandstone occurring above the siltstone-dominant lower portion of the stratigraphy were likely due to deposition from turbidite flows, and are unlike any part of the Waugoola Group stratigraphy described by Jenkins (1978). The relatively coarser grain size and irregular, interbedded nature of this unit suggest deposition in a proximal submarine fan environment. Of particular interest is the source of quartz-rich detritus that makes up the fine- to medium-grained sandstones at the uppermost portion of the stratigraphy. No quartz-rich rocks are locally present, so this material must have been sourced regionally and transported.

The correlation of the sedimentary cover sequence in the Cadia district regionally with the Waugoola Group indicates that rift-basin formation and sedimentation was widespread in the Late Silurian (regionally, known to extend into the Devonian). Basins filled with Waugoola Group sedimentary rocks were probably much more laterally extensive than their present-day configuration as isolated belts suggests.

Similarities between the sedimentary cover sequence in the Cadia district and more regional Waugoola Group are significant for two reasons: firstly, that early Waugoola Group sedimentation was controlled by local basin geometries that developed across the collapsing Macquarie Arc. Second, sedimentary detritus may have been in part sourced regionally and transported rather than derived entirely from local sources. This may explain the provenance of carbonates in the basal limestone as well as the micaceous arkose and the quartz-rich sedimentary rocks in the higher portions of the Waugoola Group stratigraphy in the Cadia District. This supports the rift-sag sequence interpretation for the Cadia district, and the cover rocks across the Macquarie Arc (coincide with development of the Molong High) on a regional scale.

## IMPLICATIONS

Changes in sedimentary processes and lithology in the Cadia District reflect the eastern migration of the active centre of Macquarie Arc magmatism during the Late Ordovician, and the transition to an extensional tectonic setting in the Silurian (Figure 2.15). These major cycles of deposition, punctuated by periods of uplift and erosion (notably during the Early Silurian and the Devonian) correspond to regional tectonic events and orogenesis.

Following mineralization, intrusions of the Cadia Intrusive Complex and the Forest Reefs Volcanics were uplifted and eroded to various levels across the Cadia district. This phase of uplift is preserved as a depositional hiatus between the Ordovician basement rocks and the Waugoola Group sedimentary cover sequence. Variable uplift and erosion is recorded by differences in the relative stratigraphic position of the Forest Reefs Volcanics subjacent to the unconformity.

Calcareous sandstone horizons in the upper portion of the Forest Reefs Volcanics host skarn deposits, and can be used as a marker horizon in district reconstructions (Harris, 2007a). Where the skarn-bearing horizon is preserved, as in Cadia East and Central Cadia, relatively high units in the FRV stratigraphy are subjacent to the Waugoola Group sedimentary cover sequence (Figure 2.16). In the footwall of Cadiangullong Fault, exposed in the south wall of the Cadia Hill open pit, and on Sharps Ridge, to the east, the skarn-bearing horizon was removed prior to Waugoola Group deposition, with relatively low stratigraphic units of the FRV at the unconformity.

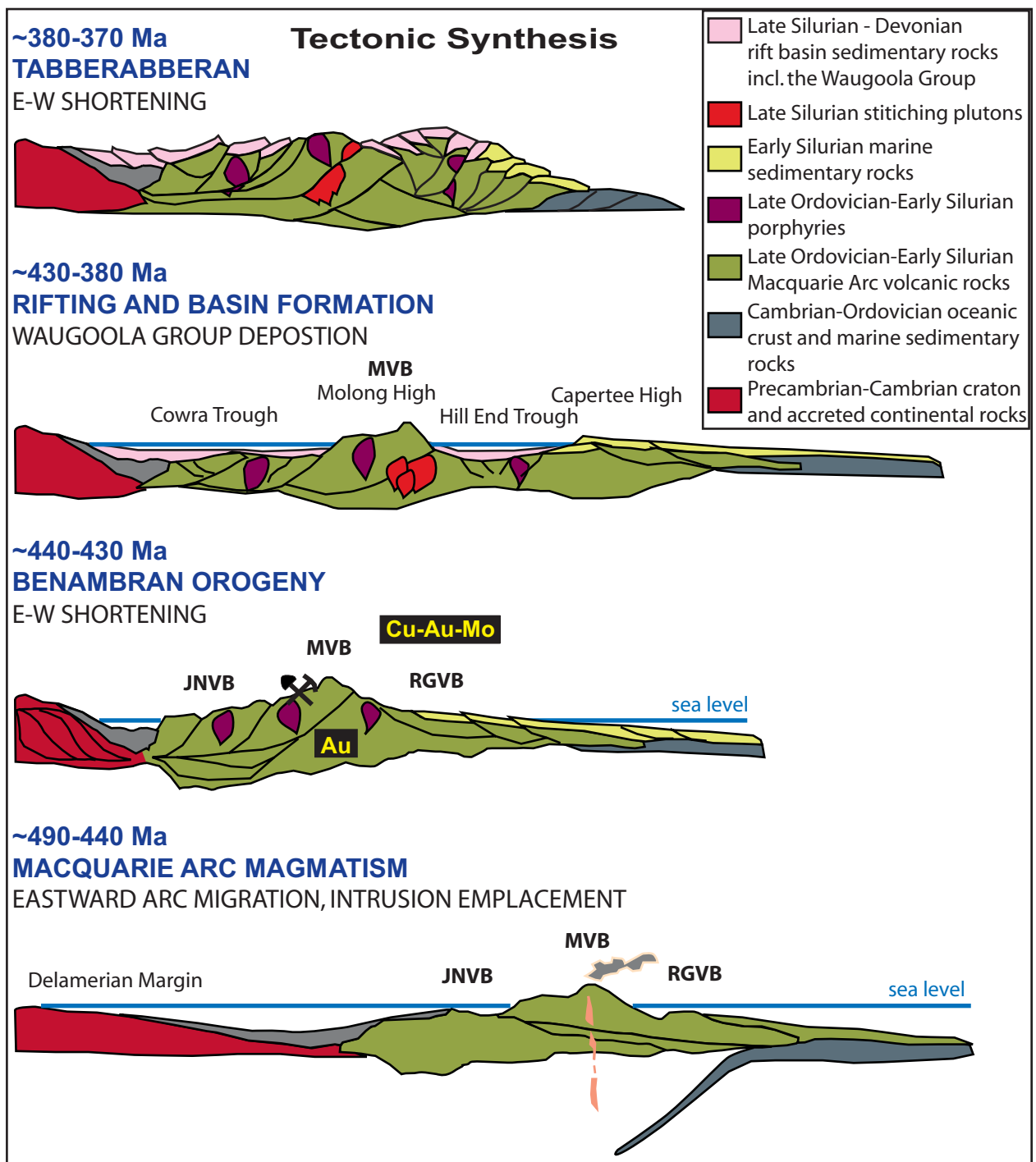


**Figure 2.15:** Regional tectonic controls on changing depositional environment in the Cadia District. JNVB=Junee-Narromine Volcanic Belt, MVB=Molong Volcanic Belt, RGVB=Rockley-Gulgong Volcanic Belt. The Weemalla Formation was deposited in the forearc as the volcanic center of the Macquarie Arc migrated eastward. The Forest Reefs Volcanics were deposited during formation of the Molong Volcanic Belt. The Ordovician basement rocks of the Cadia district were subsequently shortened during the Benambran Orogeny. A phase of rifting followed the Benambran Orogeny, and rift basins were filled with sedimentary packages such as the Waugoola Group. Early in rifting, local basin geometry controlled deposition. Thermal relaxation of the lithosphere resulted in basinal sagging, and local topographic barriers were overcome as basin filling progressed, and widespread transgressive marine sequences were deposited. This is known as a rift-sag sequence. During the Devonian, Tabberabberan Orogeny, the Waugoola Group was faulted and folded, as discussed in Chapter Three. Timing and regional vergence from Glen et al., 2007.

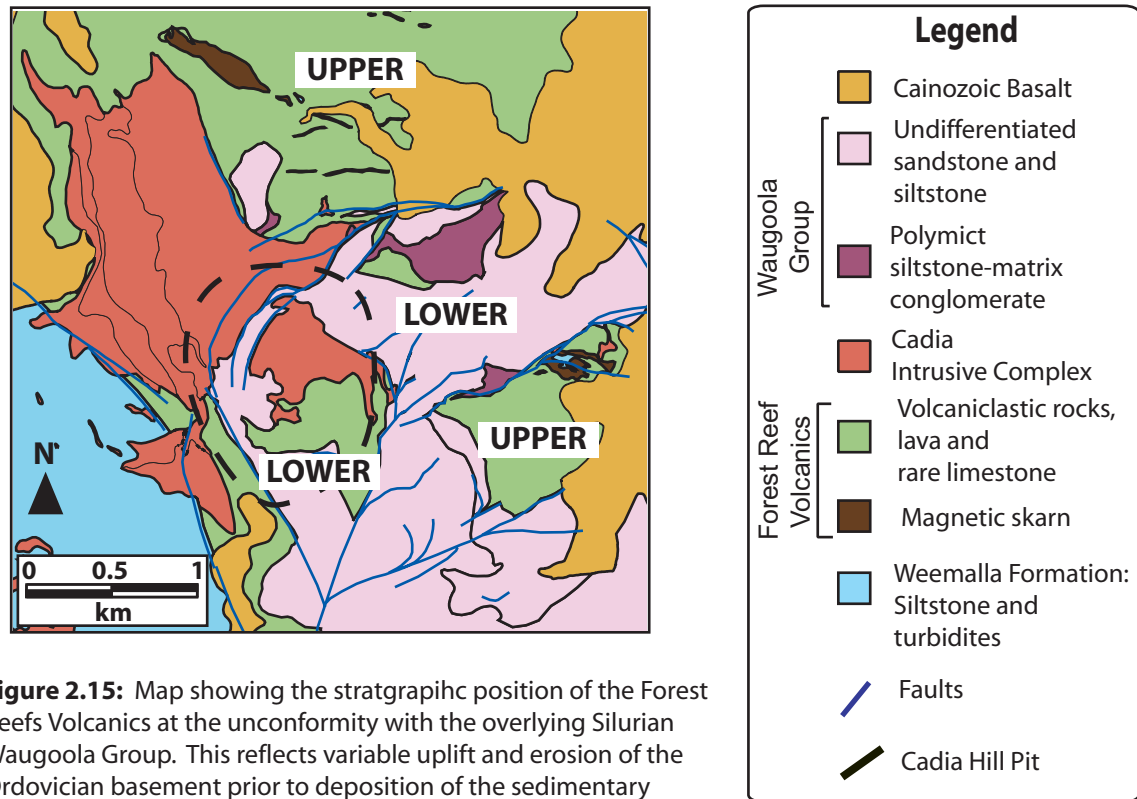


**Figure 2.15:** Map showing the stratigraphic position of the Forest Reefs Volcanics at the unconformity with the overlying Silurian Waugoola Group. This reflects variable uplift and erosion of the Ordovician basement prior to deposition of the sedimentary cover sequence.

Differences in the erosional level of the FRV suggest significant uplift and generation of topography in the early Silurian.

The Waugoola Group represents the drowning and dismemberment of the Macquarie Arc during rifting in the late Silurian. Variations in the basal unit across the district suggest that early in Waugoola Group deposition, local basin geometry was fault controlled, and significant topography influenced lithological distribution. This topography persisted into the later stages of Waugoola Group deposition, as evidenced by the absence of siltstone on Sharps Ridge. On Sharps Ridge relatively low levels of the Ordovician volcanic stratigraphy are preserved below the Silurian unconformity and only the upper portion of the Waugoola Group are preserved.

The Forest Reefs Volcanics at the unconformity in the hanging wall of the Gibb fault are also at a relatively low stratigraphic level. In the hanging wall of the Gibb fault, redbeds and boulder conglomerate at the base of the stratigraphy signify subaerial deposition in local fault-bounded basins. This facies relationship suggests that topographic highs formed during uplift and exhumation of the Cadia Intrusive Complex in the earliest Silurian persisted into the late Silurian. Finer-grained marine sedimentation followed initial rifting and clastic sedimentation was replaced by prograding wedges of regionally derived material as local basins were overwhelmed during continued subsidence related to basinal sagging.

Variable uplift of the Forest Reefs Volcanics following the Benambran Orogeny resulted in preservation of different stratigraphic levels at the unconformity across the district. It also produced long-lived topography that appears to be fault related. Furthermore observed variations in the basal unit of the Waugoola Group reflect

deposition into locally developed, fault controlled basins. Therefore, faults must have been present prior to Waugoola Group deposition in the Cadia District. Shortening during the Devonian Tabberabberan Orogeny inverted the basin bounding faults and disrupted the Waugoola Group stratigraphy in the Cadia District.



## **Chapter Three: Structural Relationships in the Cadia District**

### **INTRODUCTION**

In order to better guide future exploration and development activities in the Cadia district it is important to recognize the extent and magnitude of post-mineralization deformation. Major reverse faults of the Cadiangullong Fault system dismember the orebody at Cadia Hill and juxtapose different levels of the intrusive complex across the district. Furthermore, each deposit is preserved in a different fault block and a distinctive structural domain (Harris, 2007a). Understanding the role of post-mineral deformation is therefore critical to recognizing the dismemberment of mineralized zones and thereby refining the ore deposit model for the Cadia District.

The late Silurian Waugoola Group sedimentary cover sequence at Cadia is the key to understanding the structural effects of post-mineral deformation on the orebody. Magmatism associated with mineralization ceased during the earliest Silurian at the end of the Benambran Orogeny. Subsequent uplift and erosion removed approximately 2km of material, and brought the orebodies to the surface. Deposition of the Waugoola Group cover sequence in extensional basins during the Silurian was followed by regional shortening, which locally produced complex fold-and-thrust geometries. Due to the relative timing of Waugoola Group deposition, faults and folds preserved therein record only post-mineral deformation. The goal of this project is to document the deformation of the cover sequence in order to reconstruct the Cadia District, and to better understand

the role of post-Benambran deformation on the current distribution of ore-bearing lithologies.

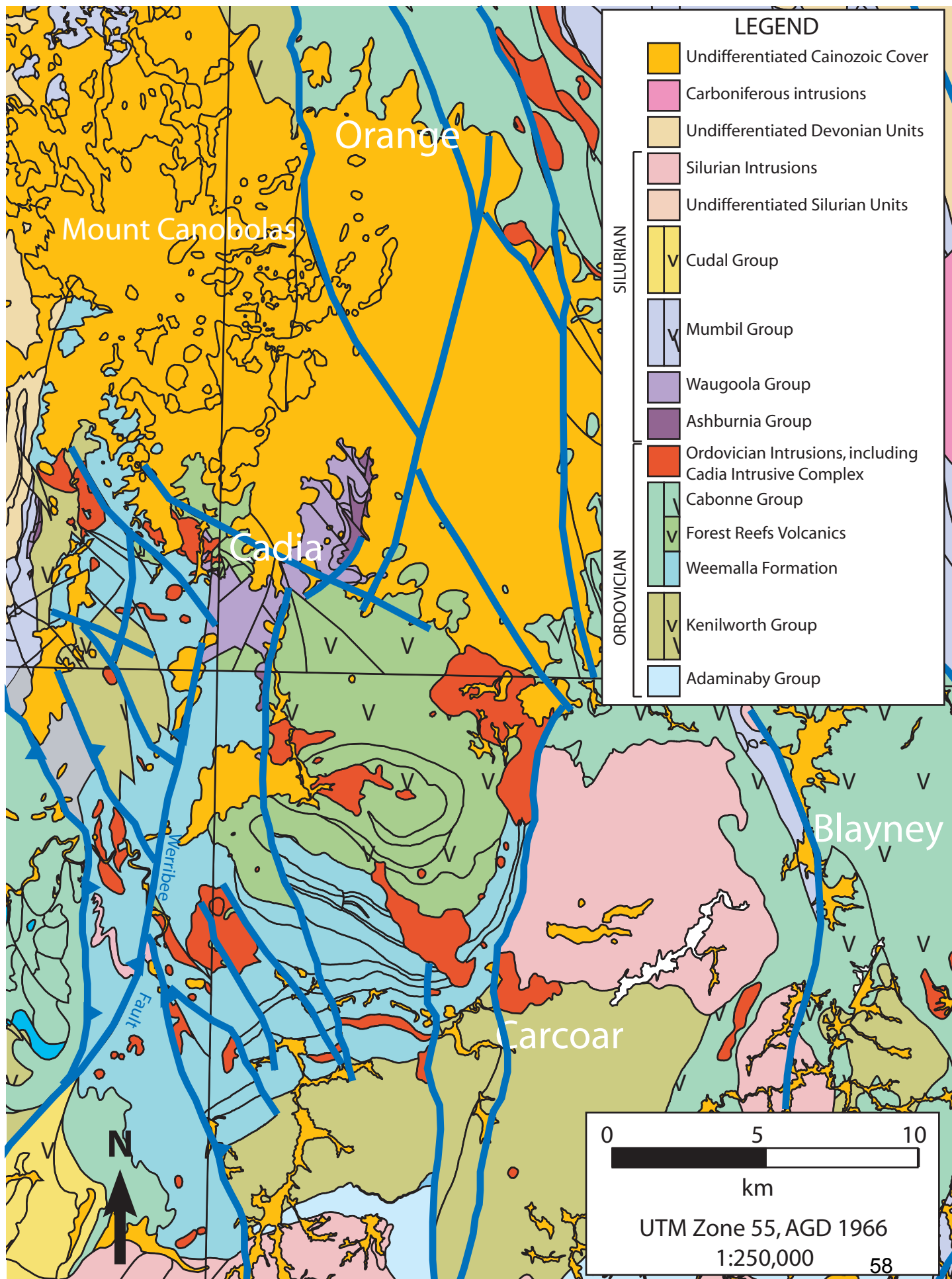
## **REGIONAL AND DISTRICT-SCALE STRUCTURE**

### **Regional Structure**

The dominant regional structural fabric in the Cadia District and surrounding areas is exemplified by north trending reverse faults and related splays, such as the Wyangalla-Werribee Fault System (Figure 3.1). These reverse faults are moderately west-dipping, curvilinear, and may have a strike slip component (Glen, 1998; Pogson and Watkins, 1998). The Werribee Fault extends into the Cadia District, where it is locally mapped as the Cadiangullong Fault system, and superposes Ordovician volcanic rocks and turbiditic sandstone and siltstone on the west against Silurian sedimentary rocks to the east (Pogson and Watkins, 1998). Overall, the Werribee-Cadiangullong fault extends for 30 km to the south (Wilson, 2003).

A second set of regionally important faults are NW-striking, and are typically cross-cut by and more weakly developed than the N-striking set, which suggests an older age of formation (Wilson, 2003). These structures are similarly oriented with the WNW-striking Lachlan Transverse Zone, a deep crustal lineament which is inferred to have localized mineralizing intrusions on a regional scale (Glen and Walshe, 1999; Finlayson et al., 2002; Wilson, 2003). The Cadia District occurs at the regional intersection of the

**Figure 3.1:** Regional map, modified from Bathurst 1:250,000 map by Pogon and Watkins, 1998. Faults shown in blue.

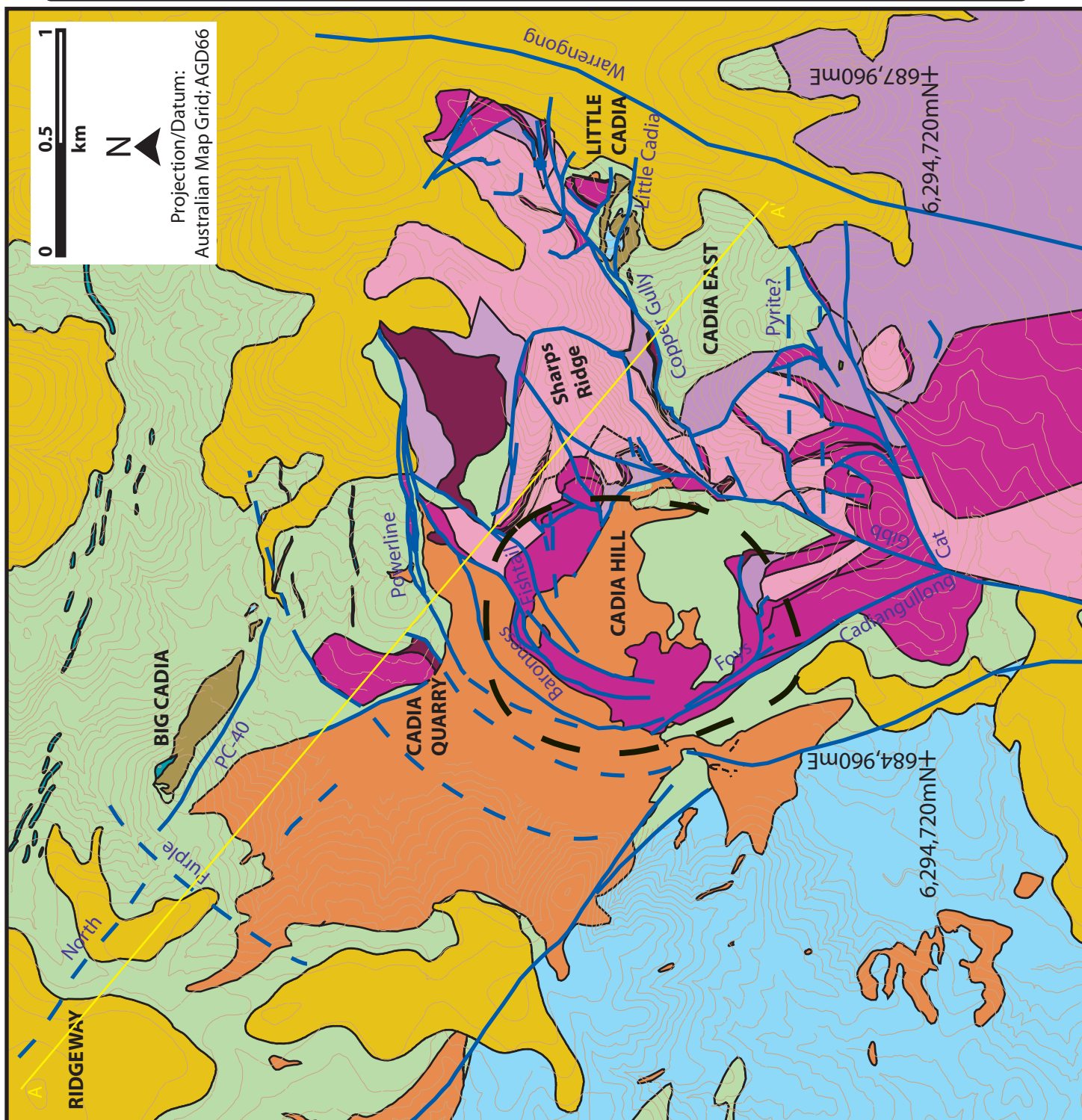


north-northeast striking reverse faults and the west-northwest striking Lachlan Transverse Zone.

### **District-Scale Structural Trends**

Structures in the Cadia District can be generally subdivided into three major sets based on orientation: (1) N-striking, W-dipping reverse faults and associated folds and fault splays, (2) NE- striking, NW-dipping faults and associated folds that are locally developed at the district scale, and (3) WNW striking, steeply N-dipping oblique- reverse faults (Figure 3.2, Table 3.1, Figure 3.3). Newcrest Mining Ltd. has recognized these faults in the Ordovician basement rocks based on drillcore intersections, but until this study, the interaction of these faults with the sedimentary cover rocks was incompletely understood. N-striking faults include the Cadiangullong Fault System (part of the regional Wyangala-Werribee Fault System), and the Gibb fault, which bound the Cadia Hill deposit (Figure 3.4). NE-striking faults in the Cadia District include the Copper Gully Fault System, the Cat Fault, and the Powerline Fault (Figure 3.2). Across the district, N- and NE- striking faults generally steepen to the W and NW respectively. The Little Cadia Fault and the PC40 Fault belong to the WNW striking group, and are related to skarn mineralization near Cadia East and Ridgeway, respectively. The Pyrite Faults at Cadia East are also west-striking (and do not outcrop). None of the W-striking faults are expressed in the Silurian Waugoola Group sedimentary cover sequence, although N- and NE- striking faults disrupt both basement and cover rocks.

**Figure 3.2:** Generalized geology map of the Cadia District. Geology of the Waugoola Group shown in shades of pink and purple. Faults shown in blue. Basement units mapped by Newcrest Mining, Ltd. Section line (A-A') for figure 3.3 shown in yellow.



<b>FAULT</b>	<b>STRIKE</b>	<b>DIP</b>	<b>MIN. VERT. DISP.</b>	<b>LOCATION</b>
Powerline Fault	NE	steep -> N	600m	N of Sharps Ridge
Cadiangollung Fault	N	steep -> W	300m	W of Cadia Hill
Gibb Fault	N	moderate -> W	300m	E of Cadia Hill
Cat Fault	NE	moderate -> N	200m	Cadia East
Copper Gully Fault	NE	steep -> N	20m	S of Sharps Ridge

**Table 3.1:** Orientation and displacement on major basement thrusts in the Cadia District. Minimum vertical displacement is estimated from offset of the unconformity. Orientation and displacement documented by Newcrest Mining Ltd. and in Harris, 2007a.



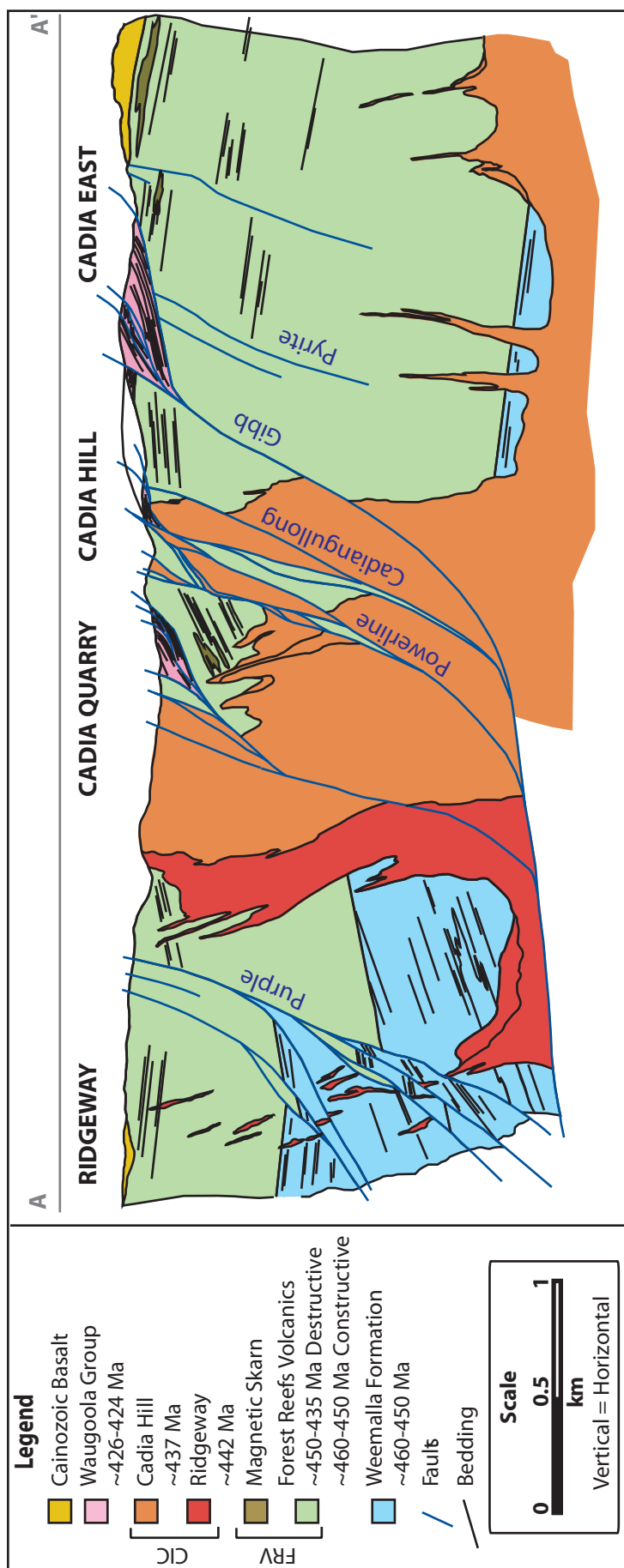


**Figure 3.3:** Long NW-SE section across the Cadia District. Section line shown in yellow on Figure 3.2. Skarn-bearing and bedded units in the Forest Reefs Volcanics (FRV) represent the upper, destructive facies of the stratigraphy. Lower portions of the Forest Reefs Volcanics are more massive, and represent the constructive facies. The Cadia Intrusive Complex (CIC) has been separated into 2 phases at Ridgeway and Cadia Hill based on different ages of emplacement (Wilson et al., 2007b). Ages that appear in the legend are from Packham et al., 1999; Rickards et al., 2002; Holliday et al., 2002; Wilson et al., 2007, and Harris, 2007. Figure after Harris, 2007.

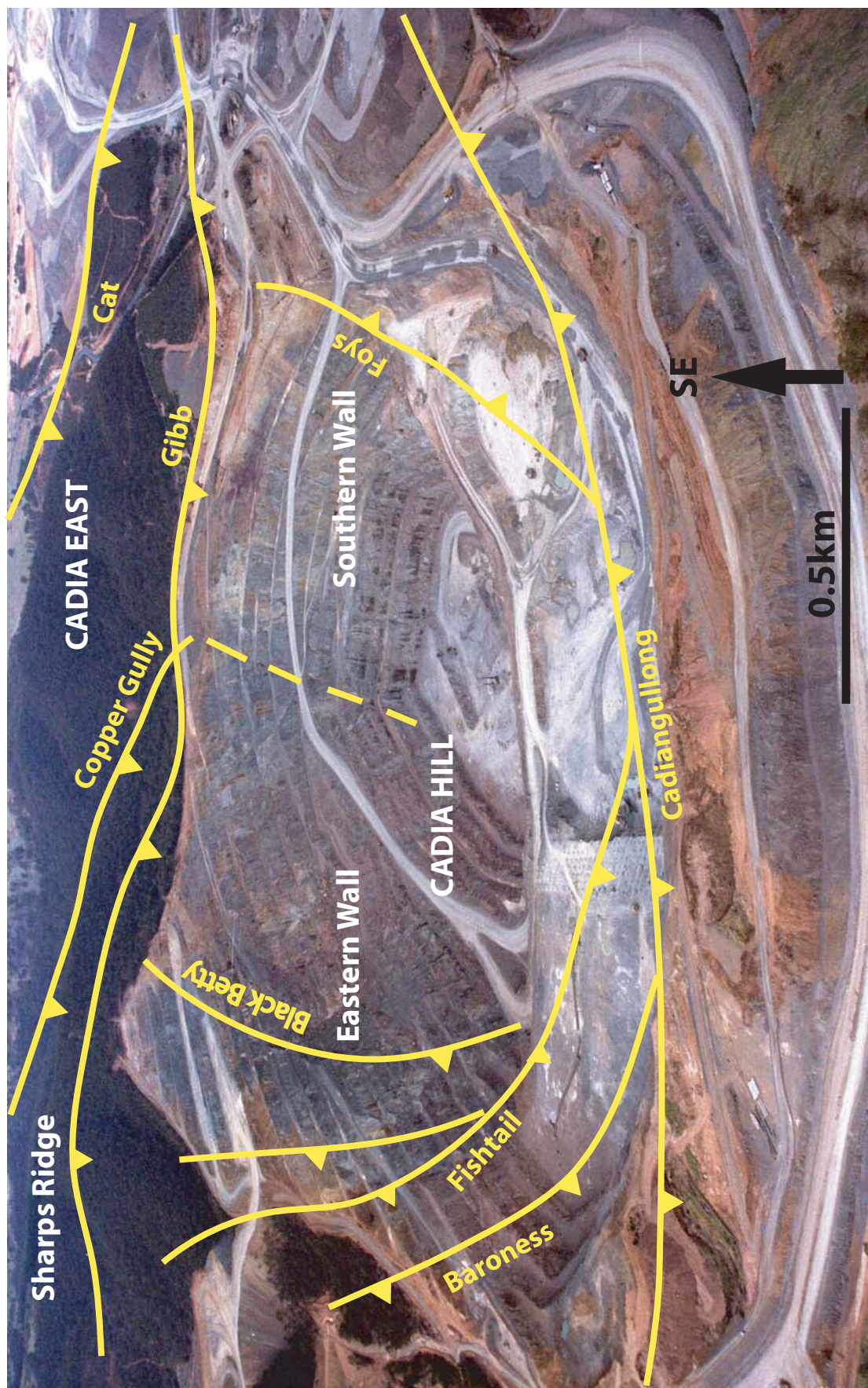


**Figure 3.4:** Annotated aerial photograph of Cadia Hill open pit looking southeast toward Sharps Ridge and Cadia East. Major reverse faults mapped in the Ordovician basement by Newcrest Mining Ltd. are shown in yellow. Southern and eastern walls of Cadia Hill pit (figures 3.8 and 3.10, respectively) are marked for reference.

## N- STRIKING FAULTS

The Cadiangullong Fault is a system of anastomosing, curvilinear, moderate-to-steeply west-dipping reverse faults with an estimated minimum vertical offset of 300m, based on offset of the unconformity at the base of the Waugoola Group sedimentary cover (Figure 3.3). It superposes rocks of the Late Ordovician Cadia Intrusive Complex to the west against the Silurian sedimentary cover sequence to the east. It is exposed in the northwest wall of the Cadia Hill pit, where it appears as a 1m-10m wide zone of black cataclasite gouge and intensely fractured wallrocks. In the Cadia District, the Cadiangullong Fault extends from the south, where it connects with the regional Werribee Fault. To the north, it curves around the Cadia Hill deposit and merges with the NE-striking Powerline fault. Whether the Cadiangullong Fault system continues to the north is uncertain, due to thick Mesozoic cover. Splays off the Cadiangullong Fault include the Foys fault and the Baronness-Fishtail faults.

The Foys fault is a SE-striking, steeply W-dipping thrust splay off the Cadiangullong fault system. In the South wall of the Cadia Hill pit, the fault is a 20m wide zone of intensely fractured siltstone-dominant Waugoola Group sedimentary rock. Silurian siltstone occurs in the footwall of the Foys fault at depths up to 300m. In the Waugoola Group cover, the Foys fault superposes siltstone from the lower portion of the stratigraphy over interbedded siltstones and sandstones of the upper sandstone-dominant portion of the stratigraphy. The Fishtail/Baronness faults are NE-striking splays off the Cadiangullong system. In the northeast corner of the Cadia Hill open pit, the faults are steeply dipping and fold the massive sandstone of the Waugoola Group. These faults link

the Cadiangullong fault system with the Powerline fault, and are also filled with black cataclasite gouge.

The Gibb Fault is another N- striking, moderate-to-steeply west-dipping reverse fault with west-over-east vertical displacement of ~300m (Figure 3.3). It occurs to the east of the Cadia Hill open pit, and has been intersected in the Cadia East Decline, where it superposes high-level destructive facies of the Forest Reefs Volcanics over the Silurian Waugoola Group. In the Silurian Waugoola cover, the Gibb Fault is manifest as a 0.5m-2m wide zone of milled rock-matrix breccia and clay gouge. Folds parallel to the fault are present in the surrounding area.

#### NE- STRIKING FAULTS

The Powerline fault lies north of and is roughly parallel to Sharps Ridge. It consists of a complex system of northwest-dipping faults, and appears to be a splay off the N-striking Gibb Fault. Faults of the Powerline system separate the Cadia Hill deposit from the Cadia Quarry deposit. Slivers of intrusive, volcanic, and sedimentary cover rocks are bounded by the faults. The displacement on individual faults is unknown, but overall offset of internal intrusive contacts suggests a net vertical displacement of ~600m across major NE-striking faults in Central Cadia (Figure 3.3; Harris, 2007a).

The Copper Gully fault is exposed in the southeast corner of the Cadia Hill Pit. It is planar and narrow, and has a reddish clay gouge. The Copper Gully fault bounds Sharps Ridge on the south. Powerline and Copper Gully faults appear to have been important during post-mineral uplift and erosion of the Cadia Intrusive Suite and the

enclosing Forest Reefs Volcanics, and also to have been important in controlling distribution of Waugoola Group sedimentary facies during late Silurian deposition (see chapter 2).

The Cat Fault is a major NE-striking fault in Cadia East. This study has also identified a significant parallel structure to the Cat fault ~500m to the north in the Waugoola Cover. Juxtaposition of sedimentary lithologies, changes in bedding contours, and folding in the sedimentary cover sequence at the surface are attributed to proximity to these faults.

## **STRUCTURES IN THE SILURIAN WUAGOOOLA GROUP**

Shortening in the late Ordovician-early Silurian basement rocks of the Cadia District was accommodated along a few moderate-to-steeply dipping major faults, including those of the N-striking Cadiangullong and Gibb fault systems, and the NE-striking Powerline, Copper Gully, and Cat faults (Figure 3.5). These faults were identified by Newcrest Mining Ltd. using drillcore. Basement fault blocks are mostly composed of massive volcanoclastic and intrusive rocks, which preserve little evidence for deformation (i.e. folds) outside of discrete fault zones. Therefore, basement fault blocks probably behaved as relatively rigid blocks during shortening. This is consistent with the behavior of fault blocks in thick-skinned thrust belts (e.g. Chambers et al., 2004; Molinaro et al., 2005; Grey et al., 2006; Mouthereau and Lacombe, 2006; and references therein). In the sedimentary cover rocks of the Waugoola Group, shortening was accommodated by a variety of structures, including faults, folds, and low-angle slip along



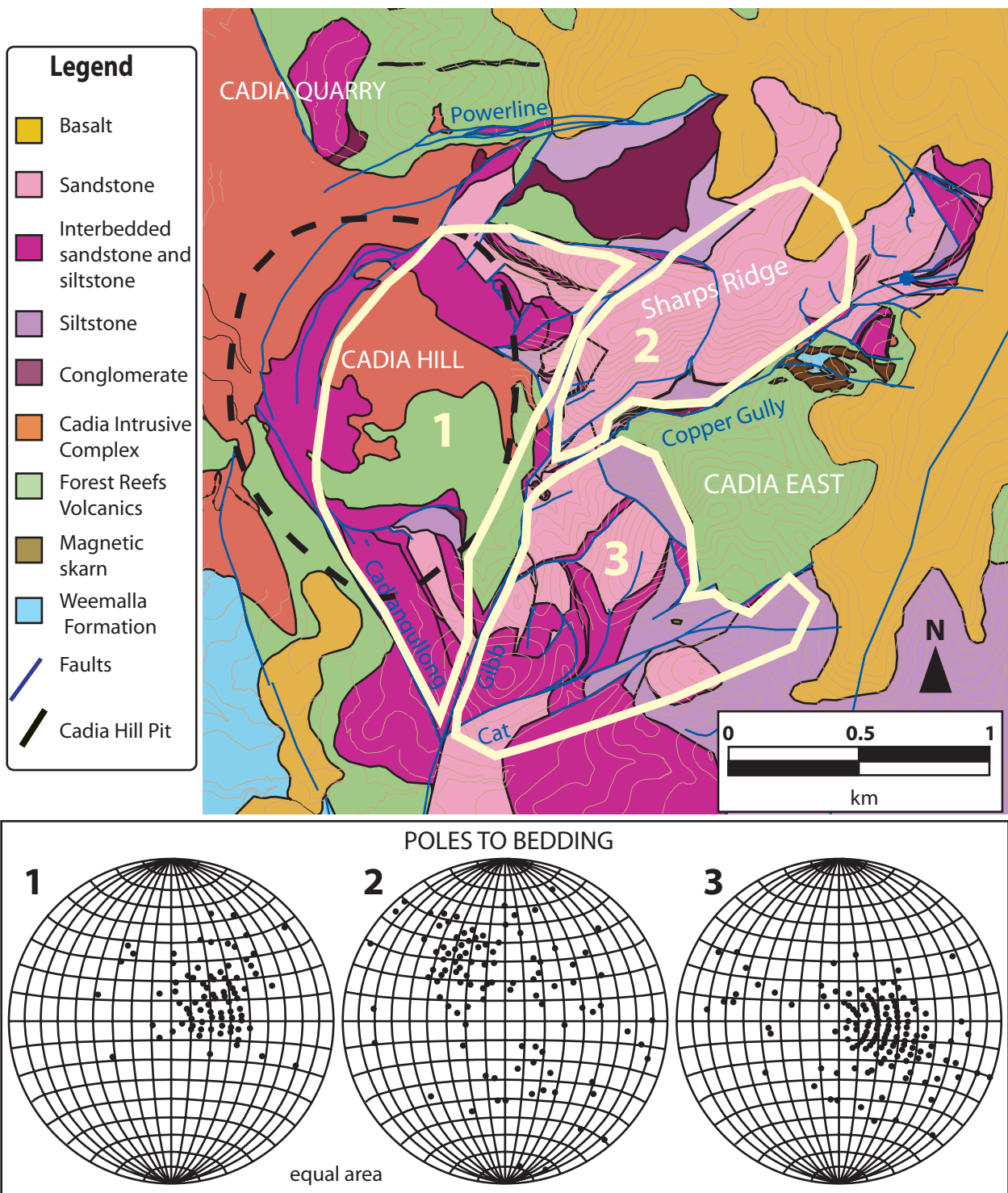


**Figure 3.5:** Domain analysis of bedding measurements from the Silurian Waugoola Group in the Cadia District. Domain 1 consists of Cadia Hill, in the footwall of the Cadiangullong fault, and the hanging wall of the Gibb fault. Domain 2 is Sharps Ridge, in the footwall of the Gibb fault, but the hanging wall of Copper Gully Fault. Domain 3 is Cadia East, in the footwall of the Gibb fault and the Copper Gully fault. Differences in bedding orientation across domains provide evidence for fault block rotation and basement fault control on orientation in the cover rocks.

bedding planes and the unconformity with the underlying Ordovician basement rocks. This style of deformation is characteristic of thin-skinned thrusting (Chambers et al., 2004; Molinaro et al., 2005; Mouthereau and Lacombe, 2006). The differences in deformation style reflect rheological contrasts between relatively strong basement rocks and the weaker bedded cover rocks.

In order to constrain the effects of post-mineral deformation on the ore-bearing lithologies, the interaction between structures in the sedimentary cover rocks of the Silurian Waugoola Group and major faults in the basement were examined in detail. The strike of thrust faults and related folds in the sedimentary cover sequence is similar to that of underlying basement faults identified in during exploration and resource drilling by Newcrest Mining Ltd. Qualitatively, the intensity of deformation recorded in the Waugoola Group sedimentary cover rocks increases approaching major basement faults. Therefore, basement faults control the orientation and distribution of faults and folds in the cover rocks (Figure 3.6). Slip along basement faults is manifested in the Waugoola Group sedimentary cover sequence as a combination of through-going faults and intra-cover faults and folds.

The scale and character of intra-cover faults differ from basement structures that have broken through the cover sequence. In general, through-going faults that link directly with basement faults are steeper and produce wider zones of deformation in the cover sequence. Where major basement faults cut up into the overlying cover rocks, the resultant structures in the sedimentary cover occur up-dip of, and trend parallel, to the faults below. Where these faults disrupt the Waugoola Group stratigraphy, sedimentary bedding steepens and is intensely fractured. Intra-cover faults are at a low angle or

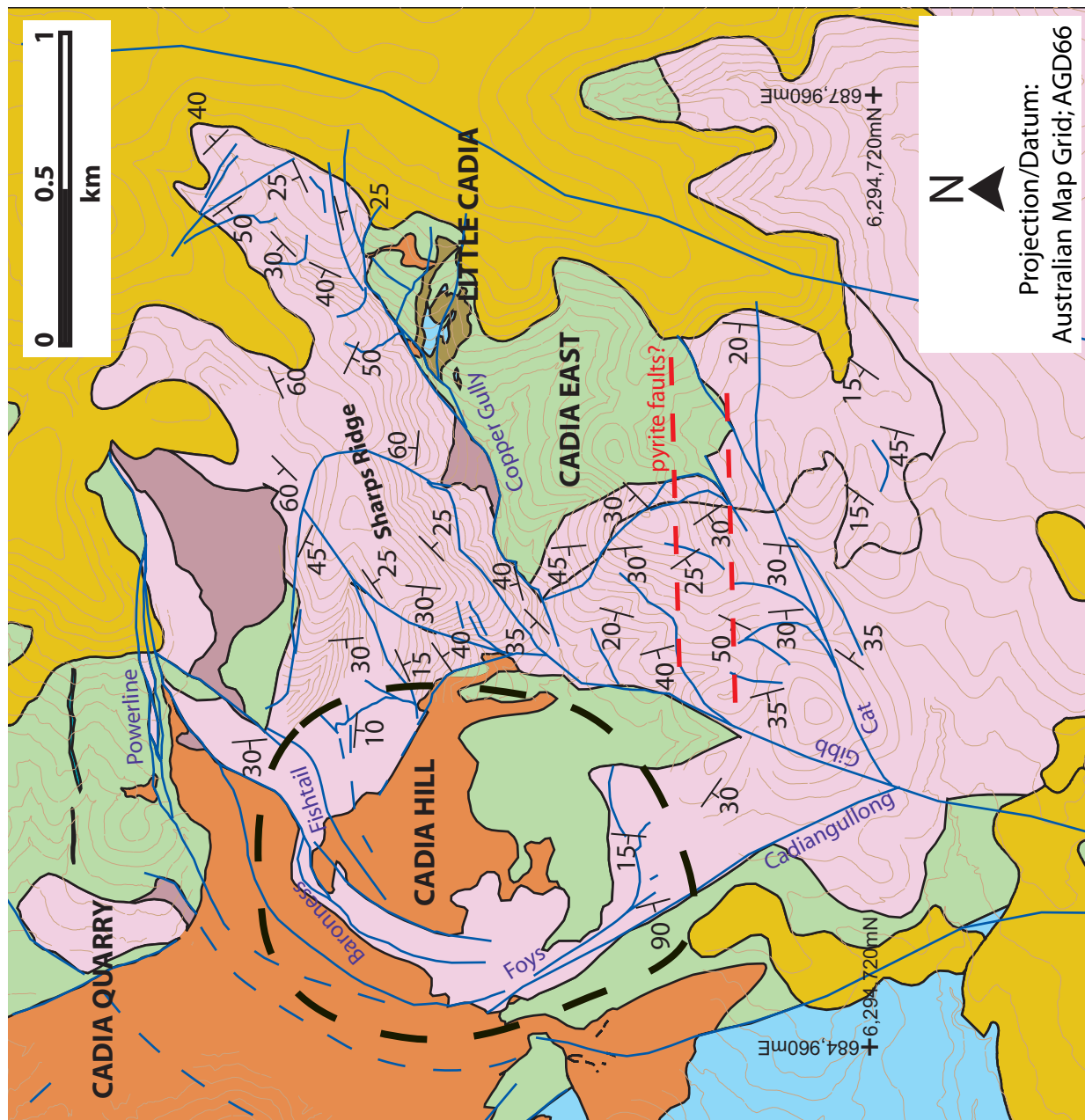


**Figure 3.6:** Map showing structural measurements mapped in the Waugoola Group sedimentary cover sequence in the Cadia District. Note that pyrite faults, shown with a red dashed line, do not appear in the cover rocks.



parallel to bedding and may be very narrow, with little to no fault gouge. These faults are connected to basement structures via a complex network of interconnected faults and folds (Figure 3.7, Figure 3.8).

The geometry produced by interaction between basement and cover structures results in steep basement faults appearing to become flatter at the unconformity. This relationship is visible on the southern wall of Cadia Hill pit, where the Foys fault brings Ordovician basement rocks over Silurian cover (Figure 3.7, Figure 3.8). The southern wall of Cadia Hill pit represents a fault-bounded block that occurs in the footwall of the Foys fault and the hanging wall of the Gibb Fault. In the basement rocks, the Foys fault and the Gibb fault both dip  $\sim 75^\circ$  to the west. In the sedimentary rocks, the Foys fault is a steeply dipping zone ( $>80^\circ$  to the west) of intensely fractured rock and sheared gouge where it continues through the cover rocks as an up-dip extension of the basement fault. Shortening accommodated along the Foys fault in the basement is also distributed in the cover sequence among multiple detachments, including the unconformity and bedding planes. These detachments cut through the cover rocks at a low angle to bedding and produce intra-cover faults and folds in the overlying sedimentary rocks (Figure 3.8).

The average dip of the unconformity and the overlying sedimentary cover rocks on the southern wall of Cadia Hill pit is  $\sim 30^\circ$  to the west. This is consistent with Waugoola Group bedding measurements from Cadia East (Figure 3.5). It is geometrically reasonable that the unconformity and the bedding of the sedimentary cover rocks was tilted due to rotation of basement blocks during reverse faulting, as is characteristic of thick-skinned thrust belts (e.g. Chambers et al., 2004; Molinaro et al., 2005; Grey et al., 2006; Mouthereau and Lacombe, 2006; and references therein). This

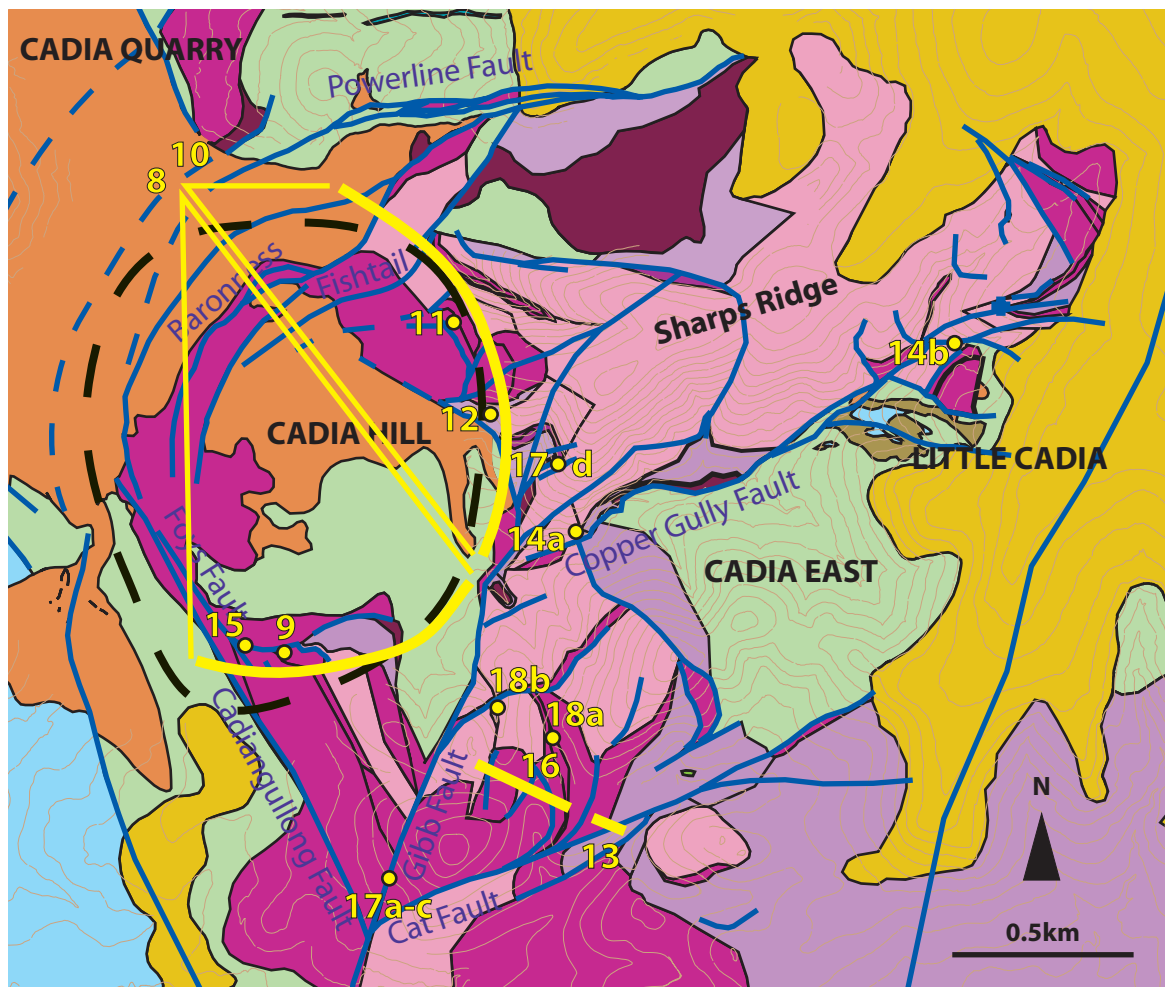


**Figure 3.7:** Reference map for locations of photographic figures in chapter 3. Photographic subject is shown with a yellow dot or a line. Numbers correspond with figure numbers, and are positioned where the photograph was taken to illustrate the direction of point-of-view. Heavy yellow lines represent panoramic photographs. Figure 8 is a panorama of the southern wall of Cadia Hill pit, taken from location 8 looking south, as shown by thin yellow lines. Figure 10 is a panorama of the eastern wall of Cadia Hill pit taken from location 10 looking southeast, shown by thin yellow lines. Figures 13 and 16 are panoramic photographs of roadcuts on the Cadia Hill access road. Figure 16 is taken looking south, and figure 13 is taken looking north. Figures 14 a-c were taken underground, in the Cadia East Decline, and are each ~20m apart.

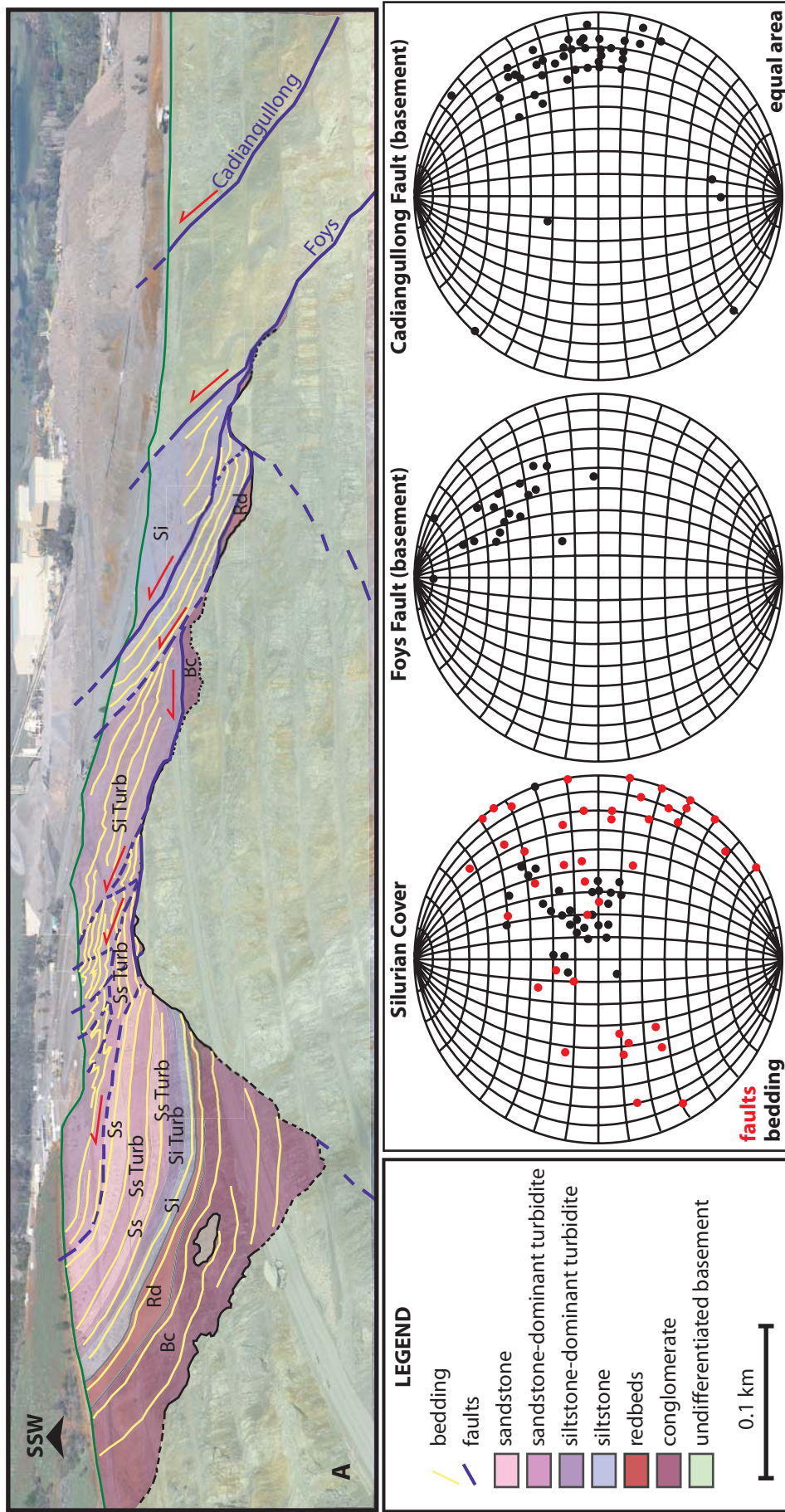


**Figure 3.8:** Relationships between basement faults and faults in the Waugoola Group sedimentary cover sequence on the southern wall of Cadia Hill pit. Location of panorama shown on figure 3.7. A: panoramic photograph of the Waugoola Group with stratigraphy overlain. Faults are shown in blue. Bedding is traced in yellow. Bc=boulder conglomerate; Rd=redbeds; Si=siltstone; Ss Turb= siltstone dominant turbidite; Ss Turb= sandstone-dominant turbidite; Ss=sandstone. Foys Fault flattens at the unconformity and shortening in the cover sequence is partitioned among many faults at a low angle to bedding, including along the unconformity. These detachments are shown in blue. Foys fault is a footwall splay off the Cadiangullong Fault. Stereonets are provided to show the spatial relationship between bedding and faults in the cover rocks and underlying basement faults. This relationship suggests that tilting of Waugoola Group bedding down to the west was the result of thrust-block rotation.

would have brought the Silurian unconformity and bedding planes into a favorable orientation to accommodate shallow-level thrusting (Figure 3.9).

Along the southern wall of Cadia Hill pit, the unconformity between altered Ordovician volcanic rocks and unaltered Silurian sedimentary rocks outcrops for ~100m along a single bench. Locally, the irregular unconformity surface has acted as a detachment; slip along the unconformity has produced clay gouge and small-scale faults and folds in the Waugoola Group sedimentary rocks above (Figure 3.9). Where local lows in the unconformity surface occur, the detachment climbs section into the sedimentary rocks and follows bedding planes. In this way, shortening on the Foys fault is accommodated in the cover sequence along minor planes of weakness at a low angle to Waugoola Group bedding that flatten at the interface between basement and cover.

The eastern wall of Cadia Hill pit essentially provides an *in situ* cross-section of Sharps Ridge (Figure 3.7, Figure 3.10). The position of the unconformity is topographically high relative to elsewhere in the district, and approximately 35m of Waugoola Group is preserved. Farther to the east along Sharps Ridge, the unconformity is at least 100m beneath the cover. During Waugoola Group deposition in the Late Silurian, Sharps Ridge was a relative topographic high in the basin (see chapter 2). During subsequent shortening and basin inversion, reverse movement on faults to either side of Sharps Ridge produced a complex fold-and-thrust geometry in the surrounding cover rocks.

On the eastern wall of Cadia Hill pit, bedding in the Waugoola Group sedimentary cover sequence is deflected at a minor basement fault (Figure 3.7, Figure 3.11). The fault is steeply dipping and strikes at a high angle to bedding of the cover



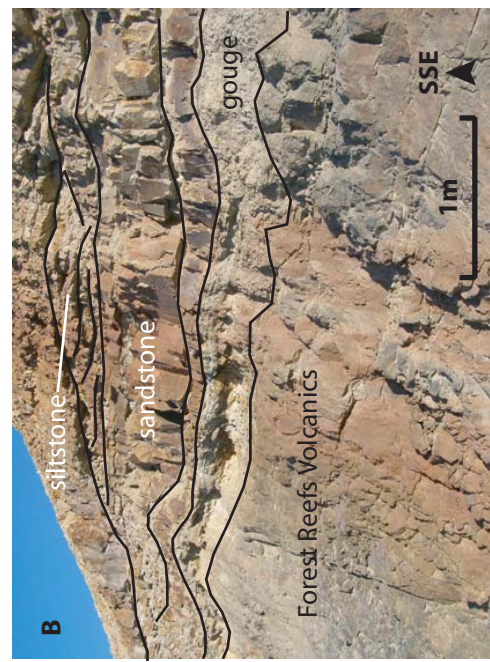
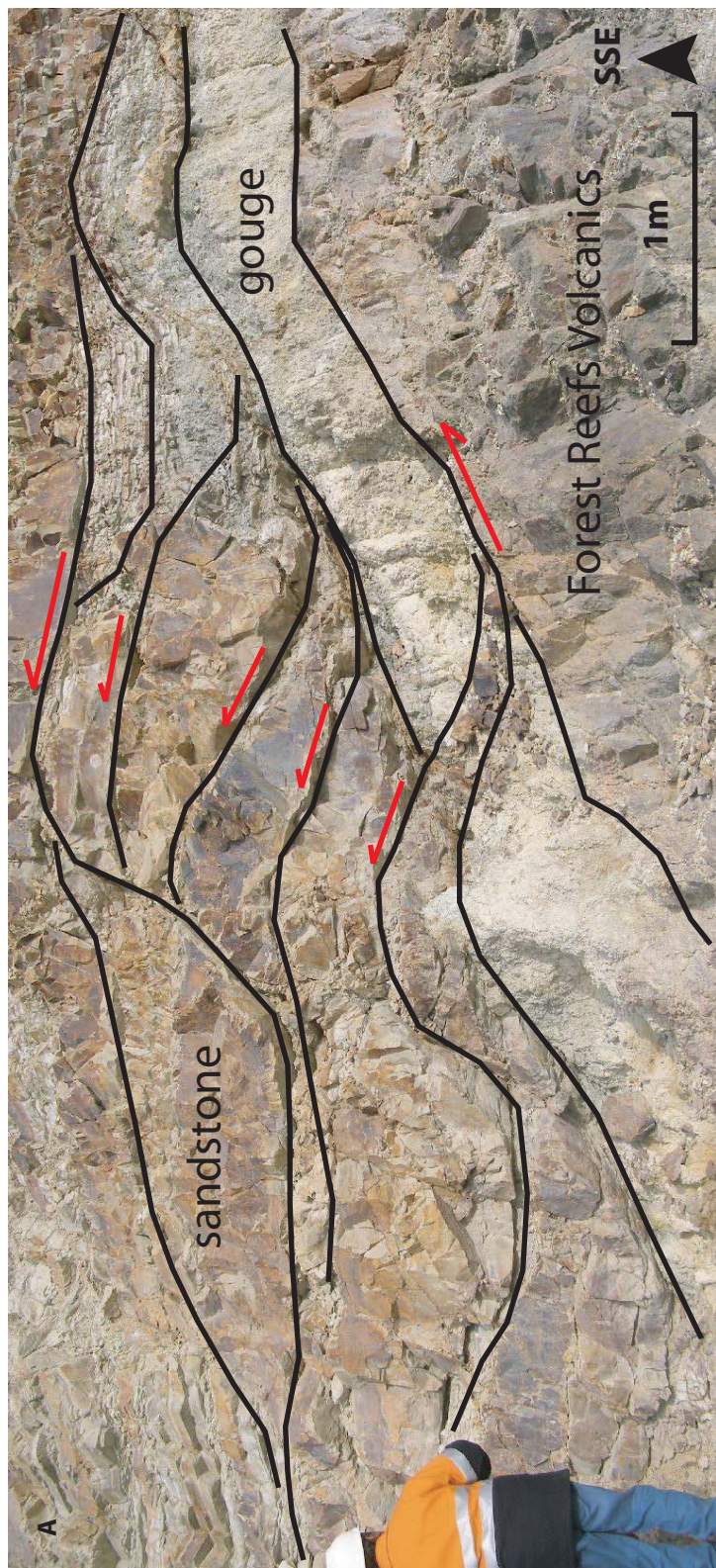


**Figure 3.9:** Photographs of unconformity features on the southern wall of Cadia Hill Pit. Locations are shown on Figure 3.7. A: duplex in the sandstone immediately above a local high on the unconformity. A sliver of siltstone is also present. The unconformity is locally covered by a thick zone of gouge. B: slip along local highs on the unconformity surface produces gouge. Detachments break up-section and slip is partitioned into siltstone horizons.



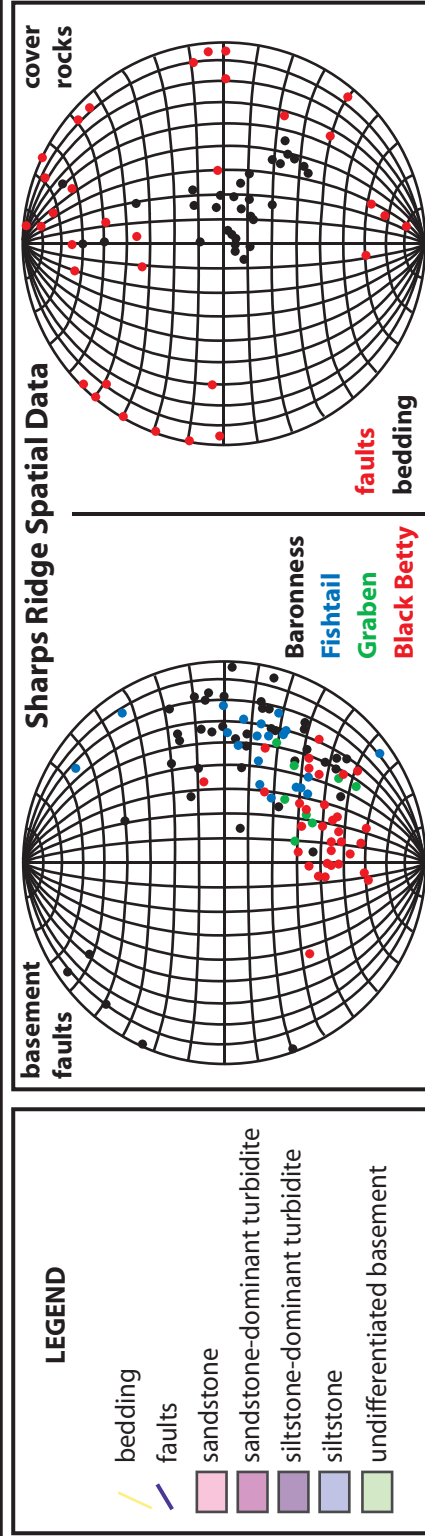
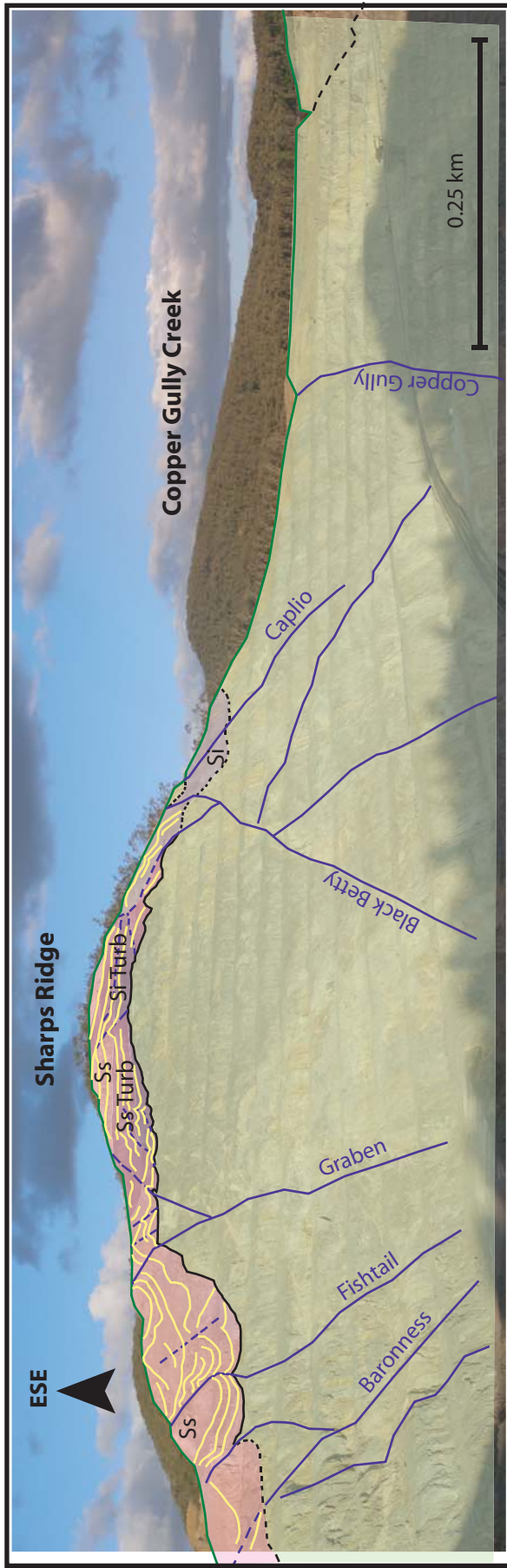


**Figure 3.10:** Panoramic photograph of the eastern wall of Cadia Hill pit highlighting the stratigraphy of the Waugoola Group sedimentary cover sequence across Sharps Ridge and important basement faults. Location of this photograph is shown on Figure 3.7. Bedding is shown in yellow. Faults are shown in blue. Relatively flat-lying beds of sandstone (Ss) and interbedded sandstone and siltstone (Ss turb, Si turb) have experienced relatively low levels of deformation, except adjacent to faults. Thick-bedded to massive sandstone on the northern slope of Sharps Ridge are folded against the Fishtail and Baroness faults. Siltstone (Si) on the southern side of Sharps Ridge dips steeply to the south, following the unconformity, and is more intensely faulted and folded. Sharps Ridge is a popped up block, and was relatively high in elevation during Waugoola Group deposition. Subsequent shortening reactivated reverse faults on either side and resulted in complex deformation of the cover sequence around the margins of the basement pop-up.



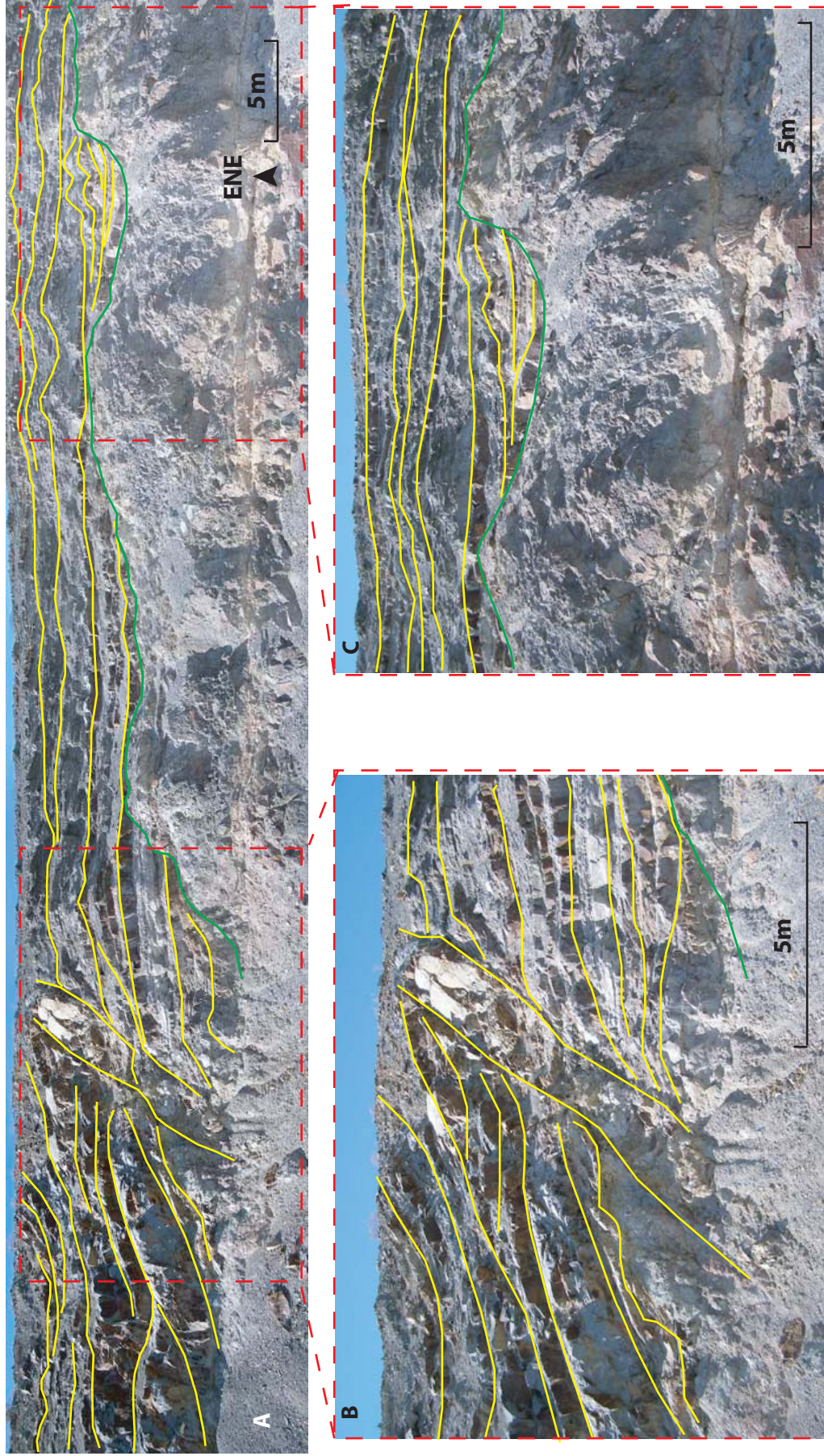


**Figure 3.11:** Photographs of the eastern wall of Cadia Hill pit. Locations shown on Figure 3.7. Unconformity shown in green. Bedding in the Waugoola Group shown in yellow. A: panoramic photograph showing relatively flat-lying bedding in the sedimentary cover sequence near the top of Sharps Ridge disrupted locally by faults (B) and local irregularities on the unconformity (C). Thick zones of gouge along the unconformity on the southern wall of the Cadia Hill pit are absent here. B: A splay off the Graben Fault, which outcrops 50m to the north. Thick-bedded sandstone on the left is juxtaposed against interbedded siltstone and sandstone on the right across a steeply dipping fault at a high angle to bedding. C: Faults and folds in sedimentary rocks draped in local basement lows. these features reflect relatively small amounts of deformation compared to unconformity features on the southern wall of Cadia Hill pit.

rocks. Thick-bedded, to massive sandstones occupy the hanging wall of the fault, whereas interbedded siltstone and sandstone are in the footwall. Steeply dipping beds of massive sandstone are folded against the fault (Figure 3.11b). This fault is similar in orientation to the nearby Graben fault, which outcrops 50m to the north in the hanging wall, and is associated with open folds and steep bedding in massive sandstone. It is plausible that this fault is a splay off Graben fault, and accommodated shortening in the Sharps Ridge pop-up fault block.

Away from faults bedding in the Waugoola Group on Sharps Ridge is relatively flat-lying, and the sedimentary cover sequence appears less deformed than on the southern wall of the Cadia Hill open pit, where bedding is tilted down to the west  $\sim 30^\circ$ . Slip along the unconformity on top of Sharps Ridge is probably less significant than along the southern wall, except where this surface is intersected by major faults, such as the Fishtail/Baroness fault complex. Some deformation of the cover rocks is associated with local irregularities on the unconformity (Figure 3.11c). Rather than the rounded peaks and troughs observed on the south wall, the unconformity at the top of Sharps Ridge appears to have a scalloped edge with sedimentary rocks draped in the lows (Figure 3.11c).

On the sides of Sharps Ridge, faults are more numerous and the Waugoola Group rocks are more deformed. For example, on the southern side of Sharps Ridge, Waugoola Group bedding dips moderately to the south, where it is parallel with the unconformity (Figure 3.12a). Cover rocks are folded and faulted against the unconformity. Small fault slivers of siltstone are preserved in the hanging wall of the Black Betty fault, which outcrops  $\sim 50\text{m}$  to the south (Figure 3.12b). These features suggest that the Silurian



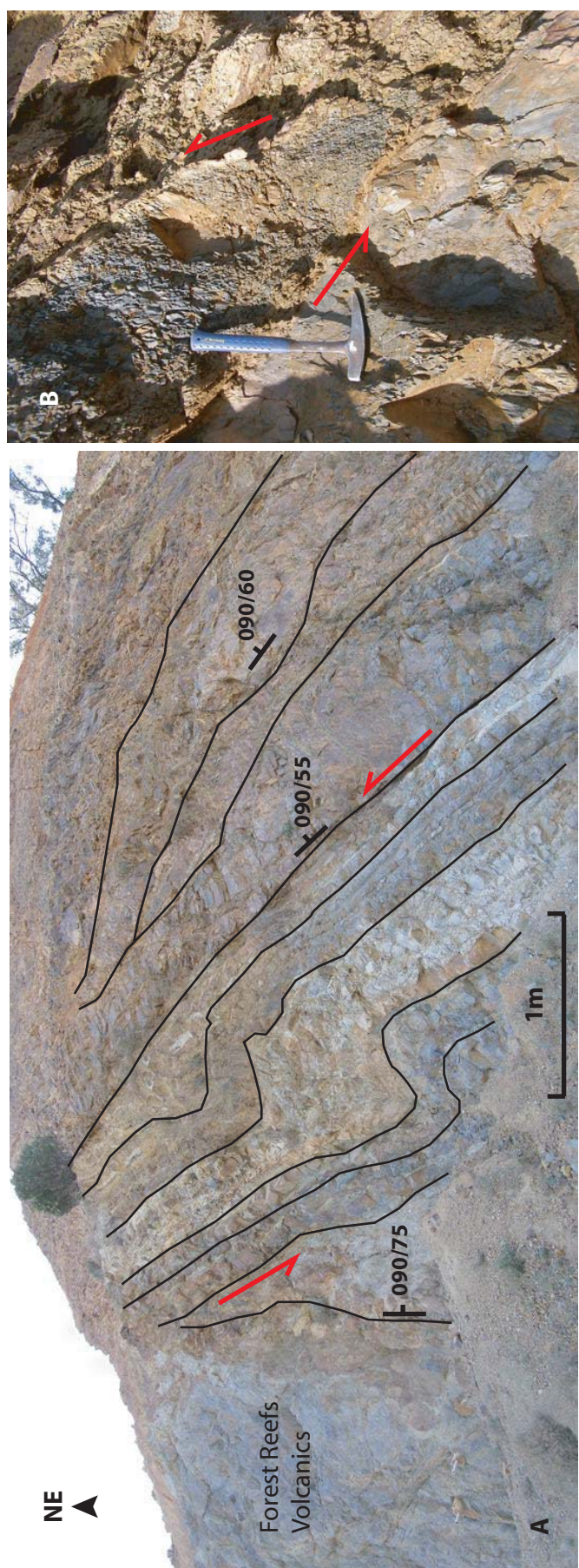


**Figure 3.12:** Faults and folds in siltstone on the southern slope of Sharps Ridge. Location is shown on figure 3.7. A: steeply dipping bedding in the Waugoola Group sedimentary rocks against the unconformity. Measurements are given in strike/dip format, with dip always to the right, and are in the projection Australian Map Grid; datum AGD66. B: fault sliver of intensely fractured siltstone showing deformed nature of Waugoola Group sedimentary rocks between Black Betty Fault, which outcrops ~50m to the south, and the unconformity.

sedimentary cover rocks on the Sharps Ridge pop-up fault block experienced the most intense deformation along the margins.

Where basement faults are exposed, as in the examples described above, deformation in the cover sequence can be related directly to reactivation of the controlling basement faults. These relationships can be used to make inferences about basement faults where only the cover rocks are present. For example, in Cadia East, the Cat fault is expressed in the overlying cover sequence as a steep fault that outcrops on the Cadia Hill access road (Figure 3.7, Figure 3.13). Interbedded siltstone and sandstone in the hanging wall is folded, with fold hinges sub-parallel to the fault plane. Minor thrusts in the hanging wall with ramp-flat geometry are also present (Figure 3.13). Siltstone in the footwall is relatively undeformed. Minor intra-cover faults and folds relate directly to the Cat fault, which can be identified in the cover rocks by the steep dip, the high angle of the fault plane to Waugoola Group bedding, and juxtaposition of interbedded sandstone and siltstone against massive siltstone.

Folds in the cover rocks can also be used to identify basement faults. This is because folds are typically spatially restricted to the cover rocks where underlying faults in the basement are present, and are related to controlling faults (Figure 3.13). Open folds in Waugoola Group cover rocks commonly overlie basement thrusts where they fail to break through the cover sequence. In Copper Gully, an open fold in thick bedded- to massive sandstones has a shallowly SW-plunging axis that is parallel to the Copper Gully fault in the basement (Figure 3.7, Figure 3.14a). An open fold with a similar geometry is present near Little Cadia (Figure 3.14b), implying that a basement fault lies below.



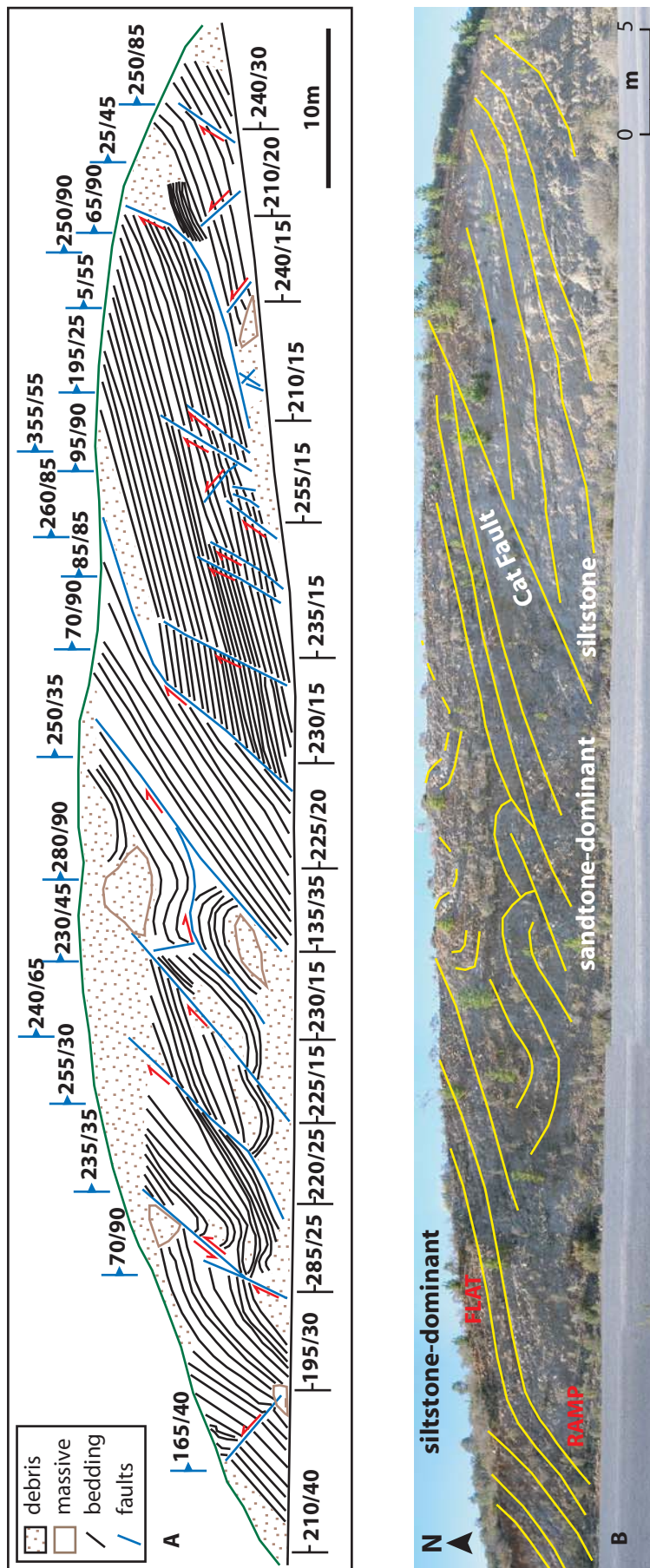
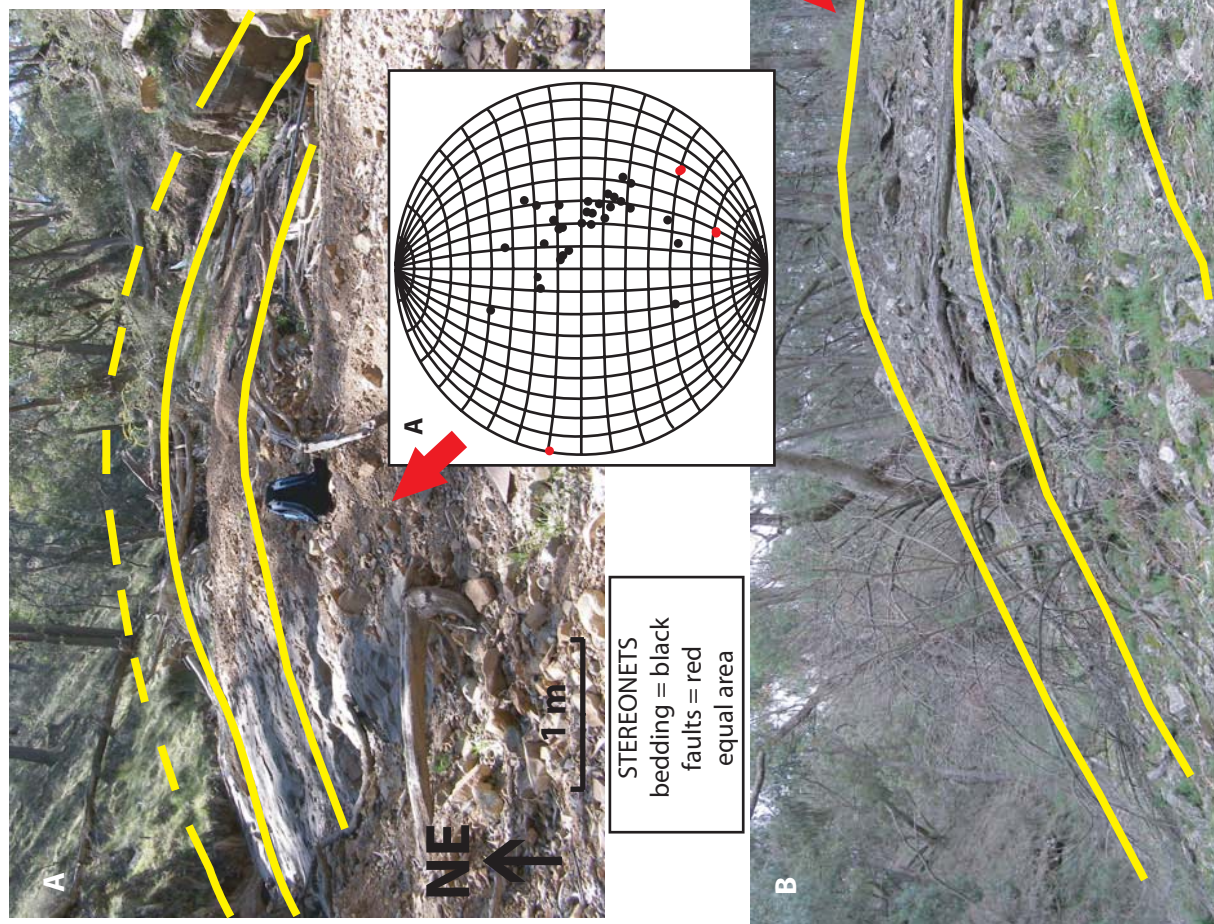


**Figure 3.13:** Detailed field sketch and panoramic photograph showing faults and folds related to the Cat Fault in an outcrop of Waugoola Group sedimentary rocks along Cadia Hill Access Road. Location of photographs shown on figure 3.7. Bedding highlighted in yellow. A: Detailed field sketch of the outcrop. Bedding measurements, in the format strike/dip, are shown approximately below where they were taken. Fault measurements are shown above the measurement position. Measurements are relative to Australian Map grid, AGD 66, and dip is always to the right of strike direction. Ramp-flat fault geometry in the siltstone-dominant portion of the outcrop give way to folds in the sandstone-dominant unit approaching the cat fault. fold hinge is approximately parallel to the fault plane. Cat fault is steeply dipping and at a relatively high angle to bedding in the sedimentary rocks. Cat Fault juxtaposes sandstone-dominant turbidites against siltstone. B: detail of most intensely deformed zone, including drag folds.



**Figure 3.14:** Open folds in sandstone above basement faults. Location of photographs is shown on figure 3.7. Stereonets A and B (equal area) show bedding (black) and fault (red) measurements from Waugoola Group rocks exposed at the surface at each photograph location. Stereonet C shows the orientation of the Copper Gully Fault measured in the Ordovician Basement rocks in the Cadia Hill pit. A: Open fold from Copper Gully Creek. Fold hinge plunges gently to the southwest and trends parallel to the underlying Copper Gully Fault. B: An open fold defines the shape of a hillside near Little Cadia, roughly along strike of the Copper Gully Fault. This fold hinge also dips gently to the southwest. Open fold geometry represents warping of bedding in the Waugoola Group rocks over the Copper Gully Fault or a related splay that has not broken through the cover rocks.



## **Intra-Cover Deformation**

Over most of Cadia East, the Silurian sedimentary cover sequence generally dips to the west at ~20-40°. Thickening via low-angle and bedding parallel intra-cover faults and related folding is the dominant mechanism by which shortening is accommodated in the Silurian sedimentary rocks. Slip has also occurred along bedding planes. Relatively weak units, such as the siltstone horizons of the turbidite and the micaceous arkose, commonly display sheared fabrics that resulted from bedding-parallel slip along these planes (Figure 3.15). The magnitude of shortening recorded by individual intra-cover faults and folds is estimated qualitatively based on field observations as being on the scale of meter-to-tens of meters.

As mentioned in the previous chapter, the stratigraphy of the Waugoola Group at Cadia East can be essentially divided into upper sandstone-dominated and lower siltstone-dominated sections. Fault and fold geometries in the upper, sandstone-dominated lithology differ from those in the lower, siltstone-dominated lithology.

Folds in sandstone-dominant lithologies are open and faults cut bedding at a low angle. In the outcrops along the Cadia Hill access road, top-to-the-east thrust faults at a low angle to bedding display a ramp-flat geometry typical of thin-skinned thrusting (Figure 3.16). Along-strike variations in orientation create wedges of deformed material that pinch out, and meter-scale fault-related folds (Figure 3.16). Displacement on these shallowly dipping faults is probably on the order of tens of meters or less, although it is impossible to quantify precisely due to the lack of marker horizons and because the fault juxtaposes rocks from the same lithologic package.



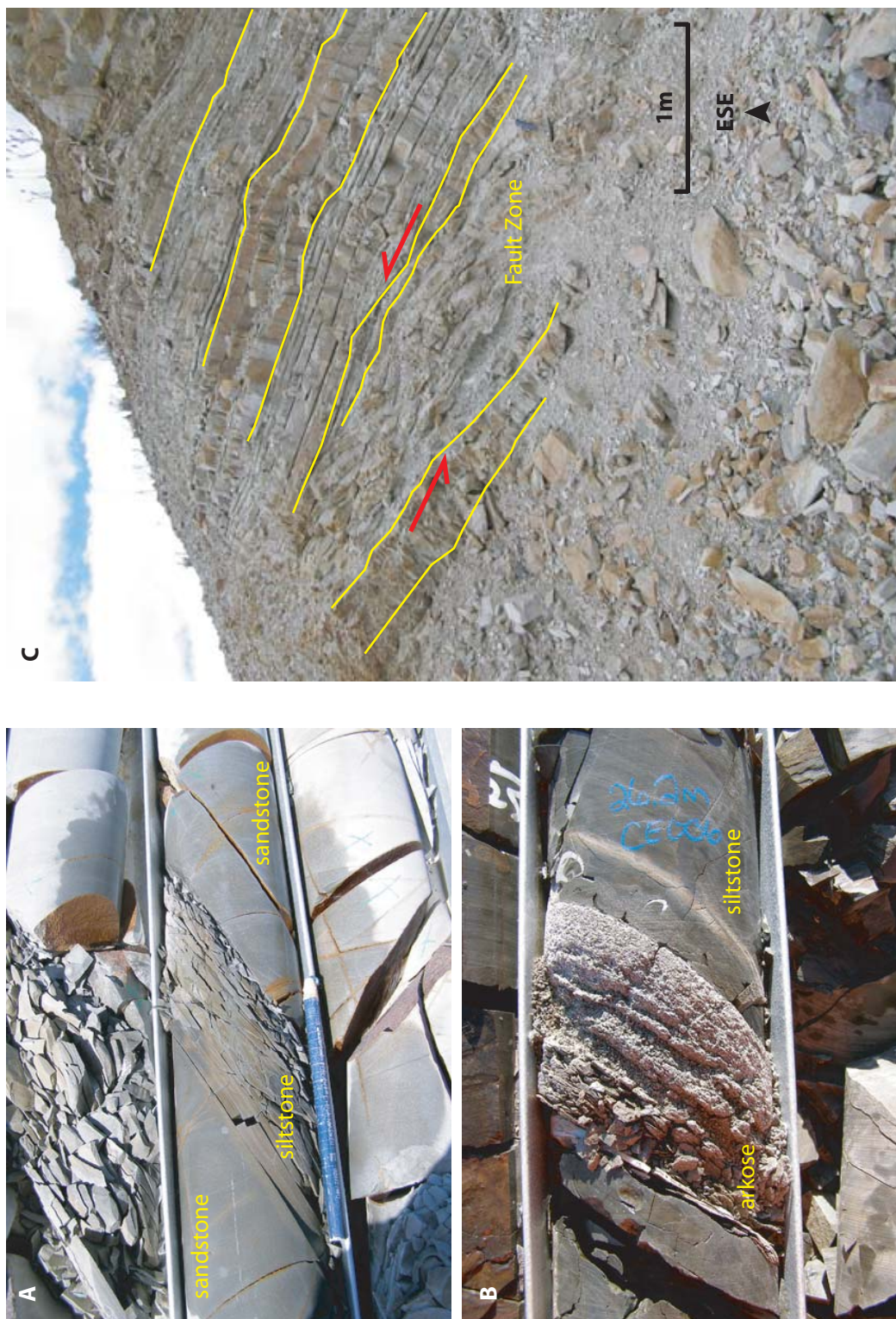


**Figure 3.15:** Photographic examples of bedding plane parallel slip. A: intense fracturing of siltstone horizon in interbedded siltstone and sandstone from drillcore. Siltstone is less competent than sandstone, so slip is partitioned along weaker planes. Graded bedding is evident in the gradational nature of fracture density. B: micaceous arkose horizons are less competent than the enclosing siltstones, so bedding-parallel slip in these units is expressed as bedding-parallel fabric development. C: The bedding parallel fault zone in interbedded sandstone and siltstone from the southern wall of Cadia Hill pit is probably a splay off the Foy's Fault. Intensely fractured rock and gouge occupy the fault zone. Photograph location is shown on figure 3.7.



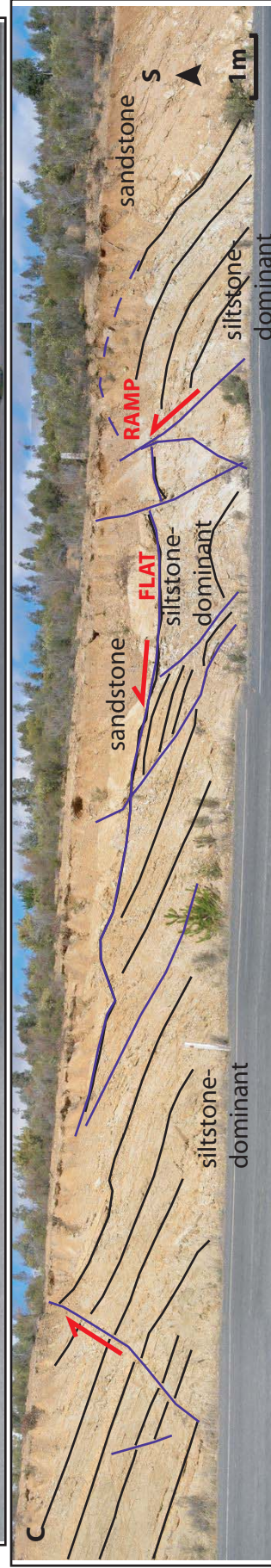
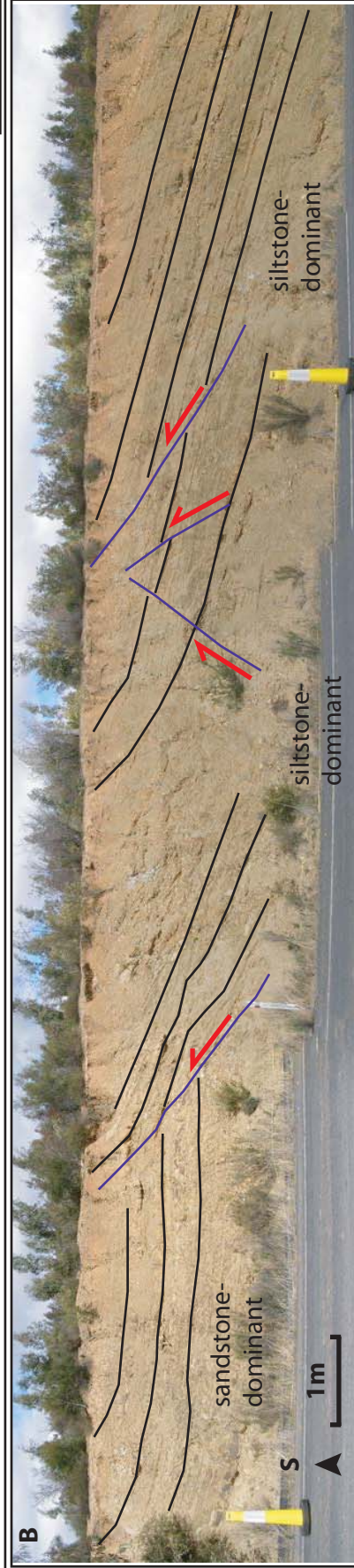
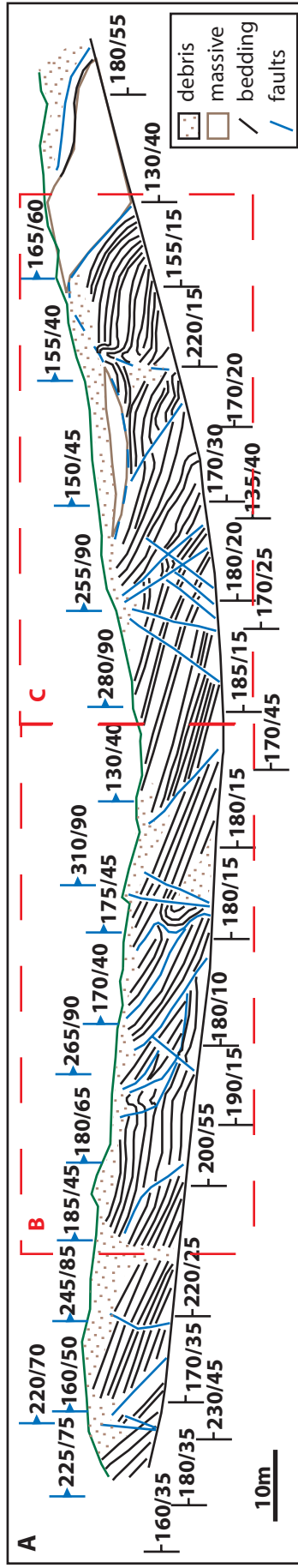


**Figure 3.16:** Folds and thrusts in sandstone and interbedded sandstone and siltstone from a continuous roadcut on the Cadia Hill Access Road. Photo location shown on figure 3.7. A: detailed field sketch of the roadcut. Bedding measurements, in the format strike/dip, are shown approximately below where they were taken. Fault measurements are shown above the measurement position. Measurements are relative to Australian Map grid, AGD 66, and dip is always to the right of strike direction. Locations of panoramic photographs below (B and C) are shown in a red dashed line. B: parallel thrusts bring siltstone-dominant turbidite over sandstone-dominant turbidite with a zone of more intense deformation in between them. C: sandstone thrust over siltstone-dominant turbidite displaying a ramp-flat geometry. Thrusts are at a relatively low angle to bedding. Complex fault and fold geometry occurs where faults bend.

Tight-to-isoclinal folds and chevron folds are common in the lower siltstone-dominant units near faults. In the Cadia East decline (Figure 3.17), the chevron folds occur in the footwall of the N- striking Gibb fault. The folds have horizontal to shallowly plunging fold axes that trend parallel to the Gibb fault. Another tight fold in siltstone related to the Gibb fault outcrops on the southern slope of Sharps Ridge (Figure 3.17). Because of geometric similarities, folds in siltstone at Cadia East (Figure 3.18) might also be related to major basement faults that have not yet been identified in the basement rocks in drillcore.

Bedding-parallel thrust faults which occur in the sandstone-dominated upper stratigraphy are not as common in the siltstone. Instead, steeply dipping faults cross-cut bedding in the siltstone. These high angle faults are identified in drillcore by rapid changes in the orientation of flaser bedding, and zones of disrupted or chaotic siltstone-in-siltstone breccia (Figure 3.19).

Slip along apparently minor detachments in the cover rocks can not be quantified because these surfaces typically do not juxtapose different lithologies. Where stratigraphic juxtaposition does occur, a lack of laterally extensive marker horizons in the Waugoola Group sedimentary cover rocks makes balancing sections not viable. Likewise, it is not possible to quantify slip along the unconformity and bedding planes. As a result, attempts at producing measured stratigraphic sections and facies reconstructions have been hindered. Additionally, the Waugoola Group is preserved discontinuously throughout the district, and erosion between the Devonian and the Mesozoic may have removed portions of the original stratigraphy, so true depositional thickness is unknown. The combination of these factors makes it unlikely that post-mineral shortening can be



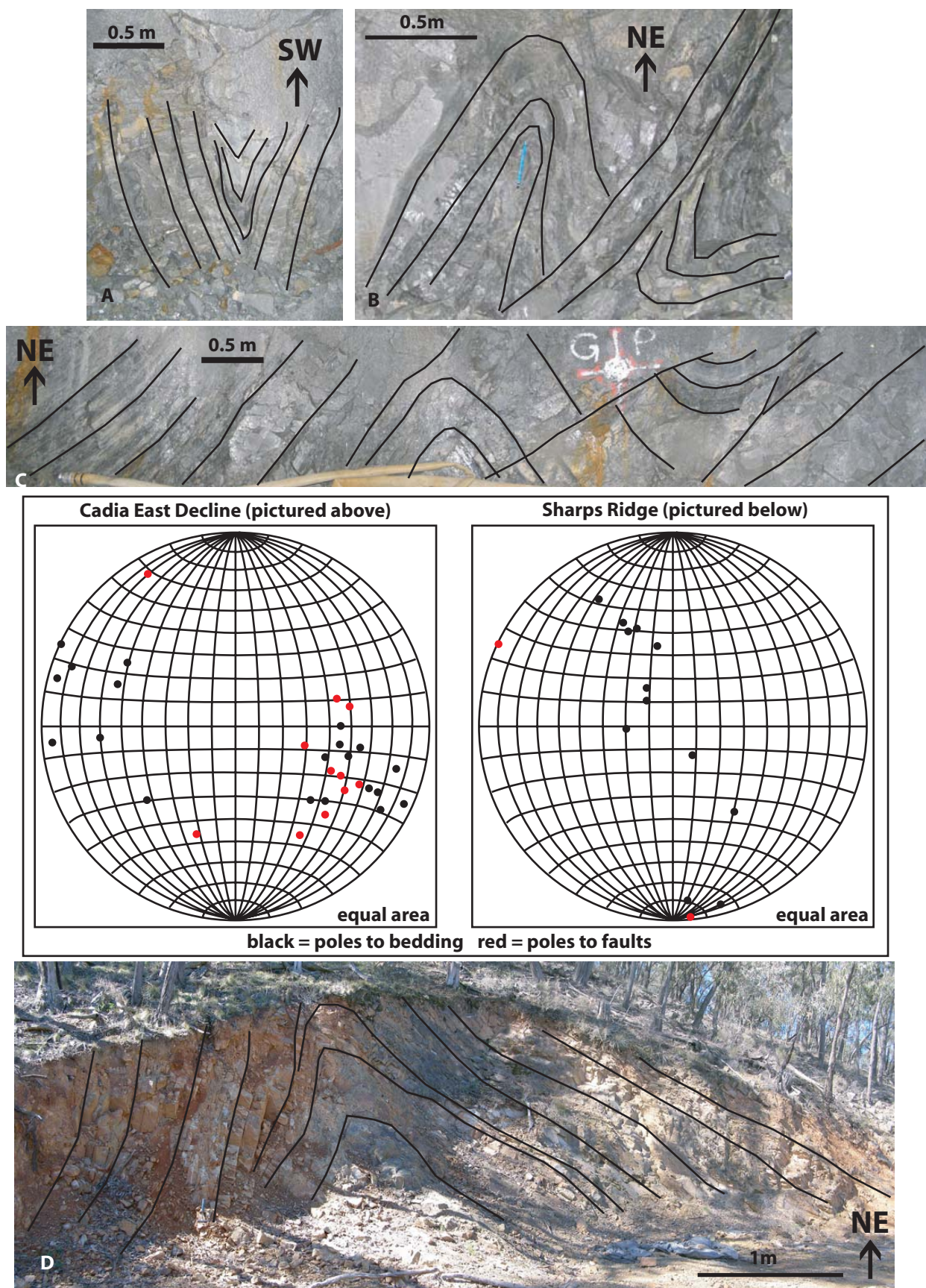


**Figure 3.17:** Tight fault-related folds in slitstone in the footwall of the Gibb Fault. Photo locations shown on figure 3.7. A, B and C are from the Cadia East decline. D is from Sharps Ridge. The relationship between folded bedding and related faults in cover rocks at both of these localities is shown on stereonets.



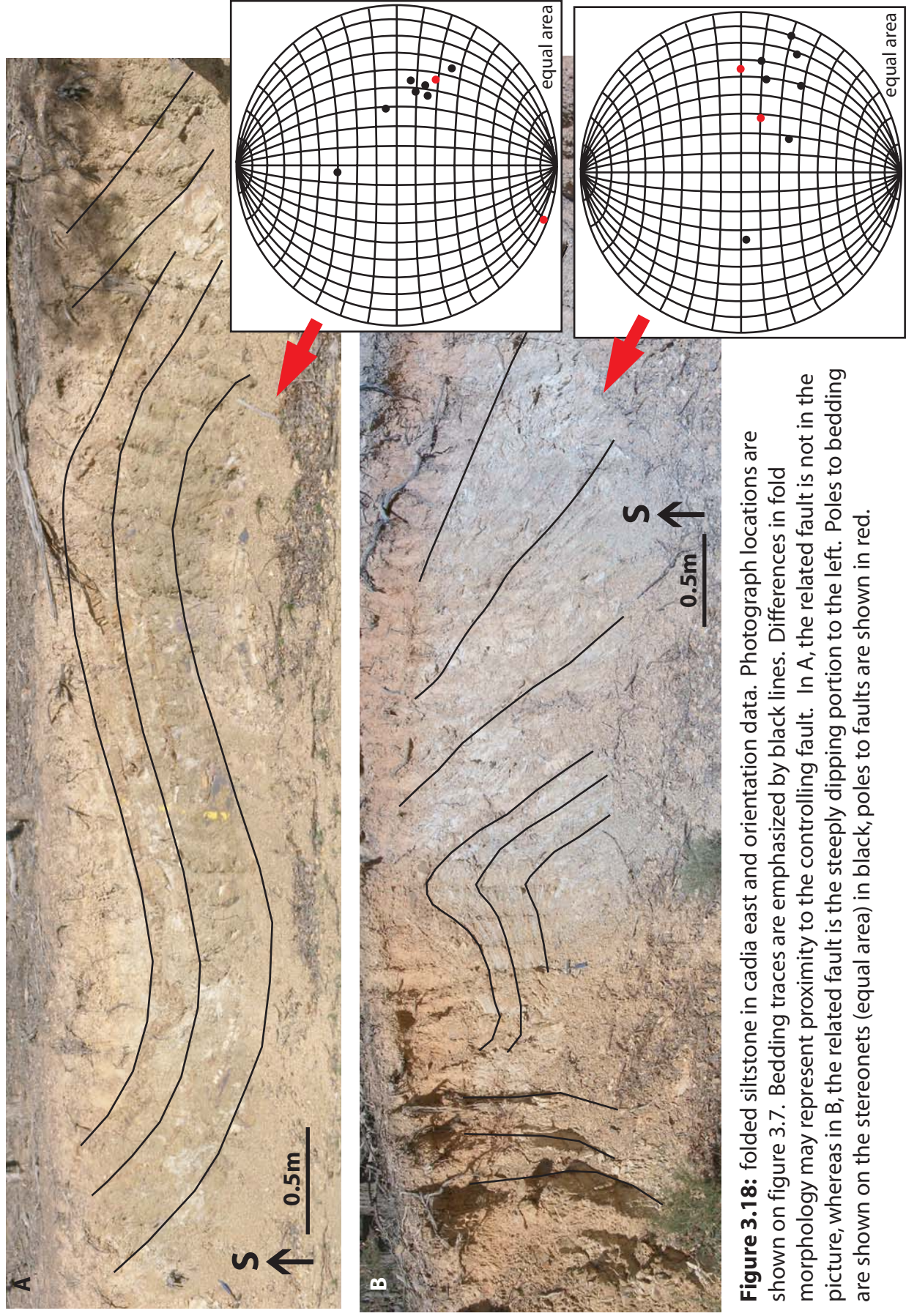


**Figure 3.18:** folded siltstone in cadia east and orientation data. Photograph locations are shown on figure 3.7. Bedding traces are emphasized by black lines. Differences in fold morphology may represent proximity to the controlling fault. In A, the related fault is not in the picture, whereas in B, the related fault is the steeply dipping portion to the left. Poles to bedding are shown on the stereonets (equal area) in black, poles to faults are shown in red.





**Figure 3.19:** Flaser bedded siltstone from drillcore (CE097, 95-109 m). Purple lines indicate bedding orientation. Bedding at 102m is chaotic. At 97m, bedding dips at a steep angle relative to the core axis. At 95m, siltstone-in-siltstone breccia is present. Therefore, it is likely that this drillhole intersects a fault or fold near 96m. This structure is a minor intra-cover feature, rather than a major, basement penetrating fault.

quantified using faults and folds measured in the Waugoola Group sedimentary cover rocks.

## **FAULT REACTIVATION HISTORY**

Faults and folds in the Late Silurian Waugoola Group provide evidence for a major deformation event following deposition of the sedimentary cover sequence. Tilting of bedding down to the west, and west-over-east thrusting on N-S oriented faults suggests that shortening was oriented E-W. Temporally and kinematically, this makes the Devonian Tabberabberan Orogeny (~380 Ma) the best candidate for post-mineral deformation in the Cadia district (e.g., Powell, 1984).

Because the orientation of structures in the sedimentary cover is essentially similar to that of major faults in the basement, it is suggested that all significant displacement was due to shortening after deposition of the Waugoola Group, in the latest Silurian. However, an equally plausible scenario is that major faults formed earlier in the Ordovician and were subsequently reactivated.

A complex tectonic history is recorded in the Cadia district. Regional deformation began during the Ordovician, and may have produced faults early in the tectonic, even the sedimentary history of the Cadia district. Once faults form, it is likely that brittle failure will continue to occur along these pre-existing planes of weakness as long as they are oriented favorably relative to the prevailing stress regime (Sibson, 2000). Reactivation of faults elsewhere in the region due to multiple episodes of orogenesis in

the Lachlan Fold Belt is well documented in the literature (e.g., Gray and Foster, 1998; Glen and Watkins, 1999; Offler and Gamble, 2002; Glen, 2005).

Stratigraphic reconstructions of the Weemalla Formation and the Forest Reefs Volcanics have shown that faults in the Cadia District influenced deposition of Ordovician units (Harris, 2007b). Additionally, recent advances in understanding the Ordovician stratigraphy in the Cadia District have shown that early faults may have facilitated intrusive emplacement (e.g. Wilson, 2001; Holliday et al., 2002; Kitto, 2005; Harris, 2007b). Geometric relationships between basement faults and the distribution of Waugoola Group lithologies suggest that many of these faults may have been active prior to deposition of the Silurian sedimentary cover sequence. Therefore, any related structures in the cover sequence may be attributed to reactivation.

The depositional environment for the basal unit of the Waugoola Group has been interpreted as local fault-bounded basins (see chapter 2). Topography was produced by fault activity during cycles of uplift/subsidence following intrusion and mineralization in the Early Silurian. The basin geometry, and therefore the distribution of the Waugoola Group, was controlled by pre-existing basement structures. Stratigraphic thickness variations and lateral facies changes appear to be influenced by N-striking and NE-striking reverse faults. Three lines of sedimentological evidence exist to support this hypothesis, concerning 1) the spatial distribution of the boulder conglomerate, 2) the role of Sharps Ridge as a pop-up fault block, and 3) the occurrence of Waugoola Group sedimentary rocks in isolated wedges across the Cadia district.

## **Boulder Conglomerate**

The boulder conglomerate at the base of the Waugoola Group is restricted to basement lows which are spatially associated with major basement faults. This is especially evident in Copper Gully and along the Gibb fault (Figure 3.20). A thick package of boulder conglomerate to the north of Sharps Ridge, known locally as the Hoares Creek Breccia, also represents a local basement low between the Powerline fault system and Sharps Ridge. This suggests that conglomerates formed at the base of fault scarps from material shed off local highs.

Clast populations in the boulder conglomerate include skarn, monzonite porphyry and hydrothermally altered volcanic clasts, reflecting local provenance. Unaltered clasts of siltstone and limestone, consistent with the lower stratigraphy of the Waugoola cover sequence, also occur in the boulder conglomerate; the polymict nature of some conglomerates suggests that they formed coeval with early phases of deep water sedimentation elsewhere in the Cadia district.

## **Sharps Ridge**

Whereas boulder conglomerate accumulated in basement lows that developed due to vertical fault displacement, basement highs underwent erosion (e.g., Sharps Ridge). Siltstone, which is thick over much of Cadia East is absent from Sharps Ridge. Limestone and boulder conglomerate are also absent. Interbedded siltstones and sandstones similar to those at the top of the Waugoola stratigraphy elsewhere in the Cadia

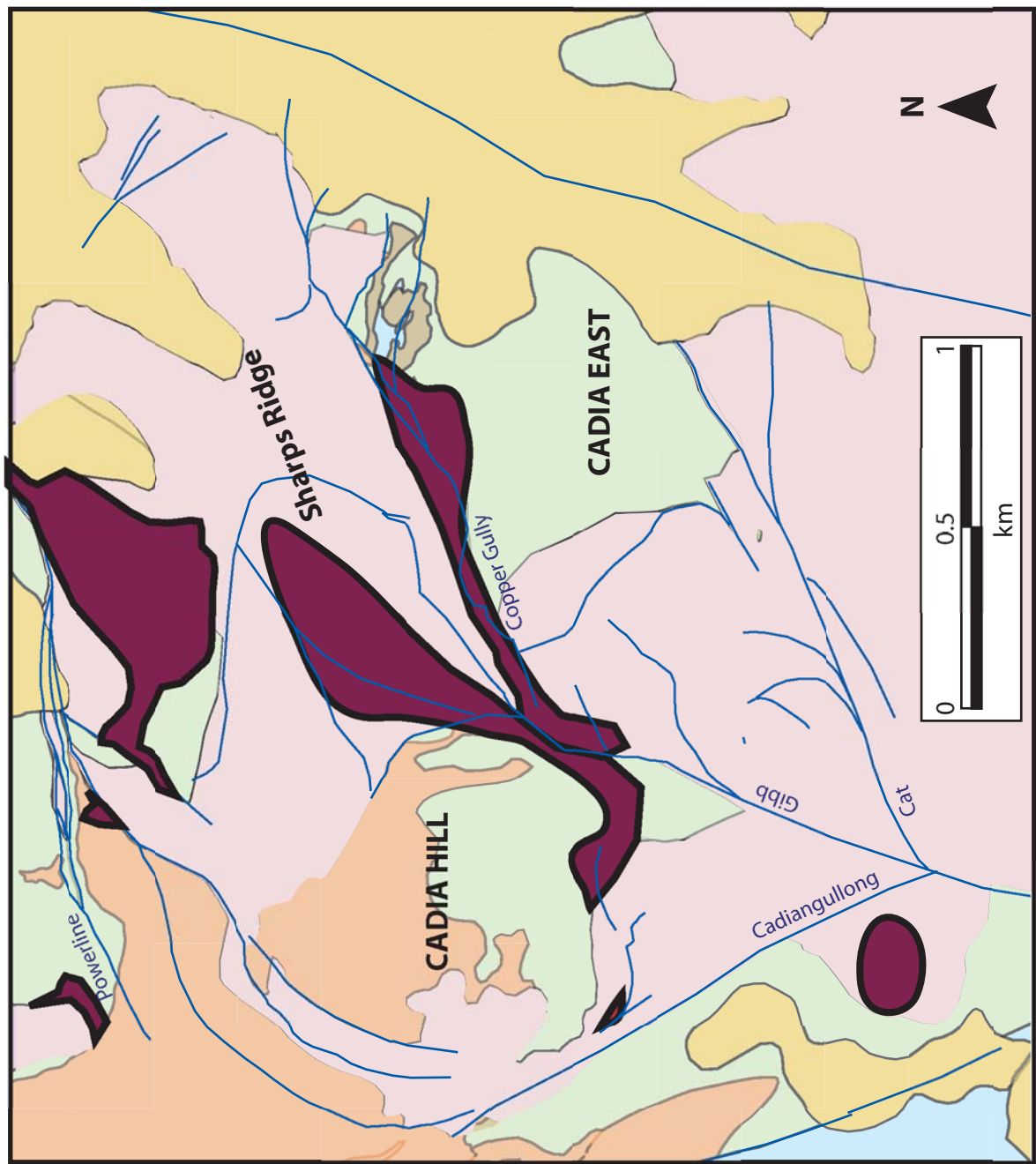


**Figure 3.20:** Map showing spatial distribution of conglomerate at the base of the Waugoola Group both at the surface and in drillcore. Conglomerate is interpreted as fault scarp deposits. This provides insight into the paleogeography of the Cadia District and the important role basement faults played in the development of topography prior to Late Silurian Waugoola Group deposition.

district dominate the cover sequence in this area. This indicates deposition of the Waugoola Group commenced on Sharps Ridge late relative to the rest of the district, once local basins filled and topography was overwhelmed.

### **Waugoola Group Geometry**

Variations in thickness of the siltstone package and differences in the basal unit of the Waugoola Group reflect pre-existing basin architecture. For example, a relatively thin siltstone package is present in the hanging wall of the Gibb Fault, where it overlies redbeds and boulder conglomerate (Figure 3.21). However, the siltstone package in the footwall of the Gibb Fault is thicker, and overlies the basal limestone. Some variations in apparent thickness of the siltstone may reflect structural thickening near the controlling fault. For example, siltstone in the footwall of the Gibb fault is intensely folded and faulted. However, tight folds and faults that appear to repeat stratigraphy in the cover rocks have only been observed proximal to major basement faults, whereas these structures are not typical with increasing distance from the controlling basement fault. Therefore, some observed thickness variations across major basement faults probably reflect depositional control. Therefore, these stratigraphic variations suggest that basin architecture in the late Silurian was controlled by normal faults similar in orientation and configuration to reverse faults present today.

Additionally, units high in the Waugoola Group stratigraphy were deposited on relatively low portions of the Forest Reefs Volcanics (see chapter 2). Deformation and erosion prior to Waugoola Group deposition was responsible for variable relative uplift of



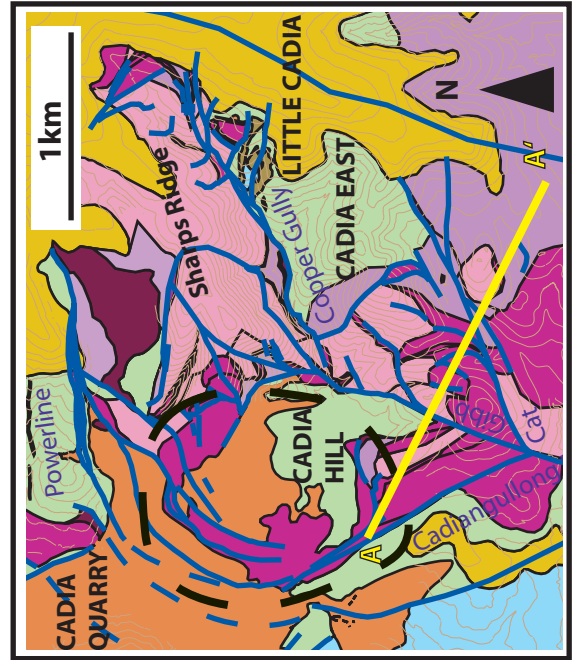
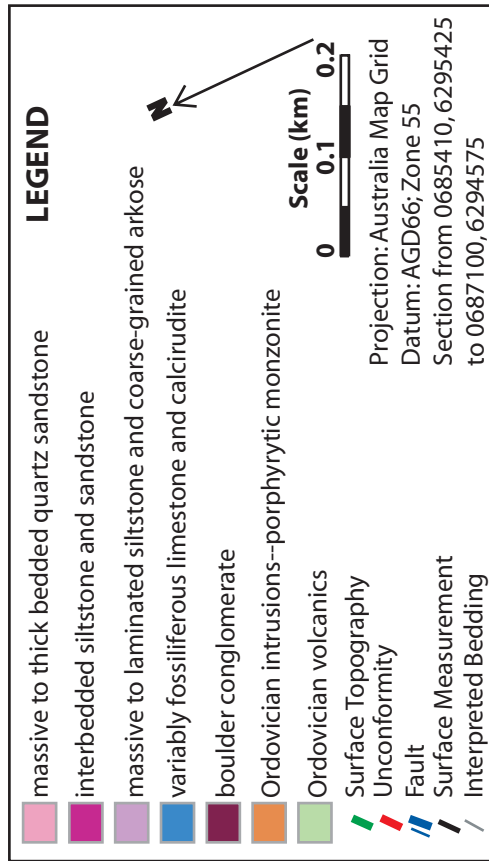
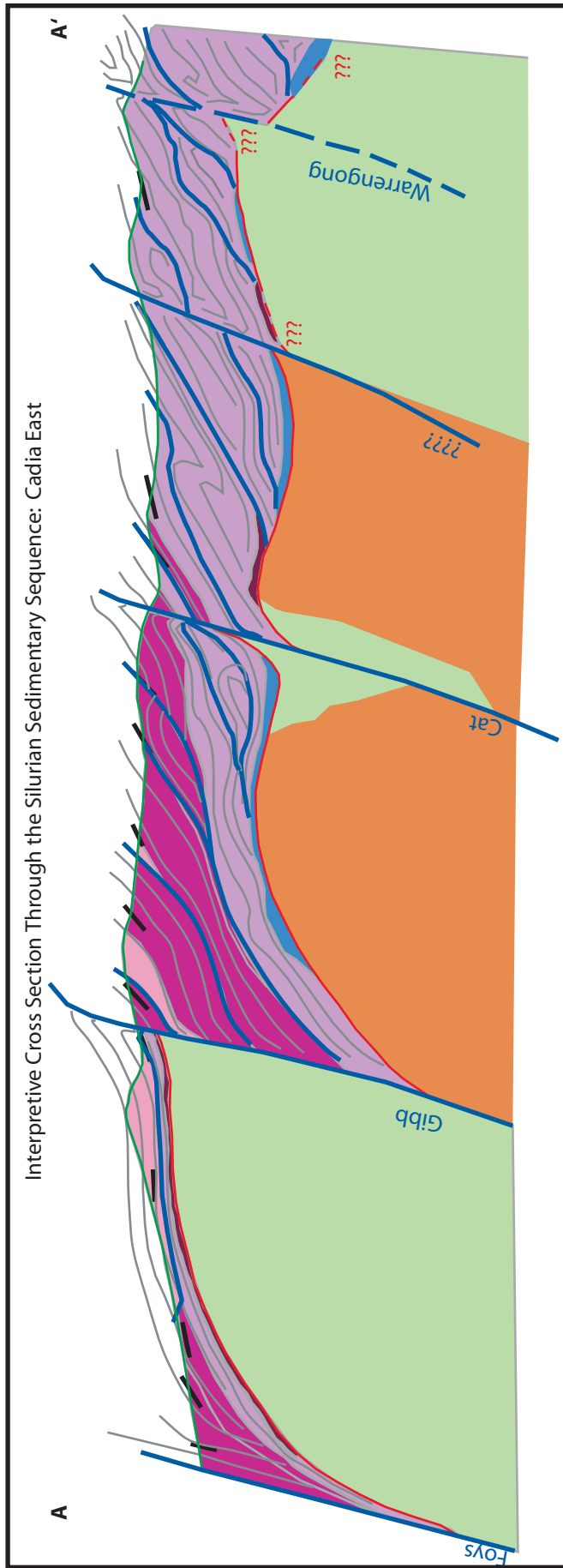


**Figure 3.21:** Cross-section showing basement faults and related faults and folds in Waugoola Group sedimentary cover rocks at Cadia East. Vertical scale=horizontal scale. Section line A-A' shown in yellow on reference map. Drillcore logs used to constrain this section are included in appendix 2.

basement rocks, which produced this geometry. Therefore, basin-bounding faults were actively producing topography at least as early as the Early Silurian, and that topography was maintained throughout much of Waugoola Group deposition in the Cadia district.

## **SUMMARY AND CONCLUSIONS**

Post-mineral shortening in the Cadia district is in part associated with the Devonian Tabberabberan Orogeny, and was accommodated by a complex, anastomosing network of meter-scale to tens-of-meters-scale intra-cover faults and folds in the Silurian sedimentary cover sequence to the Ordovician volcanic complex in the Cadia district. This deformation event was also expressed as reverse separation on basement penetrating faults and slip along the Silurian-Ordovician unconformity. Faults and folds in the Waugoola Group are similar in orientation to related faults in the Ordovician basement rocks.

### **Heirarchy of Faults**

The stratigraphic and structural framework of the Cadia district indicates that N-striking basement faults formed in the Ordovician as normal sedimentary basin-bounding faults (Harris, 2007a; Wilson, 2003; Figure 3.22). NE-striking faults were produced in response to fault propagation through the relatively strong intrusions, and apparent fault curvature resulted from connectivity of NE- and older N- striking faults. These faults were inverted during shortening, so measured offsets of marker beds provide only

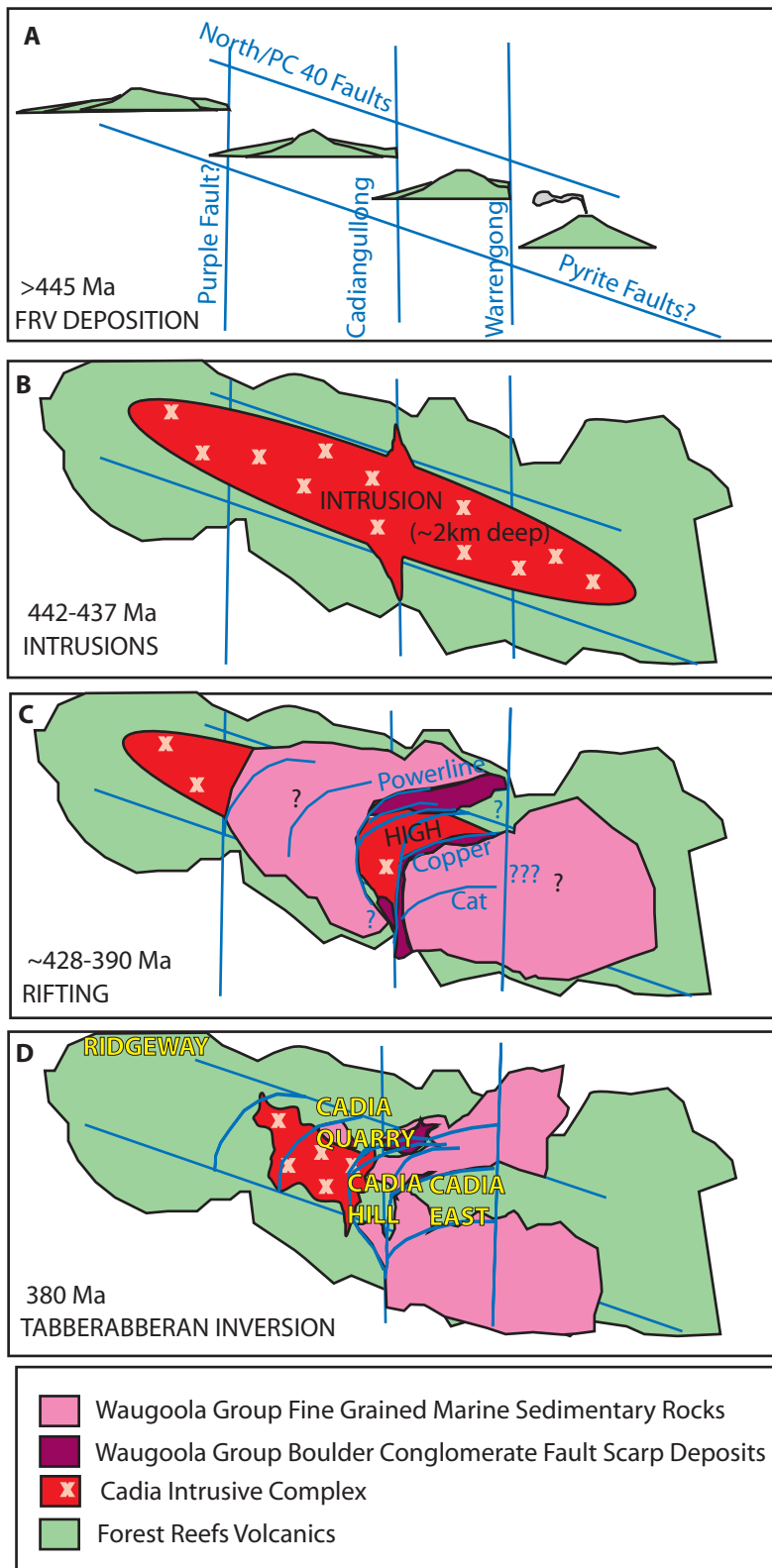


**Figure 3.22:** Interpretive map-view timeslices showing the structural evolution of the Cadia District. Geometry of faults and geologic units is idealized. Dates from Wilson et al., 2007. A: The volcanic center migrates eastward across the district, and the Forest Reefs Volcanics are deposited in fault bounded basins. This provides evidence for the earliest structural fabrics in the district. B: Intrusions are emplaced. This phase marks the introduction of major rheological contrasts into the district. Intrusion shown in map view is ~2km below the surface. C: NE-striking faults develop as fault-bounded basins form during rifting. Waugoola group sedimentary rocks are deposited therein. Topography is maintained until local basins are filled. Lateral extent of Waugoola Group rocks to the east and west are unknown. D: Rift basins filled with Waugoola Group sediments are inverted during Devonian shortening. Fault connectivity develops between NE- and older N- striking faults across the resistant intrusion, producing an apparent curvature in map view.

N  
↑  
MAP VIEW  
(NOT TO SCALE)

minimum constraints on the magnitude of vertical separation on reverse faults. E-W shortening during the Devonian Tabberabberan Orogeny was accommodated in the basement along these older faults and produced similarly oriented structures in the Silurian sedimentary rocks. The inverted faults can be sorted into three categories based on orientation and inferred timing relationships.

The earliest structural fabric to have formed was probably W- to NW- striking faults, such as the PC40 fault at Big Cadia, the North fault at Ridgeway, and the Pyrite faults in Cadia East (Holliday et al., 2002; Wilson et al., 2007b; Harris, 2007a; Figure 3.22a). Stratigraphic relationships (including thickness variations and sedimentary facies associations) suggest that these structures controlled deposition of Ordovician units in the Cadia district and were important during intrusion and mineralization events (Figure 3.22b; Wilson, 2003; Harris, 2007a). It is likely that they defined the boundaries of depositional domains during periods of trans-tension early in the tectonic history of the district (>455 Ma).

On the south wall of Cadia Hill pit, local W-striking faults produced half-graben basins that contain Waugoola Group sedimentary rocks. The half-graben basin geometry is preserved because these faults were not inverted during Devonian shortening. However, the similarly oriented (W- striking) Pyrite faults in Cadia East do not appear to control depositional distribution of Waugoola Group rocks, nor are they reflected in faults and folds in the sedimentary cover rocks. It is therefore interpreted that the Pyrite faults were not reactivated following the Benambran Orogeny in the earliest Silurian. This is probably a result of misorientation of W- and NW- striking fault planes to the regional tectonic stress.

N-striking faults of the Cadiangullong fault system and the Gibb fault probably formed as normal faults during extension of the Macquarie Arc (~455 Ma) and remained important in localizing deposition of the Forest Reefs Volcanics (Figure 3.22a). Rifting following the Benambran Orogeny may have reactivated N- striking faults as normal faults (Figure 3.22c, Figure 3.23a). Different stratigraphic levels of the Forest Reefs Volcanics preserved at the unconformity across N- and NE- striking faults provides evidence that these faults were important during rifting (Figure 3.23a-c). This phase of extension generated the basins into which the Silurian Waugoola Group was deposited (Figure 3.22c, Figure 3.23a-c). Renewed E-W shortening during the Devonian Tabberabberan Orogeny (~380 Ma) initiated reverse motion along major basement faults, and tilted, folded and faulted the Waugoola Group cover rocks (Figure 3.22d, Figure 3.23d-e).

NE- striking faults such as Copper Gully and Cat fault formed as normal faults during post-Benambran extension. Sharps Ridge and other fault-related topography developed at this time (Figure 3.23b). Normal slip along these faults during post-orogenic extension influenced basin geometry and controlled deposition of the Waugoola Group. During the Tabberabberan Orogeny, NE-striking structures experienced reverse separation, which produced similarly oriented folds and faults in the overlying Silurian sedimentary cover rocks. During this phase of basin inversion, N-striking faults were also reactivated, and curvilinear fault segments developed connecting the N-striking and NE-striking faults.

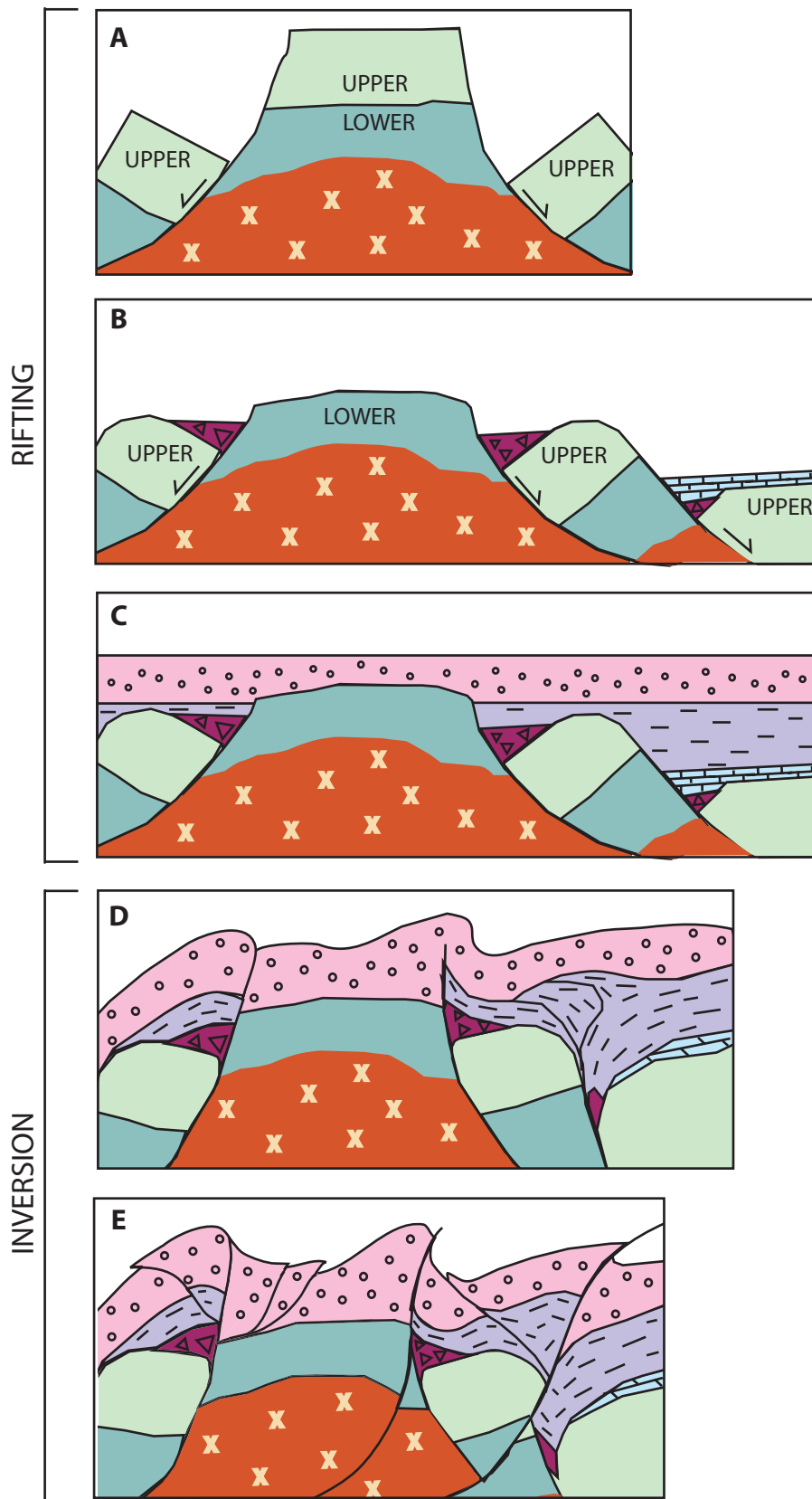


**Figure 3.23:** Tectonic model for rifting and basin inversion in the Cadia District. A: simple fault geometry at the onset of rifting. A local topographic high forms as a horst in the Forest Reefs Volcanics (green). B: Erosion exposes the lower stratigraphy of the Forest Reefs Volcanics (dark green) at the unconformity with the overlying Waugoola Group rocks on topographic highs. Upper Forest Reefs Volcanics (light green) are preserved in relative topographic lows. Clastic units at the base of the Waugoola Group, such as the boulder conglomerate (dark purple) and the calicrudite limestone (light blue) are deposited in local half-graben basins as subsidence continues. C: during the sag phase of the rift-sag sequence, siltstone (light purple) and sandstone (pink) is deposited across the district as basins fill. D: basin inversion begins in the Devonian during Tabberabberan shortening. Faults steepen as they are reactivated and blocks are rotated. Folds and faults form in the sedimentary cover rocks that are parallel to basement faults. E: as shortening continues, older faults are abandoned and thrusting is transferred to new faults that cut through the cover rocks.

## **Basement-Cover Interaction**

Faults that controlled the geometry of the Silurian Waugoola Group sedimentary cover sequence were reactivated as reverse faults during Devonian shortening. Basins into which the Waugoola Group was deposited were inverted. Differences in the relative strength of basement and cover rocks as well as irregularities in the shape of the unconformity produced complexity at the interface. During thrusting, basement fault blocks were displaced and rotated relative to one another, which tilted the cover sequence down to the west. Steep basement faults flatten approaching the surface, up into the cover rocks; shortening is accommodated along multiple detachments including the unconformity and along low angle bedding-parallel faults. Deformation is dispersed through the cover sequence via a complex network of relatively small-scale faults and folds that are related to major faults at depth. The intensity of deformation in the sedimentary cover rocks increases approaching major basement structures. Therefore, structures measured in the Waugoola Group sedimentary cover rocks can be used to make inferences about the geometry of the underlying basement.

## **Basin Inversion**

Basin inversion occurs when shortening is superposed on an extensional environment (e.g. Williams et al., 1989; Gelabert et al., 2004; Camus, 2006; Butler et al., 2006; Zanchi et al., 2006; Konstantinovskaya et al., 2007). This change in deformation reflects a change in orogen-scale tectonics. In extensional settings, normal faults cause

rotation of older rocks in fault blocks that step out toward the margins of the developing basin along a series of progressively flatter faults (e.g. Konstaninovskaya et al., 2007, and references therein). The sedimentary cover sequence is deposited in the basin at this time. When shortening commences, basin-bounding faults are reactivated as reverse faults. Older basement rocks are rotated and thrust over sedimentary cover rocks along faults that rotate to steeper orientations as the foreland propagates and new faults are formed in the footwall of older faults (Camus, 2002; Camus, 2003). Reactivated basement faults typically flatten as they intersect the sedimentary cover sequence, and may branch out into a number of smaller faults (Camus, 2006). The sedimentary cover sequence is faulted and folded around the basement fault, while the basement blocks behave as relatively rigid blocks that are displaced relative to one another via reverse faults (e.g. Chambers et al., 2004; Molinaro et al., 2005; Grey et al., 2006; Mouthereau and Lacombe, 2006; and references therein). Deformation of basement blocks typically entails both a rotational and a translational component. Basin inversion is globally recognized and can be documented at a variety of scales (Figure 3.24).

In the Cadia district, the geometry of basement and cover fault interaction is consistent with the basin inversion model. Basement faults control the orientation and distribution of faults and folds in the sedimentary cover sequence. Relatively steep basement faults flatten at the unconformity and fan into multiple low-angle detachments. Across the district, basement faults progressively steepen toward the west and northwest, i.e., toward the hanging wall of the next thrust.



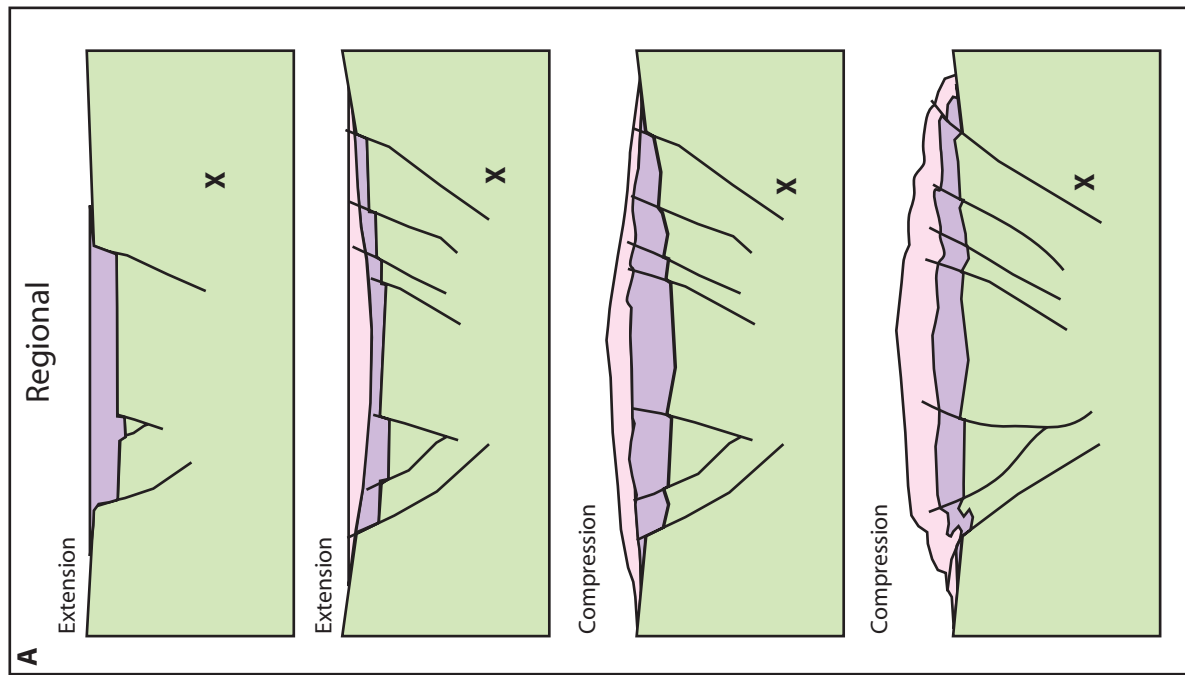
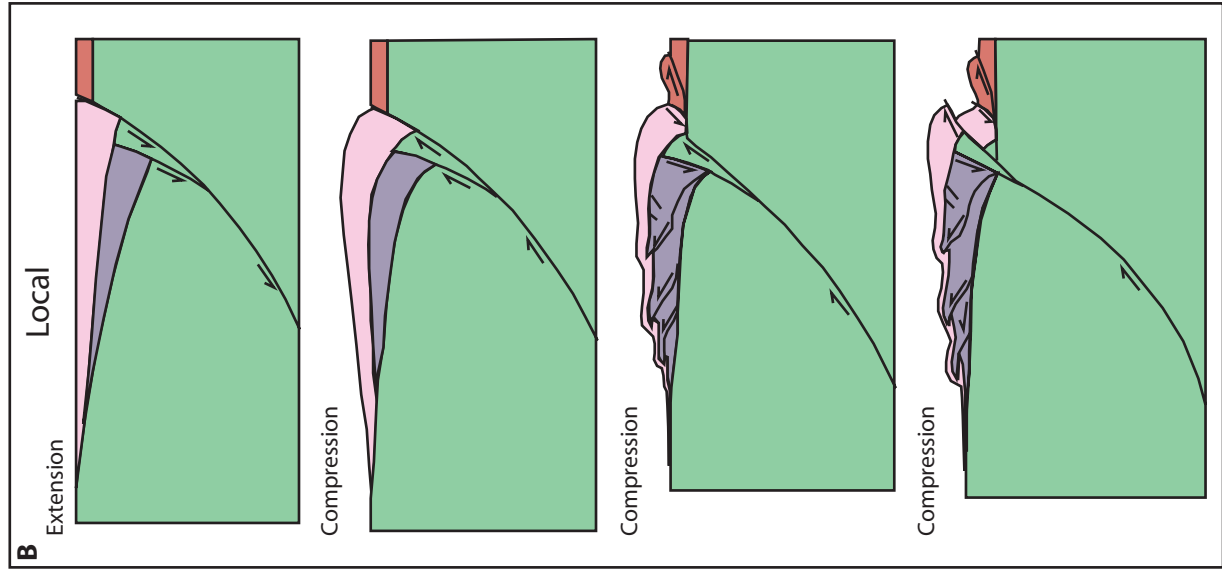


**Figure 3.24:** basin inversion models modified from Konstantinovskaya et al, 2007 (A) and Camus, 2006 (B). A: Orogen-scale phases of basin inversion. Extension leads to normal faulting and basin development. Basins fill progressively as extension continues, and normal faults are rotated to flatter orientations in the center of the basin as new faults form on the margins. When compression commences, normals faults are reactivated as reverse faults. As compression continues, faults break through the sedimentary cover rocks and flatten along the margins. A two-sided orogenic wedge is the result, with steeper thrusts at the core of the orogen and flatter faults toward the margins. B: detail of basin inversion on half-graben geometry produced locally at a single fault, similar to the one shown in position X on figure A. Following basin development and sedimentary cover sequence deposition, compression first causes folding of cover sequence rocks before faults break through. As shortening continues, deformation of the cover sequence intensifies and the fold-thrust geometry becomes more complex. In the Cadia District, half-graben basins on the southern wall of the Cadia Hill pit are not inverted because east-dipping faults are not reactivated. However, major westdipping reverse faults, such as the Cadiangullong Fault and Cat fault produced similar fault geometry to that predicted in the Camus model.



## **Chapter Four: Conclusions**

### **INTRODUCTION**

In the Cadia District, as with many other mineralized systems worldwide, study is focused on the intrusive history, alteration assemblages, and mineralization events (e.g. Holliday et al., 2002; Wilson et al., 2007a; Wilson et al., 2007b). However, this provides information on only a small portion of the district history. It is important to develop a holistic model that accounts for pre- syn- and post mineral evolution of the district in order to fully understand the ore deposits, especially in areas with a complex geologic history.

Stratigraphic reconstructions of the Ordovician basement in the Cadia District have improved the district scale structural model (e.g. Wilson, 2003; Harris, 2007a). Likewise, refining the stratigraphy of the Waugoola Group sedimentary cover sequence has been critical in understanding post-mineral deformation. Recognition of facies variations, particularly in the basal unit, has provided constraints on the paleogeography of the district, and has demonstrated the importance of basement faults in controlling basin geometry (Wilson, 2003; Harris, 2007b).

Based on the stratigraphy of the Waugoola Group cover rocks, it is possible to better understand the faults and folds at the surface and the relationship to basement faults. At the unconformity, moderate-to-steeply dipping basement faults flatten and branch out into a complex network of detachments that disrupt the tilted sedimentary cover package. This geometry suggests that post-mineral deformation was characterized

by basin inversion. Therefore, not only can the faults and folds in the Waugoola Group sedimentary cover sequence be used to characterize post-mineral deformation and orebody dismemberment, but they provide new insight into the protracted influence of basement faults on the structural architecture of the Cadia District.

## CONCLUSIONS

**1) Paleo-topography related to basement faults controlled distribution of Silurian sedimentary lithologies.** Major, through-going basement structures controlled basin geometry, defined depositional regimes, and influenced facies distribution in the Cadia District. In particular, half-graben basins and fault-scarps have been recognized as sedimentological boundaries. Variations in the basal unit across the Cadia District provide evidence that significant topography was present at the onset of Waugoola Group deposition in the Late Silurian.

The Waugoola Group in the Cadia District represents a rift-sag sequence. Fault related topography that controlled the deposition of lower clastic units of the Waugoola Group stratigraphy in the Cadia District was overwhelmed by marine sedimentation as local basins filled. The transition from isolated basins into regional marine transgression recorded by the Waugoola Group represents the thermal evolution of the extending crust.

**2) Orientation of structures in the sedimentary cover sequence is controlled by basement faults.** Major faults in the basement rocks of the Cadia District are similar in orientation and spatially related to faults and folds in the Waugoola Group cover rocks.

Faults and folds in the cover succession formed as a result of E-W directed shortening during the Devonian Tabberabberan Orogeny. Inversion of sedimentary basins occurred at this time, and N- and NE-striking basement faults experienced reverse movement.

Thrusting along basement faults and rotation of basement fault blocks resulted in tilting of the Waugoola Group sedimentary cover rocks down to the west. Steeply dipping basement faults flatten at the unconformity and shortening is accommodated in the cover rocks along slip surfaces at a low angle to bedding, including the unconformity. Where basement faults break through, deformation of the cover rocks is intense. Intra-cover faults and folds are parallel to the controlling basement fault. Where basement faults do not penetrate the cover rocks, open folds are produced. Differences in fault and fold geometry reflect rheological contrasts between adjacent rocks.

**3) Basement faults formed prior to deposition of the Waugoola Group and have probably been reactivated multiple times throughout the tectonic history of the Cadia District.** Major faults in the Cadia District can be grouped into three sets based on orientation and relative timing relationships. The earliest faults were W- and NW-striking and are parallel to the Lachlan Transverse Zone. These faults were important in mineralization at Ridgeway and Cadia East (E.g. Holliday et al., 2002; Wilson, 2003; Wilson et al., 2007b). Additionally, the NW- elongation of the Cadia Intrusive Complex and the NW-trending corridor in which deposits are localized at the district-scale suggest that this fabric developed as early as ~435 Ma (Wilson, 2003; Harris, 2007a).

N-striking faults, including the regionally significant Cadiangullong Fault System, formed during deposition of the Forest Reefs Volcanics. These faults controlled the

distribution of volcanic facies across the district, and therefore formed at least as early as the late Ordovician-early Silurian (Harris, 2007b). NE-striking faults in the Cadia District formed during rifting as a result of difficulty propagating N-striking faults through the relatively strong Cadia Intrusive Suite. NE- and N- striking faults connected during basin inversion, producing the curved step-over fault geometry preserved today.

Intrusive rocks associated with mineralization in the Cadia District and the enclosing host rocks were uplifted and eroded in the early Silurian. A transition to an extensional environment occurred when rifting commenced at ~428 Ma. Basin evolution in the Cadia District is recorded by the Late Silurian Waugoola Group. N- and NE-striking faults experienced normal slip during post-mineral extension and controlled the geometry of basins into which Waugoola Group rocks in the Cadia District were deposited. Subsequent Devonian shortening during the Tabberabberan Orogeny resulted in basin inversion and produced faults and folds in the cover sequence parallel to underlying basement faults. Because W- striking faults were not oriented favorably to the E-W shortening direction, they were not reactivated at this time, and are therefore not manifested in the cover sequence.

## **IMPLICATIONS**

### **Post-mineral Deformation and Orebody Dismemberment**

Post-mineral deformation affects the preservation potential of ore deposits, and must therefore be taken into account when considering exploration strategies. The dismemberment of ore systems by faults has been documented globally in both extensional and compressional settings. For example, normal faults related to Basin-and-Range extension in Nevada have dismembered and effectively rotated the Yerington porphyry system 90° (e.g. Dilles and Proffett, 1995). The Potrerillos deposit in Chile is dismembered by thrust faults (Davidson et al., 1991; Thompson et al., 2004). Similarly, orebody dismemberment due to post-mineral deformation has played an important role in the Cadia District.

Mineral deposits at Ridgeway, Cadia Hill, and Cadia East are separated by major basement faults with a prolonged history of reactivation in extensional and compressional environments. Reconstructions of the enclosing stratigraphy show that each deposit represents a different level in the intrusive system (e.g. Holliday et al., 2002; Wilson et al., 2006; Harris, 2007a). N- and NE-striking faults, including the Cadiangullong and Gibb faults, are responsible for dismemberment of the ore system. Post-mineral slip along these faults determines the preservation potential of ore deposits in the Cadia District. However, present-day configuration of faults and apparent displacement does not necessarily represent only post-mineral deformation, because faults were active prior to mineralization and were subsequently reactivated. Therefore, it is critical to



understand the role of these faults throughout the history of the district to constrain the magnitude of orebody dismemberment. Relationships in the Waugoola Group sedimentary cover sequence were instrumental in recognizing the importance of fault reactivation, and will continue to provide insight into post-mineral deformation as the structural model for the Cadia District evolves.

### **Using Structure in the Cover Sequence to Understand the Basement**

Faults and folds in the Waugoola Group rocks are related to underlying basement faults. Therefore, the orientation and nature of faults and folds in the Silurian sedimentary cover sequence can be used as a predictive tool to identify Ordovician faults at depth. Basement faults are expressed in the cover rocks as steep to moderately dipping planes that cut Waugoola Group bedding at a high angle and juxtapose different units in the Waugoola Group stratigraphy. Thrust faults in the cover rocks strike parallel to, and dip toward controlling basement faults.

Folds in the cover rocks are commonly associated with underlying basement faults. Where basement faults fail to penetrate the cover rocks, open folds are present. Local, minor folds related to basement- and intra-cover faults have also been identified. Folds in siltstone are generally tighter than folds in sandstone. Fold hinges trend parallel to underlying basement faults. Asymmetrical folds may provide a sense of vergence, with the steeper limb closer to the related fault. The intensity of folds and faults in the cover rocks increases proximal to basement faults.

There are some limitations associated with using faults and folds measured at the surface in the sedimentary cover rocks to identify basement faults. First, the dip of basement faults is steeper than corresponding faults in the cover rocks. Consequently, faults at the surface can not be projected through the basement. If the thickness of the cover rocks is known, faults measured at the surface can be projected to the unconformity. Likewise, basement faults measured in drillcore cannot be projected through the cover rocks.

Second, only faults that were reactivated following deposition of the Silurian Waugoola Group can be identified using faults and folds in the cover rocks. W-striking faults, such as the Pyrite faults at Cadia East, do not appear in the cover rocks. As a result, W-striking faults were not reactivated during post-mineral deformation. This is probably due to the misorientation of these faults to the dominant shortening direction. While this provides insight into the hierarchy of faults in the Cadia District, it restricts the predictive capability of faults and folds in the cover rocks.

In addition to structural measurements, stratigraphic observations in the Waugoola Group sedimentary cover sequence can provide insight into faults in the underlying basement. Boulder conglomerate at the base of the Waugoola Group is interpreted as fault scarp deposits. Therefore, where the boulder conglomerate is present at the surface, basement faults are probably present at depth. Variations in the basal unit across the district reflect different depositional environments due to fault related topography, and therefore may also delineate faults.

Because basement faults were reactivated during post-mineral deformation, analysis of faults and folds in the cover rocks can help to understand the structural

architecture of the district. Additionally, structural data obtained from surface exposed of the Waugoola Group sedimentary cover sequence can be used to better design drill programs, identify potential geotechnical problems, and target subsurface water sources.

## **FUTURE WORK**

Refining the stratigraphy of the Waugoola Group in the Cadia District has improved the understanding of paleogeography in the Silurian. Further improvements in the stratigraphy may continue to constrain the timing of deformation and basin evolution in the Cadia District. For example, a detailed study of carbonate facies in the basal limestone and calcirudite across Cadia East may provide insight into local irregularities in the unconformity. Additionally, improved age constraints on depositional stages can be obtained through continued fossil work and zircon provenance studies in sandstone and arkose units. Finally, comparison of Waugoola Group stratigraphy from the Cadia District with regional occurrences can broaden the understanding of rifting and basin development during the Silurian and place the Cadia District into a tectonic context.

Testing the predictive capability of faults and folds in the cover rocks by continued surface mapping and comparison with basement faults identified in drillcore data is a logical next step. Additionally, comparison of structural orientations, including veins and faults, in both basement and cover rocks across structural domains could provide insight into fault block rotation and orebody dismemberment. This would be particularly useful in Cadia Hill, where the deposit is completely fault-bounded. In

general, characterizing the structural evolution of the Cadia District can place the ore system in a tectonic context and provide insight into present-day ore distribution.

## References

- Betts P.G., Lister G.S., 2001. Comparison of the "strike-slip" versus the "episodic-rift-sag" models for the origin of the Isa Superbasin. *Australian Journal of Earth Sciences* 48, 265-280.
- Bierlein F.P., Gray D.R., Foster D.A., 2002. Metallogenic relationships to tectonic evolution; the Lachlan Orogen, Australia. *Earth and Planetary Science Letters* 202, 1-13.
- Bischoff G.C.O., 1986. Early and Middle Silurian conodonts from midwestern New South Wales. *CFS.Courier Forschungsinstitut Senckenberg* 89, 337.
- Butler R.W.H., Holdsworth R.E., Matthews S.J., 2006. Styles of basement involvement in the Moine thrust belt, NW Scotland; Styles of continental contraction. *Special Paper - Geological Society of America* 414, 133-151.
- Camus F., 2003. Debemos encontrar herramientas mas eficientes para explorar los porfidos. We need more efficient tools for porphyry copper exploration. *Mineria Chilena* 23, 125.
- Camus F., 2002. The Andean porphyry systems; Giant ore deposits; characteristics, genesis and exploration. *Special Publication - Centre for Ore Deposit and Exploration Studies (CODES)* 4, 5-21.
- Camus, F., 2006. The Andean porphyry copper systems; in *Great Metallogenic Provinces of the World*, The University of British Columbia, Mineral Deposit Research Unit Short course, Vancouver.
- Cawood P.A., 2005. Terra Australis Orogen; Rodinia breakup and development of the Pacific and Iapetus margins of Gondwana during the Neoproterozoic and Paleozoic. *Earth-Science Reviews* 69, 249-279.
- Chambers J.L.C., Carter I., Cloke I.R., Craig J., Moss S.J., Paterson D.W., 2004. Thin-skinned and thick-skinned inversion-related thrusting; a structural model for the Kutai Basin, Kalimantan, Indonesia; Thrust tectonics and hydrocarbon systems. *AAPG Memoir* 82, 614-634.

- Coney P.J., 1992. The Lachlan belt of eastern Australia and Circum-Pacific tectonic evolution; The Palaeozoic eastern margin of Gondwanaland; tectonics of the Lachlan fold belt, southeastern Australia and related orogens. *Tectonophysics* 214, 1-25.
- Cooke D.R., Hollings P., Walshe J.L., 2006a. Tectonic triggers for giant porphyry and epithermal deposits of the Circum-Pacific region; Abstracts of the 16th annual V. M. Goldschmidt conference. *Geochimica et Cosmochimica Acta* 70, A110.
- Cooke D.R., Wilson A.J., Harper B.J., Deyell C.L., 2006b. Sulfur isotopic zonation in the Cadia porphyry Au-Cu deposits, NSW; Abstracts of the 16th annual V. M. Goldschmidt conference. *Geochimica et Cosmochimica Acta* 70, A110.
- Cooke D.R., Wilson A.J., House M.J., Wolfe R.C., Walshe J.L., Lickfold V., Crawford A.J., 2007. Alkaline porphyry Au-Cu and associated mineral deposits of the Ordovician to Early Silurian Macquarie Arc, New South Wales; Geological evolution and metallogenesis of the Ordovician Macquarie Arc, Lachlan Orogen, New South Wales. *Australian Journal of Earth Sciences* 54, 445-463.
- Cooke D.R., Hollings P., Walshe J.L., 2005. Giant porphyry deposits; characteristics, distribution, and tectonic controls; A special issue devoted to giant porphyry-related mineral deposits. *Economic Geology and the Bulletin of the Society of Economic Geologists* 100, 801-818.
- Cooke D.R., Wilson A.J., Davies A.G.S., 2004. Characteristics and genesis of porphyry copper-gold deposits; 24 ct Au workshop. Special Publication - Centre for Ore Deposit and Exploration Studies (CODES) 5, 17-34.
- Davidson J., Mpodozis C., Sillitoe R.H., Camus F., 1991. Regional geologic setting of epithermal gold deposits, Chile; A special issue devoted to gold deposits in the Chilean Andes. *Economic Geology and the Bulletin of the Society of Economic Geologists* 86, 1174-1186.
- Dilles J.H., Einaudi M.T., 1992. Wall-rock alteration and hydrothermal flow paths about the Ann-Mason porphyry copper deposit, Nevada; a 6-km vertical reconstruction. *Economic Geology and the Bulletin of the Society of Economic Geologists* 87, 1963-2001.



- Dilles J.H., Gans P.B., 1995. The chronology of Cenozoic volcanism and deformation in the Yerington area, western Basin and Range and Walker Lane. *Geological Society of America Bulletin* 107, 474-486.
- Dilles J.H., Proffett J.M., 1995. Metallogenesis of the Yerington Batholith, Nevada; Porphyry copper deposits of the American Cordillera. *Arizona Geological Society Digest* 20, 306-315.
- Direen N.G., Crawford A.J., 2003. The Tasman Line; where is it, what is it, and is it Australia's Rodinian breakup boundary? *Australian Journal of Earth Sciences* 50, 491-502.
- Dore A.G., Stewart I.C., 2002. Similarities and differences in the tectonics of two passive margins; the Northeast Atlantic margin and the Australian North West Shelf; The sedimentary basins of Western Australia 3; proceedings of the West Australian basins symposium [modified]. The = Sedimentary Basins of Western Australia: Proceedings of Petroleum Exploration Society of Australia Symposium 3, 89-117.
- Fergusson C.L., Coney P.J., 1992. Convergence and intraplate deformation in the Lachlan fold belt of southeastern Australia; The Palaeozoic eastern margin of Gondwanaland; tectonics of the Lachlan fold belt, southeastern Australia and related orogens. *Tectonophysics* 214, 417-439.
- Fergusson C.L., VandenBerg A.H.M., 1990. Middle Palaeozoic thrusting in the eastern Lachlan fold belt, southeastern Australia; Australasian tectonics. *Journal of Structural Geology* 12, 577-589.
- Finlayson D.M., Korsch R.J., Glen R.A., Leven J.H., Johnstone D.W., 2002. Seismic imaging and crustal architecture across the Lachlan transverse zone, a possible early cross-cutting feature of eastern Australia; Evolution of the Tasmanides, eastern Australia. *Australian Journal of Earth Sciences* 49, 311-321.
- Forster D.B., Secombe P.K., Phillips D., 2004. Controls on skarn mineralization and alteration at the Cadia deposits, New South Wales, Australia. *Economic Geology and the Bulletin of the Society of Economic Geologists* 99, 761-788.
- Foster D.A., Gray D.R., Bucher M., 1999. Chronology of deformation within the turbidite-dominated, Lachlan Orogen; implications for the tectonic evolution of eastern Australia and Gondwana. *Tectonics* 18, 452-485.

- Foster D.A., Gray D.R., Kwak T.A.P., Bucher M., Arne D.C., 1998. Chronology and tectonic framework of turbidite-hosted gold deposits in the Western Lachlan fold belt, Victoria; A-40/Ar-39; Mesothermal gold mineralization in space and time. *Ore Geology Reviews* 13, 229-250.
- Gelabert, B., Sabat, F., Hardy, S., Rodriguez-Perea, A. 2004. Significance of inherited normal faults during inversion tectonics: an example from the Tramuntana Range, Mallorca. *Geodinamica Acta* 17/6.
- Glen R.A., 1995. Thrusts and thrust-associated mineralization in the Lachlan Orogen; A special issue on the metallogeny of the Tasman fold belt system of eastern Australia. *Economic Geology and the Bulletin of the Society of Economic Geologists* 90, 1402-1429.
- Glen R.A., 1992. Thrust, extensional and strike-slip tectonics in an evolving Palaeozoic orogen; a structural synthesis of the Lachlan Orogen of southeastern Australia; The Palaeozoic eastern margin of Gondwanaland; tectonics of the Lachlan fold belt, southeastern Australia and related orogens. *Tectonophysics* 214, 341-380.
- Glen R.A., Crawford A.J., Cooke D.R., 2007a. Tectonic setting of porphyry Cu-Au mineralisation in the Ordovician-Early Silurian Macquarie Arc, eastern Lachlan Orogen, New South Wales; Geological evolution and metallogenesis of the Ordovician Macquarie Arc, Lachlan Orogen, New South Wales. *Australian Journal of Earth Sciences* 54, 465-479.
- Glen R.A., Crawford A.J., Percival I.G., Barron L.M., 2007b. Early Ordovician development of the Macquarie Arc, Lachlan Orogen, New South Wales; Geological evolution and metallogenesis of the Ordovician Macquarie Arc, Lachlan Orogen, New South Wales. *Australian Journal of Earth Sciences* 54, 167-179.
- Glen R.A., Dallmeyer R.D., Black L.P., 1992. Isotopic dating of basin inversion; the Palaeozoic Cobar Basin, Lachlan Orogen, Australia; The Palaeozoic eastern margin of Gondwanaland; tectonics of the Lachlan fold belt, southeastern Australia and related orogens. *Tectonophysics* 214, 249-268.

- Glen R.A., Hancock P.L., Whittaker A., 2005. Basin inversion by distributed deformation; the southern margin of the Bristol Channel basin, England. *Journal of Structural Geology* 27, 2113-2134.
- Glen R.A., Korsch R.J., Direen N.G., Jones L.E.A., Johnstone D.W., Lawrie K.C., Finlayson D.M., Shaw R.D., 2002. Crustal structure of the Ordovician Macquarie Arc, eastern Lachlan Orogen, based on seismic-reflection profiling; Evolution of the Tasmanides, eastern Australia. *Australian Journal of Earth Sciences* 49, 323-348.
- Glen R.A., Meffre S., Scott R.J., 2007c. Benambran Orogeny in the eastern Lachlan Orogen, Australia; Geological evolution and metallogenesis of the Ordovician Macquarie Arc, Lachlan Orogen, New South Wales. *Australian Journal of Earth Sciences* 54, 385-415.
- Glen R.A., Walshe J.L., 1999. Cross-structures in the Lachlan Orogen; the Lachlan transverse zone example. *Australian Journal of Earth Sciences* 46, 641-658.
- Glen R.A., Walshe J.L., Barron L.M., Watkins J.J., 1998. Ordovician convergent-margin volcanism and tectonism in the Lachlan sector of East Gondwana. *Geology (Boulder)* 26, 751-754.
- Glen R.A., Watkins J.J., 1999. Implications of Middle Devonian deformation of the eastern part of the Hill End Trough, Lachlan Orogen, New South Wales. *Australian Journal of Earth Sciences* 46, 35-52.
- Glen R.A., 2005. The Tasmanides of eastern Australia; Terrane processes at the margins of Gondwana. *Geological Society Special Publications* 246, 23-96.
- Gray D.R., Cull J.P., 1992. Thermal regimes, anatexis, and orogenesis; relations in the western Lachlan fold belt, southeastern Australia; The Palaeozoic eastern margin of Gondwanaland; tectonics of the Lachlan fold belt, southeastern Australia and related orogens. *Tectonophysics* 214, 441-461.
- Gray D.R., and Foster D.A., 2004. Tectonic evolution of the Lachlan Orogen, southeast Australia: historical review, data synthesis and modern perspectives. *Australian Journal of Earth Sciences* 51, 773-817.

- Gray D.R., Foster D.A., 1998. Character and kinematics of faults within the turbidite-dominated Lachlan Orogen; implications for tectonic evolution of eastern Australia. *Journal of Structural Geology* 20, 1691-1720.
- Gray D.R., Foster D.A., Korsch R.J., Spaggiari C.V., 2006. Structural style and crustal architecture of the Tasmanides of eastern Australia; example of a composite accretionary orogen; Styles of continental contraction. *Special Paper - Geological Society of America* 414, 119-132.
- Gray N., Mandyczewsky A., Hine R., 1995. Geology of the zoned gold skarn system at Junction Reefs, New South Wales; A special issue on the metallogeny of the Tasman fold belt system of eastern Australia. *Economic Geology and the Bulletin of the Society of Economic Geologists* 90, 1533-1552.
- Green, D.G., 1999, The geology and origin of the Big Cadia skarn, NSW, Australia: Unpublished B.Sc. Honors thesis, Hobart, University of Tasmania, 154 p.
- Harris A.C., 2007a. 'A 'working' district-scale structural model for the Cadia Valley' End of Year Meeting October 2007, Cadia Valley Alkalic Porphyry Ore Deposits: Deconstructing the System Architecture, ARC Centre of Excellence in Ore Deposits & Newcrest Mining Limited, Orange NSW, 10.1-10.16.
- Harris A.C., 2007b. 'Building the Cadia Valley Volcanic Architecture' End of Year Meeting October 2007, Cadia Valley Alkalic Porphyry Ore Deposits: Deconstructing the System Architecture, ARC Centre of Excellence in Ore Deposits & Newcrest Mining Limited, Orange NSW, 5.1-5.23.
- Hill D., 1951. Geology. In: Mack G.. *Handbook of Queensland*, pp. 13-24. Australian Association for the Advancement of Science, Brisbane.
- Holliday J.R., Wilson A.J., Blevin P.L., Tedder I.J., Dunham P.D., Pfitzner M., 2002. Porphyry gold-copper mineralisation in the Cadia District, eastern Lachlan fold belt, New South Wales, and its relationship to shoshonitic magmatism. *Mineralium Deposita* 37, 100-116.
- Hood D.I.A., Durney D.W., 2002. Sequence and kinematics of multiple deformation around Taemas Bridge, eastern Lachlan fold belt, New South Wales; Evolution of the Tasmanides, eastern Australia. *Australian Journal of Earth Sciences* 49, 291-309.

- Hough, M.A. Bierlein, F.P., Wilde, A.R., 2007. A review of the metallogeny and tectonics of the Lachlan Orogen. *Mineralium Deposita* 42, 435-448.
- Jaques A.L., Jaireth S., Walshe J.L., 2002. Mineral systems of Australia; an overview of resources, settings and processes; Geodynamics of Australia and its mineral systems; technologies, syntheses and regional studies. *Australian Journal of Earth Sciences* 49, 623-660.
- Jenkins C.J., 1978. Llandovery and Wenlock stratigraphy of the Panuara area, central New South Wales. *Proceedings of the Linnean Society of New South Wales* 102, 109-130.
- Kitto, J.C., 2005. Lithostratigraphy, alteration, and geochemistry at the Cadia East Au-Cu porphyry deposit, NSW. BSc. Honors Thesis. University of Tasmania, Australia.
- Konstantinovskaya E.A., Harris L.B., Poulin J., Ivanov G.M., 2007. Transfer zones and fault reactivation in inverted rift basins; insights from physical modelling. *Tectonophysics* 441, 1-26.
- Kusznir N.J., Williams G.D., 1989. Geometric, thermal and isostatic constraints on basin inversion; Inversion tectonics meeting. *Geological Society Special Publications* 44, 355.
- Large R., McGoldrick P., Bull S., Cooke D., 2004. Proterozoic Stratiform Sediment-Hosted Zinc-Lead-Silver Deposits of Northern Australia. In: Deb, M., Goodfellow, W.D. (Eds.), *Sediment-Hosted Lead-Zinc Sulphide Deposits; Attributes and Models of some Major Deposits in India, Australia and Canada*. Narosa Publishing House, New Delhi, India (IND), India (IND).
- Li Z., Powell C.M., 2001. An outline of the palaeogeographic evolution of the Australasian region since the beginning of the Neoproterozoic. *Earth-Science Reviews* 53, 237-277.
- Martins-Neto M.A., 2000. Tectonics and sedimentation in a Paleo/Mesoproterozoic rift-sag basin (Espinhaço Basin, southeastern Brazil). *Precambrian Research* 103, 147-173.
- Martins-Neto M.A., Pedrosa-Soares A.C., Lima S.A.A., Eriksson P.G.(., Catuneanu O.(., Aspler L.B.(., Chiarenzelli J.R.(., Martins-Neto M.A.(., 2001. Tectono-sedimentary evolution of sedimentary basins from late Paleoproterozoic to late

- Neoproterozoic in the Sao Francisco Craton and Aracuai fold belt, eastern Brazil; The influence of magmatism, tectonics, sea level change and paleo-climate on Precambrian basin evolution; change over time. *Sedimentary Geology* 141-142, 343-370.
- Meffre S., Scott R.J., Glen R.A., Squire R.J., 2007. Re-evaluation of contact relationships between Ordovician volcanic belts and the quartz-rich turbidites of the Lachlan Orogen; Geological evolution and metallogenesis of the Ordovician Macquarie Arc, Lachlan Orogen, New South Wales. *Australian Journal of Earth Sciences* 54, 363-383.
- Miller J.M., Dugdale L.J., Wilson C.J.L., 2001. Variable hangingwall palaeotransport during Silurian and Devonian thrusting in the western Lachlan fold belt; missing gold lodes, synchronous Melbourne trough sedimentation and Grampians Group fold interference. *Australian Journal of Earth Sciences* 48, 901-909.
- Miller J.M., Wilson C.J.L., 2002. The Magdala lode system, Stawell, southeastern Australia; structural style and relationship to gold mineralization across the western Lachlan fold belt. *Economic Geology and the Bulletin of the Society of Economic Geologists* 97, 325-349.
- Miller J.M., Wilson C.J.L., Blenkinsop T.G., Vearncombe J.R., Reddy S.M., 2004. Structural analysis of faults related to a heterogeneous stress history; reconstruction of a dismembered gold deposit, Stawell, western Lachlan fold belt, Australia; Applied structural geology for mineral exploration and mining. *Journal of Structural Geology* 26, 1231-1256.
- Molinaro M., Leturmy P., Guezou J.C., de Lamotte D.F., Eshraghi S.A., 2005. The structure and kinematics of the southeastern Zagros fold-thrust belt, Iran; from thin-skinned to thick-skinned tectonics. *Tectonics* 24, 19.
- Mouthereau F., Lacombe O., 2006. Inversion of the Paleogene Chinese continental margin and thick-skinned deformation in the western foreland of Taiwan; Tectonic inversion and structural inheritance in mountain belts. *Journal of Structural Geology* 28, 1977-1993.



- O'Dea M.G., Lister G.S., Betts P.G., Pound K.S., 1997. A shortened intraplate rift system in the Proterozoic Mount Isa Terrane, NW Queensland, Australia. *Tectonics* 16, 425-441.
- Offler R., Gamble J., 2002. Evolution of an intra-oceanic island arc during the Late Silurian to Late Devonian, New England fold belt; Evolution of the Tasmanides, eastern Australia. *Australian Journal of Earth Sciences* 49, 349-366.
- Olsen, P. E., 1997. Stratigraphic record of the early Mesozoic breakup of Pangea in the Laurasia-Gondwana rift system: *Annual Reviews of Earth and Planetary Science*, v. 25, p. 337-401.
- Packham G.H., 1999. Radiometric evidence for Middle Devonian inversion of the Hill End Trough, Northeast Lachlan fold belt. *Australian Journal of Earth Sciences* 46, 23-33.
- Packham G., Percival I., Bischoff G., 1999. Age constraints on strata enclosing the Cadia and junction reefs ore deposits of central New South Wales, and tectonic implications. *Quarterly Notes - Geological Survey of New South Wales* 110, 1-12.
- Percival I.G., Glen R.A., 2007. Ordovician to earliest Silurian history of the Macquarie Arc, Lachlan Orogen, New South Wales; Geological evolution and metallogenesis of the Ordovician Macquarie Arc, Lachlan Orogen, New South Wales. *Australian Journal of Earth Sciences* 54, 143-165.
- Perkins C., Walshe J.L., Morrison G., 1995. Metallogenic episodes of the Tasman fold belt system, eastern Australia; A special issue on the metallogeny of the Tasman fold belt system of eastern Australia. *Economic Geology and the Bulletin of the Society of Economic Geologists* 90, 1443-1466.
- Pogson D.J., Watkins J.J., 1998. Bathurst geological sheet 1:250 000. 1:250000 Geological Sheets Series.Explanatory Notes SI/55-8, 430.
- Powell C.M., 1983. Tectonic relationship between the Late Ordovician and Late Silurian palaeogeographies of southeastern Australia. *Journal of the Geological Society of Australia* 30, 353-373.
- Powell C.M., 1984. Tectonic Evolution of the Tasman Fold Belt, with Emphasis on Palaeozoic Implications for Tasmania; Mineral Exploration and Tectonic Processes in Tasmania; Abstract Volume and Excursion Guide. In: Baillie, P.W.,

- Collins, P.L.F. (Eds.), Mineral Exploration and Tectonic Processes in Tasmania, Burnie, Tasmania, Australia (AUS) (Geol. Soc. Aust., Tasmania, Australia (AUS)).
- Reed A.R., Calver C., Bottrill R.S., 2002. Palaeozoic suturing of eastern and western Tasmania in the West Tamar region; implications for the tectonic evolution of Southeast Australia. *Australian Journal of Earth Sciences* 49, 809-830.
- Richards J.P., 2003. Tectono-magmatic precursors for porphyry Cu-(Mo-Au) deposit formation. *Economic Geology and the Bulletin of the Society of Economic Geologists* 98, 1515-1533.
- Rickards R.B., Percival I.G., Simpson A.J., Wright A.J., 2001. Silurian biostratigraphy of the Cadia area, south of Orange, New South Wales. *Proceedings of the Linnean Society of New South Wales* 123, 173-191.
- Scheibner E., Veevers J.J., 2000. Tasman Fold Belt System. In: Veevers, J.J. (Ed.), *Billion-Year Earth History of Australia and Neighbours in Gondwanaland*. GEMOC Press, Sydney, N.S.W., Australia (AUS), Australia (AUS).
- Schlische, R.W., Withjack, M.O., Austin, J.A., Brown, D.E., Contreras, J., Gierlowski-Kordesch, E., Jansa, L.F., Malinconico, M.L., Smoot, J.P., Wintsch, R.P., 2000. Basin Evolution. In: Olsen, P.E., and Kent, D.V. (Eds.) *Climatic, Biotic, and Tectonic Pole-to-Pole Coring Transect of Triassic-Jurassic Pangea*. International Continental Drilling Program.
- Sibson R.H., 2000. A brittle failure model plot defining conditions for high-flux flow. *Economic Geology and the Bulletin of the Society of Economic Geologists* 95, 41-47.
- Sillitoe R.H., 2002. Some metallogenic features of gold and copper deposits related to alkaline rocks and consequences for exploration. *Mineralium Deposita* 37, 4-13.
- Sillitoe R.H., 2000. Gold-rich porphyry deposits; descriptive and genetic models and their role in exploration and discovery; *Gold in 2000*. *Reviews in Economic Geology* 13, 315-345.
- Spaggiari C.V., Gray D.R., Foster D.A., 2004. Lachlan Orogen subduction-accretion systematics revisited. *Australian Journal of Earth Sciences* 51, 549-553.

- Squire R.J., Crawford A.J., 2007. Magmatic characteristics and geochronology of Ordovician igneous rocks from the Cadia-Neville region, New South Wales; implications for tectonic evolution; Geological evolution and metallogenesis of the Ordovician Macquarie Arc, Lachlan Orogen, New South Wales. *Australian Journal of Earth Sciences* 54, 293-314.
- Squire R.J., Miller J.M., 2003. Synchronous compression and extension in East Gondwana; tectonic controls on world-class gold deposits at 440 Ma. *Geology (Boulder)* 31, 1073-1076.
- Squire R.J., 2001. Volcanological and tectono-magmatic evolution of the Cadia-Neville region, southern Molong volcanic belt, Australia. Doctoral thesis, University of Tasmania, Hobart, Tasmania, Australia (AUS).
- Suppel ., 1998. The Palaeozoic in New South Wales geology and mineral resources. *AGSO journal of Australian geology geophysics* 17, 87.
- Suppel D.W., Barnes R.G., Scheibner E., 1998. The Palaeozoic in New South Wales; geology and mineral resources; Geology and mineral potential of major Australian mineral provinces. *AGSO Journal of Australian Geology and Geophysics* 17, 87-105.
- Thompson J.F.H., Gale V.G., Tosdal R.M., Wright W.A., 2004. Characteristics and formation of the Jeronimo carbonate-replacement gold deposit, Potrerillos district, Chile; Andean metallogeny; new discoveries, concepts, and updates. *Special Publication (Society of Economic Geologists (U.S.))* 11, 75-95.
- Tosdal R.M., Richards J.P., 2001. Magmatic and structural controls on the development of porphyry Cu+ or -Mo+ or -Au deposits; Structural controls on ore genesis. *Reviews in Economic Geology* 14, 157-181.
- Turner J.P., Corbin S.G., 1995. Tertiary uplift of a deep rift-sag basin, Cardigan Bay, offshore Wales, UK; Basin inversion. *Geological Society Special Publications* 88, 587.
- VandenBerg A.H.M., 1999. Timing of orogenic events in the Lachlan Orogen. *Australian Journal of Earth Sciences* 46, 691-701.

- Watson J.M., Gray D.R., 2001. Character, extent and significance of broken formation for the Tabberabbera zone, central Lachlan Orogen. *Australian Journal of Earth Sciences* 48, 943-954.
- Williams E.A., Ford M., Edwards H.E., O'Sullivan M.J., 1989. The Tectono-Sedimentary Evolution of the Late Devonian Munster Basin, South-West Ireland; International Workshop on the Rhenohercynian and Subvariscan Fold Belts; Tectonic Evolution and Genesis of Mineral Deposits; Program and Abstracts. In: Anonymous International Workshop on the Rhenohercynian and Subvariscan Fold Belts, Boppard/Rhein, Federal Republic of Germany (DEU) (Earth Evolution Sci. Interdisciplinary Res. Group, Federal Republic of Germany (DEU)).
- Willis G.F., Tosdal R.M., 1992. Formation of gold veins and breccias during dextral strike-slip faulting in the Mesquite mining district, southeastern California. *Economic Geology and the Bulletin of the Society of Economic Geologists* 87, 2002-2022.
- Willman C.E., VandenBerg A.H.M., Morand V.J., 2002. Evolution of the southeastern Lachlan fold belt in Victoria; Evolution of the Tasmanides, eastern Australia. *Australian Journal of Earth Sciences* 49, 271-289.
- Wilson A.J., 2003. The geology, genesis and exploration context of the Cadia gold-copper porphyry deposits, New South Wales, Australia. Doctoral thesis, University of Tasmania, Hobart, Tasmania, Australia (AUS).
- Wilson A.J., Cooke D.R., Harper B.J., Deyell C.L., 2007a. Sulfur isotopic zonation in the Cadia district, southeastern Australia; exploration significance and implications for the genesis of alkalic porphyry gold-copper deposits; Tectonics to mineral discovery; deconstructing the Lachlan Orogen. *Mineralium Deposita* 42, 465-487.
- Wilson A.J., Cooke D.R., Harper B.L., 2003. The Ridgeway gold-copper deposit; a high-grade alkalic porphyry deposit in the Lachlan fold belt, New South Wales, Australia. *Economic Geology and the Bulletin of the Society of Economic Geologists* 98, 1637-1666.
- Wilson A.J., Cooke D.R., Stein H.J., Fanning C.M., Holliday J.R., Tedder I.J., 2007b. U-Pb and Re-Os geochronologic evidence for two alkalic porphyry ore-forming

events in the Cadia District, New South Wales, Australia. *Economic Geology and the Bulletin of the Society of Economic Geologists* 102, 3-26.

Zanchi A., Berra F., Mattei M., Sabouri J., 2004. Tectonic inversion in the central Alborz, Iran; Italia 2004; 32nd international geological congress; abstracts. *International Geological Congress, Abstracts = Congres Geologique International, Resumes* 32, 85.

## Appendix I: Bedding Data

The following data table represents a compilation of measurements gathered over both the 2006 and 2007 field season. Measurements (in degrees) and corresponding coordinates (given as Easting and Northing) are in Australia Map Grid projection, using the datum AGD66. Strike and dip was measured with a Brunton compass, and measurements were rounded in the field to the nearest 5°. Strike measurements were always taken so that the plane being measured dipped to the right (for example, N-striking planes dip to the E). Where measurement or lithology was uncertain, it is indicated with a question mark.

The “station” column indicates a general geographic area for measurement location. CE=Cadia East, CG=Copper Gully, RC=roadcutting from the Cadia Hill access road, SR=Sharps Ridge, SW=southern wall of Cadia Hill pit, EW=eastern wall of Cadia Hill pit, DP=drill pad (Cadia East or Sharps Ridge).

The “lithology” column indicates what rock type bedding was measured in. Where a bedded contact was measured, units on either side of the contact are separated with an underscore, and the upper unit is listed first. Abbreviations are as follows: si=siltstone, ss=sandstone (undifferentiated), siturb=siltstone-dominant interbedded siltstone and sandstone, ssturb=sandstone-dominant interbedded siltstone and sandstone, mss=massive sandstone, redsi=red siltstone, blksi=black shale, bc=boulder conglomerate, sibx=brecciated siltstone, ord=Ordovician basement (undifferentiated), ark=arkose.

The “measurement” column indicates what feature was measured at each location. Abbreviations used are: bed=bedding, bedcontact=bedding-parallel contact, bedfault=bedding parallel fault, bedfaultcontact=bedding parallel faulted contact. Uncertainty is indicated with a question mark.



station	lithology	measurement	strike	dip	Easting	Northing
CE	si	bed	230	80	686752	6295005
CE	siturb	bed	25	45	686730	6294817
CE	si	bed	25	35	686738	6294812
CE	ss	bed	220	45	686101	6295123
CE	siturb	bed	5	70	686013	6295254
CE	siturb	bed	325	45	686012	6295238
CE	siturb	bed	190	45	686119	6295163
CE	ss	bed	190	25	686387	6295440
CE	ss	bed	190	40	686428	6295363
CE	ss	bed	170	40	686472	6295413
CE	si	bed	175	45	686505	6295668
CE	ss	bed	190	25	686389	6295574
CE	ss	bed	155	30	686290	6295042
CE	siturb?	bed	200	50	686229	6295083
CE	ss	bed	125	30	685819	6295246
CE	ss	bed?	330	65	685736	6295315
CE	ss	bed	200	90	686131	6295632
CG	ss	bed	165	45	687610	6296630
CG	ss	bed	145	50	687570	6296731
CG	ss	bed	135	60	687574	6296729
CG	ss	bed	135	55	687573	6296726
CG	ss	bed	20	50	687572	6296720
CG	ss	bedfault	40	85	687557	6296666
CG	ss_siturb	bedcontact	180	25	687570	6296680
CG	ss	bed	170	40	687527	6296620
CG	ss	bed	160	25	687499	6296542
CG	ss	bed	160	20	687449	6296559
CG	ss	bed	150	25	687451	6296550
CG	ss	bed?	230	70	687289	6296491
CG	ss	bed?	250	10	687289	6296491
CG	ss	bed?	20	60	687398	6296503
CG	ss	bed	220	20	687405	6296490
CG	ss	bed	225	25	687375	6296452
CG	ss	bed	200	10	687349	6296409
CG	ss	bed	230	50	687346	6296408
CG	ss	bed	200	40	687355	6296359
CG	ss	bed	80	65	687403	6296346
CG	siturb	bed	230	30	687456	6296289
CG	ss	bed	225	30	687432	6296250
CG	ss	bed	210	30	687415	6296243
CG	ss	bed	245	60	687376	6296284
CG	ss	bed	220	45	687401	6296305
CG	ss	bed	230	40	687402	6296323
CG	ss	bed	250	60	687356	6296309
CG	ss	bed?	240	50	687352	6296299
CG	siturb	bed	95	65	687355	6296317
CG	ss	bed?	60	45	687346	6296265

station	lithology	measurement	strike	dip	Easting	Northing
CG	ss	bed?	355	25	687283	6296241
CG	siturb	bed	80	35	687282	6296291
CG	ss	bed?	235	25	687252	6296290
CG	ss	bed?	265	25	687233	6296276
CG	ss	bed?	310	25	687185	6296293
CE	si	bed	15	55	686698	6295432
CE	si	bed	240	45	686695	6295432
CE	si	bed	270	40	686699	6295437
CE	si	bed?	225	30	686659	6295445
CE	siturb?	bed?	10	60	686703	6295341
CE	ss?si?	bed	190	15	686663	6295297
CG	sibx?bc?	bed?	290	35	686502	6295858
CG	si	bed	255	45	686479	6295853
CG	si_ark	bed	145	35	686426	6295791
CG	si_ark	bed	140	40	686405	6295774
CG	siturb	bed	200	50	686310	6295726
CG	ss	bed	200	45	686303	6295725
CG	ss	bed	215	55	686242	6295802
CG	ss	bed?	20	35	686329	6295811
CG	ss	bed?	250	40	686370	6295842
CG	ss	bed	220	20	686392	6295888
CG	ss	bed	230	35	686431	6295930
CG	ss	bed?	140	20	686489	6295981
CG	si?siturb?	bed	180	80	686634	6296050
CG	ss?	bed	270	40	686727	6296120
CG	ss	bed?	350	70	686740	6296127
CG	ss	bed?	230	85	686749	6296123
RC	ssturb	bed?	215	45	686193	6294910
RC	ssturb	bed	220	65	686198	6294890
RC	ssturb	bed	190	45	686195	6294891
RC	si	bed	30	75	686203	6294889
RC	ssturb?	bed	240	35	686208	6294872
RC	si	bed	215	15	687034	6294703
RC	si	bed	205	30	686884	6294649
RC	si	bed	200	40	686866	6294648
RC	si	bed	205	25	686857	6294649
RC	si	bed?	190	40	686823	6294654
RC	si	bed	30	55	686787	6294664
RC	si	bed	35	65	686785	6294664
RC	si	bed	200	65	686711	6294698
RC	si	bedfault	185	70	686600	6294751
RC	ark?ss?	bed	230	15	686600	6294752
RC	si	bed	200	25	686593	6294758
RC	si	bed	230	15	686532	6294784
RC	ssturb?	bed	220	30	686489	6294792
RC	si	bed	225	15	686544	6294788
RC	si	bed	210	25	686526	6294802

station	lithology	measurement	strike	dip	Easting	Northing
RC	ssturb	bedfaultcontact	240	10	686516	6294807
RC	si	bed?	250	55	686387	6294866
RC	si	bed	190	20	686397	6294868
RC	si	bed	190	25	686409	6294866
RC	si?ssturb?	bed	190	10	686417	6294872
RC	si?turb?	bed	180	15	686420	6294871
RC	si?turb?	bed	180	5	686425	6294871
RC	si?	bed	185	15	686427	6294878
RC	si?	bed	200	35	686431	6294881
RC	ssturb?	bed	210	5	686440	6294880
SR	ss	bed?	290	30	687031	6296652
SR	ss	bed?	100	16	687002	6296634
SR	ss	bed?	220	60	686941	6296625
SR	ss	bed?	20	20	686940	6296620
SR	ss	bed	35	45	686829	6296548
SR	ss	bed?	70	30	686820	6296504
SR	ss	bed	150	40	686801	6296475
SR	ss?	bed?	135	70	686728	6296474
SR	ss	bed?	220	25	686633	6296496
SR	ssturb?	bed?	140	55	686628	6296494
SR	ssturb?	bed?	220	60	686619	6296493
SR	ssturb?	bed?	115	45	686592	6296504
SR	ssturb	bed	110	45	686578	6296505
SR	si	bed	60	45	686444	6296552
SR	ss	bed	145	35	686439	6296534
SR	ss	bed	145	25	686437	6296533
SR	ss	bed	150	30	686408	6296524
SR	ss	bed	110	25	686355	6296518
SR	ss	bed	130	30	686316	6296498
SR	ss	bed?	200	35	686275	6296547
SR	ss	bed	185	25	686181	6296541
SR	ss?	bed?	330	35	686087	6296563
SR	siturb?	bed	250	90	686077	6296557
SR	ss?	bed	90	35	686080	6296557
SR	ss	bed	110	60	686072	6296546
SR	siturb	bed	270	5	686074	6296506
SR	ssturb?	bed	220	25	686072	6296495
SR	ss	bed	175	25	686100	6296483
SR	ss	bed	110	10	686112	6296455
SR	ss	bed	180	25	686136	6296454
SR	ssturb?	bed	170	30	686173	6296440
SR	ssturb	bed	170	25	686187	6296432
SR	ssturb	bed	170	35	686204	6296425
SR	ssturb	bed	185	30	686223	6296419
SR	ssturb	bed	185	40	686223	6296416
SR	siturb	bed	170	30	686227	6296403
SR	ssturb?	bed	130	25	686262	6296401

station	lithology	measurement	strike	dip	Easting	Northing
SR	ssturb	bed	150	10	686265	6296400
SR	siturb	bed	170	25	686271	6296398
SR	ss	bed	155	35	686271	6296388
SR	ss	bed	170	35	686316	6296367
SR	ss	bed	140	35	686326	6296386
SR	ss	bed?	130	30	686392	6296416
SR	ss	bed?	50	40	686413	6296366
SR	ss	bed?	255	25	686409	6296350
SR	ss	bed?	240	15	686440	6296371
SR	ss	bed?	10	25	686673	6296256
SR	ss	bed?	240	40	686714	6296296
SR	siturb	bed	30	40	686206	6296053
SR	ss?turb?	bed?	170	40	686254	6296087
SR	ssturb	bed	115	35	686270	6296075
SR	si	bed	125	45	686275	6296061
SR	si	bed	105	60	686275	6296053
SR	si	bed	235	15	686275	6296020
SR	si	bed	80	35	686279	6296021
SR	si	bed	355	20	686287	6296011
SR	ss	bedfault	40	90	686256	6295803
SR	si	bed	30	85	686259	6295800
SR	si?turb?	bed	70	40	686232	6296281
SR	siturb	bed	200	70	686207	6296294
SR	siturb	bed	175	30	686198	6296305
SR	siturb	bed	155	20	686196	6296302
SR	si?	bed	155	40	686188	6296305
SR	siturb	bed	175	20	686171	6296310
SR	siturb	bed	160	20	686155	6296306
SR	ssturb	bed	160	20	686148	6296312
SR	siturb	bed	170	10	686130	6296321
SR	ss?turb?	bed	160	10	686112	6296324
SR	ss	bed	190	40	686105	6296328
SR	siturb	bed	180	25	686197	6296294
SR	ss?turb?	bed?	60	40	686175	6296265
SR	ss	bed	65	50	686151	6296206
SR	siturb	bed	55	70	686180	6296166
SR	si?	bed?	55	60	686172	6296140
SR	ss	bed	40	30	686162	6296133
SR	si	bed	45	50	686159	6296084
SR	si	bed	45	45	686159	6296090
SR	ss	bed	45	45	686172	6296070
SR	ss	bed	35	40	686185	6296063
CG	ss	bed?	165	20	687597	6296618
CG	ss	bed?	175	25	687554	6296626
CG	ss	bed	155	30	687556	6296626
CG	ss	bed?	10	60	687561	6296629
CG	ss	bed?	10	70	687559	6296637

station	lithology	measurement	strike	dip	Easting	Northing
CG	ss	bed	210	30	687558	6296662
CG	ss	bed	210	40	687562	6296670
CG	ss	bed	30	60	687563	6296719
CG	ss	bed	150	45	687577	6296725
CG	ss	bed	150	55	687573	6296732
CG	ss	bed	280	55	687582	6296734
CG	ss	bed	135	60	687585	6296738
CG	siturb?	bed?fault?	325	75	687689	6296667
CG	siturb	bed	145	90	687688	6296674
CG	si?	bed	205	30	687690	6296577
CG	si?	bed?	165	60	687753	6296747
CG	siturb?	bed?	20	80	687741	6296747
CG	ssturb?	bed?	310	40	687734	6296769
CG	ssturb	bed	310	45	687726	6296775
CG	ssturb	bed	125	50	687718	6296797
CG	ssturb	bed	320	45	687727	6296798
CG	si?	bed	315	40	687723	6296784
CG	siturb?	bed	290	35	687723	6296774
CG	siturb	bed	270	45	687725	6296767
CG	ss	bed	290	40	687718	6296759
CG	siturb	bed	295	50	687718	6296755
CG	si?turb?	bed	290	40	687715	6296735
RC	si	bed	220	25	687680	6296514
RC	si	bed	190	35	687680	6296518
RC	si	bed	130	25	687678	6296512
RC	si	bed	185	35	687675	6296508
RC	si	bed	205	35	687677	6296500
RC	si	bed	245	35	687674	6296491
RC	si?	bed	200	20	687673	6296477
RC	siturb?	bed	240	55	687674	6296478
RC	ssturb?	bed	230	55	687673	6296468
RC	ssturb?	bed	155	35	687674	6296459
RC	si?turb?	bed	140	30	687674	6296459
RC	si	bed	215	60	687638	6296458
RC	ss	bed	150	45	687639	6296450
RC	ssturb	bed	70	80	687636	6296434
EW	mss	bed	185	40	685973	6296609
EW	siturb	bed	175	30	685959	6296608
EW	ss	bed	155	30	685936	6296606
EW	mss	bedfault	175	30	685866	6296587
SW	ss	bed?	95	20	685495	6295452
SW	bc_ord	bedcontact	110	45	685779	6295558
EW	si	bedfault	80	65	686034	6296154
CG	si?	bed	275	40	686511	6295846
CG	mss	bed	160	30	686395	6295779
CG	ss	bed	145	20	686360	6295638
DP	ss	bed	140	25	686452	6295218

station	lithology	measurement	strike	dip	Easting	Northing
DP	ss	bed	140	25	686530	6295300
DP	sst	bed	195	35	686550	6295394
DP	sst	bed	140	20	686635	6295418
DP	si	bed	150	10	686673	6295294
DP	si	bed	140	30	686727	6295273
RC	ss	bed	215	15	687017	6294691
CE	ss	bed?	250	25	686590	6294952
CE	ss_si	bedcontact?	240	15	686556	6294898
CE	sst	bed	210	30	686740	6294957
CE	si	bed	215	25	686567	6294992
CE	ssturb?	bed	155	20	686470	6295058
CE	sst	bed	165	30	686344	6295076
CE	ssi	bed	200	60	686327	6295079
CE	si?	bed	165	25	686325	6295104
CE	ssturb	bed	150	70	686291	6295097
EW	sst	bed	220	45	685993	6296461
EW	sst	bed	115	40	685992	6296458
CE	mss	bed	180	35	686097	6295063
CE	mss	bed	190	45	686017	6295262
CE	mss	bed	215	45	686048	6295298
CE	ss	bed	185	35	686126	6295227
CE	ss	bed	55	10	686099	6295305
CE	ss	bed	210	40	686073	6295204
CE	ss	bed	175	20	686175	6295537
CE	mss	bed	205	20	686243	6295580
CE	ss	bed	185	30	686359	6295463
CE	si?	bed?	270	25	686425	6295634
CE	si?	bed	175	30	686501	6295661
CE	ss	bed	190	45	686414	6295550
CE	ss	bed	20	25	686392	6295393
CE	mss	bed	200	35	686539	6295453
CE	mss	bed	180	40	686575	6295503
SR	mss	bed?	15	30	686534	6296273
SR	ss	bed?	5	70	686510	6296206
SR	mss	bed?	330	25	686459	6296102
SR	mss	bed?	350	70	686435	6296055
SR	ssturb	bed	45	60	686367	6296041
SR	mss	bed?	315	55	686344	6296077
SR	mss	bed	120	35	686337	6296093
SR	ssturb	bed	45	60	686412	6296115
SR	mss	bed	185	30	686406	6296139
SR	mss	bed	140	45	686398	6296140
SR	mss	bed	135	15	686124	6296255
SR	mss	bed	50	30	686156	6296125
SR	mss	bed	35	40	686168	6296072
SR	siturb	bed	30	45	686202	6296046
SR	blksi?	bed	105	60	686261	6296048



station	lithology	measurement	strike	dip	Easting	Northing
SR	blksi	bed	45	15	686286	6296033
SR	si	bed	55	20	686282	6296036
SR	ss	bed	65	60	687044	6296654
SR	ss	bed	60	60	687011	6296610
SR	ss	bed?	125	25	686992	6296602
SR	ss	bed	60	60	686960	6296607
SR	ss	bed	60	35	686913	6296535
SR	ss	bed	65	20	686882	6296579
SR	ss	bed	100	20	686849	6296514
SR	ss	bed?	275	40	686725	6296452
SR	ss	bed	60	50	686675	6296469
SR	ss	bed?	280	30	686575	6296454
SR	ss	bed	65	30	686431	6296486
SR	ss	bed	225	25	686396	6296402
SR	ss	bed	235	25	686413	6296364
SR	si	bed	70	20	686228	6296277
SR	si	bed	185	30	686195	6296280
SR	ss	bed	65	60	686196	6296264
SR	ss	bed	165	15	686125	6296267
SR	ss	bed	170	15	686135	6296290
RC	ss	bed	205	20	687064	6294700
CG	mss	bed	175	25	687596	6296612
CG	mss	bed	145	30	687557	6296620
CG	mss	bed	140	30	687554	6296631
CG	mss	bed	175	35	687558	6296603
CG	mss	bed	170	40	687545	6296590
CG	mss	bed	205	45	687546	6296575
CG	mss	bed	145	20	687503	6296565
CG	mss	bed	125	20	687402	6296538
CG	mss	bed	155	30	687480	6296537
CG	mss	bed	150	20	687473	6296530
CG	mss	bed	120	25	687459	6296528
CG	mss	bed	225	25	687455	6296527
CG	mss	bed	175	70	687454	6296522
CG	mss	bed	220	35	687451	6296522
CG	mss	bed	140	25	687451	6296527
CG	mss	bed	180	20	687450	6296520
CG	mss	bed	170	20	687436	6296523
CG	mss	bed	230	40	687432	6296520
CG	mss	bedfault	145	40	687430	6296520
CG	mss	bed	140	20	687427	6296522
CG	mss	bed	220	25	687412	6296518
CG	mss	bed	335	45	687420	6296504
CG	mss	bed	275	50	687413	6296518
CG	mss_siturb	bedcontact	230	45	687395	6296504
CG	ss_siturb	bedcontact	225	40	687409	6296498
CG	ss_siturb	bedcontact	220	25	687406	6296498

station	lithology	measurement	strike	dip	Easting	Northing
CG	ss_siturb	bedcontact	220	35	687387	6296494
CG	ss_siturb	bedcontact	210	35	687394	6296475
CG	ss_siturb	bedcontact	205	35	687384	6296475
CG	ss_siturb	bedcontact	220	25	687384	6296476
CG	ss_siturb	bedcontact	215	25	687371	6296451
CG	mss?	bed	210	35	687365	6296411
CG	ssturb	bedcontact	185	25	687364	6296428
CG	mss	bed	210	25	687350	6296413
CG	mss	bed	215	40	687392	6296394
CG	mss	bed	220	25	687381	6296392
CG	mss	bed	210	50	687354	6296372
CG	mss	bed	200	45	687342	6296343
CG	mss	bed	90	75	687334	6296315
CG	mss	bedfault	80	65	687344	6296319
CG	si	bedfault	85	70	687326	6296293
CG	siturb?	bed	195	15	687319	6296282
CG	siturb?	bed	225	60	687178	6296268
CG	ss?	bed	115	50	687155	6296365
CG	ss	bed	180	20	687198	6296211
CG	ss	bed	105	60	686756	6296117
CG	ss	bed	100	45	686731	6296113
CG	si_bc?	bedcontact	290	50	686715	6296007
CG	ss?	bed	220	35	686184	6295693
CG	siturb?	bed	50	85	686215	6295786
CG	mss?	bed	235	70	686221	6295780
CG	bc	bed?	155	20	686207	6295875
CG	mss	bed?	70	40	686116	6296005
CG	mss	bed	125	30	686144	6295862
CG	si	bed	210	35	686143	6295612
CG	mss	bed	195	30	686193	6295569
CG	mss	bed	165	30	686228	6295559
CG	mss	bed	190	35	686234	6295635
CG	mss	bed	150	35	686139	6295610
CG	mss_ssturb	bedcontact	45	85	686258	6295796
CG	siturb?	bed	255	50	687309	6296288
CG	ss	bedfault	290	45	687307	6296300
CG	mss	bed	175	35	687555	6296625
EW	mss	bed	90	60	686016	6296154
RC	siturb	bed	230	15	686331	6294893
RC	si	bed	240	30	686366	6294877
RC	si	bed	165	10	686548.6	6294764
RC	ssturb_si	bedcontact	205	15	686507.6	6294791
RC	ssturb?	bed	215	20	686460.8	6294817
RC	si	bed?	110	10	686714.8	6294686
RC	ssturb?	bed?	60	15	686695.4	6294696
RC	ss?	bed?fault?	210	15	686648.5	6294720
CG	si	bed	290	45	686465.6	6295863

station	lithology	measurement	strike	dip	Easting	Northing
CG	si	bed	145	10	686435.7	6295850
CG	si	bed	155	20	686371	6295753
EW	ssturb?	bed	310	10	685980	6296393
EW	mss	bed	195	25	685960.9	6296435
EW	mss	bed	215	40	685941.7	6296490
CG	sst	bed	205	45	686340.9	6295749
CG	mss	bed	205	25	686265	6295748
CG	mss	bed	180	20	686213.3	6295712
DP	sst	bed	200	35	686381	6295277
DP	ssturb	bed	210	40	686701	6295432
RC	ssturb	bed	220	50	687650.3	6296458
RC	ss	bed	205	20	687658.8	6296382
CE	si	bed	185	30	686534.6	6294967
CE	si	bed	155	15	686505	6295055
CE	ssturb	bed	145	20	686534	6295147
CE	sst	bed	170	30	686345.1	6294958
CE	sst	bed	175	20	686405	6295141
RC	si?	bed	180	20	687263	6295092
RC	sst	bed	180	65	685995.9	6295054
RC	si	bed	190	15	686061	6295043
RC	ssturb	bed	160	35	686127	6295025
EW	ssturb	bed	190	20	685989	6296447
EW	si	bed	90	10	686003.5	6296379
EW	ssturb_si_ord	bedcontact?	275	10	686016	6296332
EW	ssturb	bed	210	50	686035	6296382
EW	mss	bed	225	45	685971	6296500
CE	ss_siturb	bedcontact	215	55	686077.3	6295282
CE	si	bed	85	15	686121	6295310
CE	si	bed	210	30	686123	6295232
CE	ss_siturb	bedcontact	85	30	686123	6295157
CE	ss	bed	155	20	686271	6295308
CE	mss	bed	180	25	686197	6295366
CE	mss	bed	185	20	686135	6295359
CE	ss	bed	205	20	686183	6295562
CE	mss	bed	190	25	686268	6295483
CE	ss	bed	205	35	686332	6295481
CE	mss	bed	180	40	686320	6295567
CE	mss	bed	180	25	686385	6295566
CE	ss	bed	190	20	686442	6295566
CE	si_ssturb	bedcontact	170	20	686409	6295501
CE	ss	bedcontact	110	15	686342	6295411
CE	ss	bed	185	30	686424	6295353
CE	mss	bed	175	35	686464	6295402
CE	mss	bed	175	30	686513	6295483
CE	mss	bed	190	25	686461	6295218
SR	mss	bed	45	25	686508	6296146
SR	ssturb	bed	75	40	686189	6296140

station	lithology	measurement	strike	dip	Easting	Northing
SR	ssturb_si	bedcontact	50	35	686187.9	6296161
SR	mss	bed	75	45	686163.3	6296192
SR	siturb	bed	70	50	686154	6296095
SR	ssturb	bed	55	40	686160	6296085
SR	mss	bed	45	35	686194	6296060
SR	ssturb	bed?	95	55	686260.6	6296082
SR	si_ssturb	bedcontact?	80	30	686268.3	6296082
SR	siturb	bed	265	80	686284.4	6296030
SR	mss	bed	180	60	686270	6295965
SR	mss	bed	155	55	686270	6295944
SR	si	bed	50	50	686188	6296152
SW	ssturb	bed	140	50	685481	6295409
SW	mss_siturb	bedcontact	65	15	685576	6295445
SW	redsi	bed	145	50	685767	6295499
SW	siturb	bed	195	35	685730	6295463
SW	ssturb	bed	195	35	685721	6295460
SW	ss	bed	200	10	685660	6295441
SW	siturb	bed	180	15	685644	6295434
SW	mss	bed	190	30	685674	6295445
SW	ssturb	bed	160	90	685389	6295449
SW	mss_ord	bedcontact	95	15	685488	6295453
SW	ss	bed	195	15	685638	6295477
SW	siturb	bed	170	20	685686	6295494
RC	ss	bed	190	25	686288.6	6294911
RC	ss	bed	220	25	686303.5	6294905
RC	ss	bed	230	15	686313.5	6294901
RC	ss	bed	225	20	686321.8	6294896
RC	siturb	bed	215	15	686341.9	6294885
RC	ssturb	bed	220	25	686116.4	6295028
RC	si	bed	205	25	686106.7	6295030
RC	si	bed	180	15	686099	6295031
RC	si	bed	180	10	686080.8	6295035
RC	si	bed	180	15	686070.3	6295036
RC	si	bed	170	25	686039.2	6295044
RC	si	bed	170	20	686020.4	6295049
RC	si	bed	150	15	686005.2	6295052
RC	si	bed	185	20	686533.3	6294772
RC	si	bed	190	20	686516.7	6294783
RC	ss	bed	220	15	686491.9	6294795
RC	si	bed?	150	10	686701.2	6294693
RC	si	bed	160	20	686682.4	6294703
RC	mss	bed?	125	20	686674.1	6294706
RC	si?	bed	200	20	687254.5	6295061
RC	si?	bed	170	20	687233	6294993
RC	si?	bed	190	15	687243.4	6295027
RC	si	bed	120	30	687657.5	6296385
RC	si	bed	120	60	687654.6	6296397

station	lithology	measurement	strike	dip	Easting	Northing
RC	si	bed	175	25	687650.7	6296401
RC	si	bed	105	30	687649.9	6296399
RC	si	bed	120	50	687651.5	6296398
RC	si	bed	185	25	687648.4	6296407
RC	ss	bed	165	40	687644.3	6296417
RC	ss	bed	150	25	687645.2	6296419
RC	ss	bed	190	40	687644.1	6296430
RC	si	bed	250	85	687644.8	6296440
RC	ss	bed	105	55	687647.2	6296450
CG	ss	bed	185	30	686316.2	6295751
CG	si	bed	185	25	686421.8	6295789
CG	si	bed	150	25	686418	6295786
CG	si	bed	105	35	686400.3	6295766
CG	si	bed	125	20	686392.2	6295760
CG	si	bed	150	20	686377.9	6295754
CG	ss	bed	205	30	686293.5	6295755
CG	ss	bed	200	35	686281.9	6295749
CG	ss	bed	190	25	686258.4	6295734
CG	ss	bed	65	20	686234.9	6295714
CG	ss	bed	205	30	686224.1	6295720
CG	ss	bed	125	10	686221	6295712
SW	ss	bed	125	50	685415.1	6295452
SW	ss	bed	140	55	685425.1	6295452
SW	ss	bed	115	45	685439.3	6295453
SW	ss	bed	135	30	685457.9	6295453
SW	ss	bed	135	35	685484.1	6295451
SW	ss	bed	150	25	685516	6295456
SW	ss	bed	150	25	685578.7	6295465
SW	ss	bed	150	10	685616.8	6295470
SW	ss	bed	310	10	685653.5	6295482
SW	redsi	bed	150	35	685708.2	6295503
SW	redsi	bed	190	30	685744	6295521
SW	siturb	bed	150	20	685520.9	6295426
SW	ss	bed	140	25	685497.4	6295417
SW	ssturb	bed	140	20	685540.1	6295433
SW	mss	bed	180	35	685564	6295440
SW	ss	bed	150	20	685595.3	6295450
SW	siturb	bed	140	20	685616.1	6295454
SW	mss	bed	140	15	685640	6295459
SW	mss	bed	155	15	685669.6	6295468
SW	siturb	bed	180	25	685695.5	6295475
SW	siturb	bed	175	30	685717.8	6295484
SW	redsi	bed	180	30	685754.4	6295495
DP	mss	bed	185	20	686382.3	6295284
DP	ssturb	bed	240	60	686700.4	6295421
CE	si	bed	290	25	686541.5	6294979
CE	si	bed	290	5	686546.3	6294982

station	lithology	measurement	strike	dip	Easting	Northing
CE	si	bed	350	35	686549.7	6294985
CE	si	bed	175	45	686556.4	6294983
CE	si	bed	200	25	686560.5	6294977
CE	si	bed	120	35	686509.7	6295059
CE	si	bed	220	45	686518.5	6295056
CE	ssturb	bed?	10	55	686540.2	6295143
CE	mss	bed	215	20	686357.9	6294964
CE	mss	bed	150	25	686407.4	6295145
CE	mss	bed	200	25	686409.4	6295148
CE	mss	bed	195	30	686413.5	6295148
CE	mss	bed	210	30	686418.9	6295147
CE	mss	bed	180	20	686423	6295146
CE	si	bed	200	80	686079.6	6295280
CE	si	bed	235	30	686076.6	6295280
CE	si	bed	195	50	686075.2	6295283
CE	siturb	bed	205	70	686072.8	6295283
CE	siturb	bed	190	60	686073.2	6295285
CE	ss	bed	210	20	686074.2	6295288
CE	ssturb	bed	355	35	686077.6	6295278
CE	si	bed	170	25	686122.4	6295304
CE	si	bed	165	20	686122.7	6295296
CE	si	bed	165	20	686123.7	6295286
CE	si	bed	180	30	686127.4	6295269
CE	si	bed	200	30	686129.8	6295258
CE	si	bed	210	30	686129.8	6295249
CE	si	bed	155	20	686128.8	6295239
CE	si	bed	170	30	686123.4	6295156
CE	siturb	bed	205	40	686126.1	6295153
CE	siturb	bed	200	45	686127.8	6295151
CE	siturb	bed	210	60	686125.7	6295150
CE	si	bed	190	45	686122.7	6295160
CE	si	bed	195	40	686125.7	6295162
CE	mss	bed	155	30	686200.6	6295366
CE	mss	bed	165	40	686203.6	6295363
CE	mss	bed	185	20	686137.9	6295353
CE	mss	bed	185	25	686131.5	6295362
CE	mss	bed	175	20	686129.1	6295363
CE	mss	bed	185	30	686136.6	6295356
CE	mss	bed	185	45	686127.6	6295363
CE	mss	bed	200	20	686120.7	6295362
CE	ss	bed	210	30	686180.6	6295566
CE	ss	bed	200	10	686186.7	6295557
CE	mss	bed	185	25	686264.6	6295464
CE	mss	bed	170	30	686266.6	6295475
CE	mss	bed	185	25	686269.4	6295493
CE	mss	bed	185	30	686273.1	6295504
CE	ss	bed	195	25	686447.5	6295571

station	lithology	measurement	strike	dip	Easting	Northing
CE	ss	bed	200	15	686453	6295578
CE	ss	bed	200	25	686438.7	6295559
CE	si	bed	155	25	686409.4	6295506
CE	ss	bed	140	30	686408.7	6295496
CE	si	bedcontact	90	15	686341.3	6295415
SR	ss	bed	55	45	686186.7	6296166
SR	ss	bed	60	45	686182.3	6296168
SR	ssturb?	bed	85	40	686154.5	6296093
SR	siturb	bed	40	40	686155.9	6296090
SR	siturb	bed	50	45	686157.3	6296089
SR	ssturb	bed	50	40	686163.1	6296081
SR	ssturb	bed	35	40	686200.8	6296059
SR	ssturb	bed?	175	45	686256.1	6296081
SR	si	bed?	145	30	686270.3	6296077
SR	siturb	bed	255	85	686288.6	6296030
SR	si	bed	235	45	686289.9	6296029
SR	si	bed	65	45	686292	6296023
SR	ssturb	bed	60	65	686292.8	6296019
SR	ssturb	bed	65	50	686293.3	6296015
SR	ssturb	bed	70	45	686293.5	6296012
SR	mss	bed	185	65	686270	6295958
SR	mss	bed	195	80	686269.6	6295954
SR	mss	bed	190	75	686269.4	6295949
SR	mss	bed	170	50	686269.6	6295947
SW	ssturb	bed	190	30	685716.8	6295459
SW	ssturb	bed	190	25	685709.3	6295455
SW	ssturb	bed	200	30	685705.3	6295453
EW	ssturb	bed	95	10	686039.3	6296364
EW	ssturb	bed	275	5	686043	6296344
EW	mss	bed	215	45	685969.6	6296498
EW	mss	bed	210	40	685967.1	6296494
EW	mss	bed	110	75	686023.5	6296136
EW	mss	bed	90	50	686023.1	6296139
EW	ssturb?	bed	230	15	685978.1	6296399
EW	ssturb?	bed	150	25	685971.4	6296417
EW	ssturb?	bed	205	15	685968.6	6296422
EW	ssturb?	bed	225	15	685966.6	6296427
EW	mss	bed	230	45	685956.4	6296450
EW	mss	bed	175	20	685944.3	6296482
EW	mss	bed	200	30	685939.9	6296496
EW	ssturb	bed	210	20	685988.6	6296441
EW	ssturb	bed	140	20	685988.6	6296437
EW	ssturb	bed	210	5	685990	6296426
EW	si	bed	165	15	685993.7	6296411
EW	si	bed	190	5	685999.5	6296396
EW	si	bed	300	5	686000.8	6296385
EW	si	bed	240	5	686008.3	6296365



station	lithology	measurement	strike	dip	Easting	Northing
EW	si	bed	230	25	686013	6296350
RC	ss	bed	210	45	686119.8	6295022
RC	ss	bed	180	45	686123	6295021
RC	ss	bed	160	35	686125.9	6295023
RC	ss	bed	190	38	686117.9	6295026
RC	ss	bed	220	22	686114.7	6295030
RC	si	bed	170	35	686112.8	6295025
RC	si	bed	205	15	686110.5	6295028
RC	si	bed	205	23	686106.3	6295029
RC	si	bed	180	15	686098.3	6295030
RC	si	bed	202	55	686094.5	6295031
RC	si	bed	190	12	686085.8	6295031
RC	si	bed	175	15	686085.8	6295033
RC	si	bed	180	10	686083.5	6295036
RC	si	bed	185	30	686075.7	6295036
RC	si	bed	180	15	686073.4	6295031
RC	si	bed	180	15	686070.8	6295035
RC	si	bed	190	15	686061.8	6295038
RC	si	bed	160	20	686052.9	6295040
RC	si	bed	180	20	686038.1	6295044
RC	si	bed	165	20	686045.5	6295042
RC	si	bed	185	15	686044.7	6295042
RC	si	bed	170	25	686043.2	6295042
RC	si	bed	165	25	686049.5	6295037
RC	si	bed	175	40	686030.7	6295045
RC	si	bed	170	30	686028	6295046
RC	si	bed	170	20	686020.6	6295048
RC	si	bed	170	25	686016.8	6295049
RC	si	bed	220	15	686013.2	6295050
RC	si	bed	193	35	686011.3	6295050
RC	si	bed	155	15	686009	6295051
RC	si	bed	150	15	686006.9	6295051
RC	si	bed	170	40	686000.6	6295053
RC	si	bed	180	55	685998	6295053
RC	ss	bed	180	20	687262.9	6295091
RC	ss	bed	200	20	687255.7	6295056
RC	ss	bed	190	20	687252.8	6295047
RC	ss	bed	180	20	687249.6	6295036
RC	ss	bed	190	15	687241.8	6295015
RC	ss	bed	170	20	687230.8	6294981
RC	siturb	bed	210	40	686285.2	6294913
RC	ss	bed	190	25	686287.8	6294912
RC	ss	bed	195	35	686292.6	6294911
RC	ss	bed	200	20	686295.1	6294911
RC	ss	bed	180	15	686299	6294911
RC	ss	bed	235	20	686299.7	6294907
RC	ss	bed	285	25	686301.6	6294906

station	lithology	measurement	strike	dip	Easting	Northing
RC	ss	bed	220	25	686304.2	6294907
RC	ss	bed	25	60	686305.3	6294904
RC	ss	bed	225	15	686307.6	6294903
RC	ss	bed	80	15	686310.2	6294904
RC	ss	bed	230	15	686312.5	6294903
RC	ss	bed	175	30	686316.2	6294904
RC	ss	bed	235	35	686318.2	6294901
RC	ss	bed	165	15	686322.5	6294905
RC	ss	bed	225	20	686322.5	6294898
RC	ss	bed	230	15	686333.6	6294896
RC	siturb	bed	235	15	686335.1	6294892
RC	siturb	bed	205	5	686336.6	6294887
RC	siturb	bed	215	15	686341.3	6294886
RC	siturb	bed	210	15	686351.1	6294882
RC	siturb	bed	240	15	686356.5	6294879
RC	siturb	bed	230	20	686360.6	6294878
RC	siturb	bed	240	30	686365.1	6294872
RC	ssturb	bed	215	20	686500.7	6294791
RC	si	bed	165	10	686550.2	6294763
RC	si	bed	190	20	686547.2	6294764
RC	si	bed	170	10	686543.5	6294767
RC	si	bed	185	20	686533.7	6294769
RC	si	bed	175	75	686530.8	6294768
RC	si	bed	205	15	686530.1	6294772
RC	si	bed	195	5	686523.9	6294777
RC	si	bed	190	20	686517.6	6294783
RC	ssturb	bed	205	15	686504.2	6294791
RC	ssturb	bed	35	5	686499.6	6294791
RC	ssturb	bed	220	15	686497.6	6294794
RC	ss	bed	220	15	686488	6294799
RC	ss	bed	215	20	686480.8	6294802
RC	si	bed	110	10	686716.2	6294686
RC	ss	bed	125	20	686677.5	6294704
RC	si	bed	150	10	686702	6294692
RC	si	bed?	60	15	686700.4	6294693
RC	si	bed?	270	50	686700.3	6294693
RC	si	bed	160	20	686682.6	6294702
RC	ss	bed	110	15	686667.8	6294709
RC	ss	bed	125	25	686659	6294713
RC	ss	bed	100	25	686653.4	6294716
RC	ss	bed?	210	15	686649.9	6294718
RC	ss	bed?	280	40	686650.2	6294718
RC	mss	bed	205	20	687659	6296383
RC	siturb	bed	250	85	687646.4	6296443
RC	ssturb	bed	220	50	687653.4	6296459
RC	ssturb	bed	215	55	687650.4	6296457
RC	ssturb	bed	200	35	687648.9	6296455

station	lithology	measurement	strike	dip	Easting	Northing
RC	ssturb	bed	170	30	687648.7	6296454
RC	ssturb	bed	140	40	687648.4	6296454
RC	ssturb	bed	170	30	687648.9	6296452
RC	ssturb	bed	145	30	687648.7	6296451
RC	ssturb	bed	105	55	687648.2	6296450
RC	ssturb	bed	160	30	687649.4	6296448
RC	ssturb	bed	110	40	687647.2	6296447
RC	ssturb	bed	100	60	687646.9	6296445
RC	ssturb	bed	135	40	687643.4	6296438
RC	ssturb	bed	195	45	687647.1	6296436
RC	ssturb	bed	190	30	687644.6	6296436
RC	ssturb	bed	210	45	687643.9	6296433
RC	ssturb	bed	140	30	687645.9	6296432
RC	ssturb	bed	190	30	687642.1	6296430
RC	mss	bed	190	40	687646.4	6296428
RC	siturb	bed	180	25	687647.6	6296407
RC	mss	bed	190	50	687645.1	6296426
RC	mss	bed	145	40	687644.9	6296424
RC	mss	bed	195	25	687644.9	6296423
RC	mss	bed	150	25	687645.7	6296420
RC	mss	bed	120	80	687647.6	6296419
RC	mss	bed	165	40	687645.7	6296418
RC	mss	bed	170	30	687645.9	6296416
RC	siturb	bed	185	25	687646.2	6296405
RC	siturb	bed	175	25	687651.4	6296401
RC	siturb	bed	105	30	687649.9	6296399
RC	siturb	bed	195	25	687650.7	6296399
RC	siturb	bed	120	55	687650.4	6296398
RC	siturb	bed	135	25	687651.1	6296398
RC	siturb	bed	120	50	687651.5	6296398
RC	siturb	bed	95	90	687651.4	6296397
RC	siturb	bed	100	75	687654.4	6296397
RC	siturb	bed	230	15	687653.7	6296395
RC	siturb	bed	120	60	687656.2	6296396
RC	siturb	bed	115	25	687654.6	6296393
RC	siturb	bed	120	40	687656.1	6296388
RC	siturb	bed	125	40	687655.5	6296387
RC	siturb	bed	120	30	687657.2	6296386
RC	siturb	bed	130	10	687657.5	6296384
CG	si	bed	290	45	686470.3	6295861
CG	ss	bed	205	45	686343.8	6295749
CG	si	bed	240	45	686462.7	6295856
CG	si	bed?	65	45	686444.5	6295852
CG	si	bed	145	10	686439	6295847
CG	si	bed	80	20	686420	6295800
CG	si	bed	185	25	686419.7	6295791
CG	si	bed	150	25	686419.2	6295788

station	lithology	measurement	strike	dip	Easting	Northing
CG	si	bed	115	10	686417	6295784
CG	si	bed	105	35	686395.8	6295766
CG	si	bed	125	20	686389.3	6295761
CG	si	bed	150	20	686377.8	6295755
CG	si	bed	155	20	686370.2	6295754
CG	ss	bed	205	35	686343	6295752
CG	ss	bed	210	45	686343	6295754
CG	ss	bed	210	35	686322.1	6295750
CG	ss	bed	185	30	686313.7	6295756
CG	ss	bed	220	35	686297.4	6295759
CG	ss	bed	205	35	686293.3	6295758
CG	ss	bed	195	30	686286.8	6295754
CG	ss	bed	200	35	686280.8	6295751
CG	ss	bed	185	25	686264.2	6295744
CG	ss	bed	205	25	686261.5	6295743
CG	ss	bed	190	20	686260.1	6295742
CG	ss	bed	190	25	686258.2	6295741
CG	ss	bed	65	20	686236.7	6295720
CG	ss	bed	205	30	686222.3	6295720
CG	ss	bed	125	10	686221.2	6295713
CG	ss	bed	180	20	686214.2	6295712
EW	ss	bed	110	75	686024.6	6296135
EW	ss	bed	90	50	686024.4	6296139
EW	ss	bed	90	60	686017.6	6296152
EW	ss	bed	90	55	686017.6	6296157
EW	ss_ord	bedcontact	90	75	686017.8	6296159
EW	ssturb	bed?	300	15	685996.6	6296357
EW	ssturb	bed	310	10	685988.2	6296388
EW	ssturb	bed	225	5	685984.9	6296400
EW	ssturb	bed	230	15	685982.8	6296404
EW	ssturb	bed	335	15	685982.5	6296405
EW	ssturb	bed	150	25	685974.6	6296418
EW	ssturb	bed	205	15	685969.7	6296424
EW	ssturb	bed	225	15	685972.7	6296428
EW	ssturb	bed	185	15	685967.8	6296428
EW	mss	bed	220	25	685966.4	6296432
EW	mss	bed	195	25	685963.2	6296441
EW	mss	bed	155	30	685961.3	6296444
EW	mss	bed	215	35	685963.5	6296449
EW	mss	bed	230	45	685963.7	6296455
EW	mss	bed	175	20	685948.8	6296484
EW	mss	bed	200	30	685945.8	6296489
EW	mss	bed	215	40	685943.9	6296493
EW	mss	bed	200	30	685941.7	6296496
EW	ssturb	bed	115	40	685990.1	6296452
EW	ssturb	bed	190	20	685993.1	6296444
EW	ssturb	bed	210	20	685994.5	6296440

station	lithology	measurement	strike	dip	Easting	Northing
EW	ssturb	bed	140	20	685993.1	6296436
EW	ssturb	bed	205	50	685992.8	6296432
EW	ssturb	bed	210	5	685993.9	6296427
EW	siturb	bed	215	10	685992	6296420
EW	siturb	bed	55	15	685995.5	6296416
EW	siturb	bed	165	15	685996.1	6296412
EW	siturb	bed	215	25	685997.7	6296408
EW	siturb	bed	195	10	685998.8	6296405
EW	siturb	bed	175	10	685999.6	6296398
EW	siturb	bed	190	5	686000.7	6296393
EW	siturb	bed	260	2	686001.3	6296389
EW	siturb	bed	300	5	686003.4	6296382
EW	siturb	bed	90	10	686003.4	6296378
EW	siturb	bed	255	35	686006.4	6296372
EW	siturb	bed	270	10	686008.1	6296368
EW	siturb	bed	240	5	686009.8	6296362
EW	siturb	bed	50	15	686010.2	6296361
EW	siturb	bed	230	25	686012	6296355
EW	siturb	bed	230	25	686013.1	6296351
EW	siturb	bed	290	20	686015.3	6296347
EW	ssturb	bed	275	10	686023.3	6296337
SW	siturb	bed	150	10	685513	6295423
SW	ss	bed	140	50	685482	6295407
SW	ss	bed	160	55	685488.1	6295409
SW	ss	bed	120	65	685489	6295410
SW	ssturb	bed	160	30	685493.5	6295414
SW	ssturb	bed	140	25	685497.2	6295416
SW	ssturb	bed	145	20	685505.2	6295420
SW	siturb	bed	150	20	685520.1	6295425
SW	siturb	bed	155	20	685525	6295427
SW	siturb	bed	155	20	685530.4	6295429
SW	ss	bed	170	30	685533.8	6295430
SW	ss	bed	140	20	685542.9	6295433
SW	siturb	bed	140	20	685548.4	6295435
SW	siturb	bed	140	20	685555	6295435
SW	ss	bed	180	35	685565	6295437
SW	ss	bed	200	50	685570.6	6295440
SW	mss	bed	65	15	685572.2	6295443
SW	ssturb	bed	150	30	685575.2	6295445
SW	ssturb	bed	130	50	685577.5	6295445
SW	ssturb	bed	115	25	685588.7	6295447
SW	mss	bed	150	20	685598.5	6295445
SW	ssturb	bed	135	25	685605.2	6295450
SW	siturb	bed	115	30	685609.6	6295452
SW	siturb	bed	140	20	685615.9	6295453
SW	siturb	bed	145	25	685624.4	6295455
SW	mss	bed	140	15	685635.8	6295457

station	lithology	measurement	strike	dip	Easting	Northing
SW	mss	bed	130	15	685649.6	6295459
SW	mss	bed	140	10	685661.4	6295463
SW	mss	bed	155	15	685669.4	6295464
SW	mss	bed	190	10	685673.4	6295467
SW	mss	bed	160	15	685680	6295469
SW	siturb	bed	175	20	685691.4	6295474
SW	mss	bed	180	25	685702.8	6295478
SW	ssturb	bed	190	25	685711.6	6295481
SW	siturb	bed	175	30	685716.6	6295483
SW	siturb	bed	175	35	685730.8	6295488
SW	redsi	bed	180	30	685752.3	6295494
SW	redsi	bed	155	35	685760.8	6295496
SW	redsi	bed	145	50	685771.5	6295498
SW	redsi	bed	160	35	685729.1	6295512
SW	si	bed	160	90	685392.5	6295449
SW	si	bed	150	90	685394	6295449
SW	si	bed	150	90	685395.4	6295449
SW	mss	bedcontact	125	50	685414.2	6295450
SW	mss	bedcontact	130	60	685416.3	6295450
SW	si	bed	140	80	685418.2	6295451
SW	si	bed	140	55	685423.8	6295451
SW	mss	bed	150	50	685436.6	6295451
SW	mss_turb	bedfault	115	45	685439.8	6295450
SW	mss	bed	135	35	685447.7	6295451
SW	mss	bed	135	40	685452.3	6295451
SW	siturb	bed	135	30	685460.8	6295451
SW	siturb	bed	140	25	685469.2	6295451
SW	siturb	bed	140	35	685475.1	6295451
SW	siturb	bed	135	30	685481	6295451
SW	mss_ord	bedcontact	135	35	685484.4	6295451
SW	mss_ord	bedcontact	95	15	685490	6295451
SW	mss_ord	bedcontact	190	5	685497	6295451
SW	mss_ord	bedcontact	355	10	685502.4	6295451
SW	mss_ord	bedcontact	150	25	685518.4	6295452
SW	mss_ord	bedcontact	20	40	685573.6	6295462
SW	ssturb	bed	150	25	685580.1	6295464
SW	ssturb	bed	140	10	685588.7	6295465
SW	ssturb	bed	150	10	685615.8	6295469
SW	ssturb	bed	195	15	685633.6	6295475
SW	ssturb	bed	310	10	685652.1	6295481
SW	ssturb	bed	180	5	685667.1	6295486
SW	ssturb	bed	220	25	685671.7	6295488
SW	siturb	bed	170	20	685685.6	6295493
SW	siturb	bed	175	35	685696.7	6295499
SW	si	bed	155	35	685706.2	6295503
SW	si	bed	155	35	685710.6	6295505
SW	si	bed	150	35	685708.6	6295504

station	lithology	measurement	strike	dip	Easting	Northing
SW	redsi	bed	170	30	685724.3	6295510
SW	redsi	bed	155	40	685730.6	6295513
SW	redsi	bed	90	30	685745.9	6295519
SW	redsi	bed	230	40	685756	6295524
SW	redsi	bed	145	40	685760.8	6295526
SW	redsi_ord	bedcontact	165	20	685761.6	6295527
RC	si	bed	210	40	686285	6294913



## Appendix II: Fault Measurements

The following data table represents a compilation of measurements gathered over both the 2006 and 2007 field season. Measurements (in degrees) and corresponding coordinates (given as Easting and Northing) are in Australia Map Grid projection, using the datum AGD66. Strike and dip was measured with a Brunton compass, and measurements were rounded in the field to the nearest 5°. Strike measurements were always taken so that the plane being measured dipped to the right (for example, N-striking planes dip to the E). Where measurement or lithology was uncertain, it is indicated with a question mark.

The “station” column indicates a general geographic area for measurement location. CE=Cadia East, CG=Copper Gully, RC=roadcutting from the Cadia Hill access road, SR=Sharps Ridge, SW=southern wall of Cadia Hill pit, EW=eastern wall of Cadia Hill pit, DP=drill pad (Cadia East or Sharps Ridge).

The “lithology” column indicates what rock type bedding was measured in. Units on either side of the fault are separated with an underscore, and the upper unit is listed first. Abbreviations are as follows: si=siltstone, ss=sandstone (undifferentiated), siturb=siltstone-dominant interbedded siltstone and sandstone, ssturb=sandstone-dominant interbedded siltstone and sandstone, mss=massive sandstone, redsi=red siltstone, blksh=black shale, bc=boulder conglomerate, sibx=brecciated siltstone, ord=Ordovician basement (undifferentiated), ark=arkose.

The “measurement” column indicates what feature was measured at each location. Abbreviations used are: fault\_bed=bedding parallel fault, fault\_contact=faulted contact within the cover rocks (i.e. juxtaposing different stratigraphic units), fault\_unconf=fault at the unconformity between the basement and cover rocks. The “sense” column indicates the general sense of separation on the measured fault observed in the field. Normal separation is indicated by “N”, reverse separation by “R”. Although faults fitting in either of these categories may have experienced motion in the third dimension, faults which appear to display a strong strike-slip component are indicated by “X”. Faults measured in the Ordovician basement rocks were mostly undifferentiated in the field, due to poor stratigraphic control, and are marked with “U”.

The “class” column shows information about the estimated magnitude of displacement along the measured fault, with 1 being the most and 3 being the least. In general, quantifying displacement was not possible due to lack of marker horizons and the prevalence of faults at a low angle to bedding, but a qualitative assessment based on the estimated width and infill (if any) of the damage zone, juxtaposition of stratigraphic units, and other related disruption (e.g. folds) was attempted. Displacement on class 3 faults was estimated to be on the mm-cm scale. Displacement on class 1 faults was estimated to exceed 20m, while class 2 faults were categorized as having experienced displacement on the meter scale. While this classification is somewhat arbitrary, it allows for division of recognized faults into groups which accommodated relatively major (10s of meters) vs. minor (less than 1 m) amounts of shortening. Faults in the Ordovician basement were not classified, and were assigned a class of 0.

station	lithology	measurement	sense	class	strike	dip	Easting	Northing
EW	ord	fault_unconf	U	0	95	75	686031	6296106
EW	ord	fault	U	0	105	50	686014	6296212
EW	ord	fault	U	0	110	50	686006	6296254
CE	mss	fault	N	2	90	90	686133	6295359
SR	si	fault	N	2	25	90	686290.9	6296025.9
SR	mss	fault	N	3?	75	80	686269.8	6295962.3
EW	ss	fault	N	2?	50	60	686014	6296360.6
EW	si	fault	N	2	75	75	685990.3	6296443.3
RC	si?	fault	N?	3	180	85	687207	6294924
SW	mss	fault	R	2	165	65	685708	6295453
SW	ss_si	fault_contact	R	2?	180	25	685690	6295449
SW	si	fault_unconf	R	1?	165	20	685764	6295535
CE	si	fault_contact	R	1?	195	55	686559.1	6294986.7
CE	si	fault	R	2	120	45	686517.1	6295059.9
CE	si	fault	R	2	135	40	686513.1	6295057.2
CE	ss_siturb	fault	N	2	180	55	686078.9	6295278.5
CE	ss_siturb	fault_contact	R	1	200	30	686073.9	6295286.3
CE	si	fault	N	2	205	50	686122.7	6295157.8
CE	ss	fault	R	2?	155	45	686343	6295408.4
SW	ssturb	fault	R	2	175	70	685719.5	6295458.9
CE	si	fault	N	2?	250	90	686545.6	6294977.2
CE	si	fault	N	3	250	90	686550.3	6294979.9
CE	ss_siturb	fault	R	3	220	90	686077.3	6295282.1
CE	si	fault	R	3	290	90	686123.7	6295153.4
CE	mss	fault	N	2	275	90	686126.7	6295365.4
SR	si	fault	R?	1	265	90	686286.5	6296030.4
EW	mss	fault	N	2?	230	85	685964.4	6296430
EW	mss	fault	R	2?	230	50	685964.6	6296429
EW	ss_si	fault	R	2	280	45	686019.5	6296340.3
EW	si	fault	R	2	270	60	686002.2	6296390.8
EW	ssf	fault	R?	1	80	80	686035	6296382
SR	ss?	fault	R?	3	15	60	686177	6296104
SW	mss	fault	R	2	165	65	685708	6295453
CG	mss	fault	R?	3	120	55	687434	6296525
CG	mss	fault	R?	2?	145	40	687430	6296520
CG	mss	fault	R	2?	170	60	687416	6296515
CG	mss	fault	R?	2?	80	65	687344	6296319
CG	si	fault_contact	R	2?	85	70	687326	6296293
CG	mss_ssturb	fault_contact	X	1	220	90	686254.1	6295797.1
CG	ord?	fault	U	0	170	55	686117	6295953
CG	mss_ssturb	fault_contact	X	1	225	85	686249.8	6295798.9
CG	ss	fault_contact	R	2?	290	45	687307.4	6296300
RC	ss_si	fault_contact	R	1	160	50	686113.7	6295027.6
RC	ss	fault	N	3	220	70	686118.7	6295025.9
RC	ss	fault	X	2	217	75	686120	6295025.7
RC	si	fault	N?	3?	170	45	686073.6	6295029.3
RC	si	fault	N	3	235	70	686071.3	6295035.2

station	lithology	measurement	sense	class	strike	dip	Easting	Northing
RC	si	fault	N	3	260	90	686071.7	6295035
RC	si	fault	R	2?	170	40	686067.5	6295036.5
RC	si	fault	R	1	170	40	686078.4	6295033.3
RC	si	fault	R	3	185	45	686095.1	6295023.6
RC	si	fault	X	2	265	90	686086.2	6295031.2
RC	si	fault	R	3	180	65	686097	6295029.9
RC	si	fault	N	3	245	85	686107.8	6295027.6
RC	si	fault_contact	R	1	165	60	685994.9	6295053.3
RC	si	fault	N?	3	155	40	686008.6	6295049.3
RC	si	fault	R?	2	150	45	686018.5	6295046.6
RC	si	fault	N	3	250	90	686031	6295045.5
RC	si	fault	N	3	220	90	686039.6	6295043.2
RC	si	fault	N	2	90	50	686043.6	6295042.2
RC	si	fault	N	3	75	60	686047.2	6295041.5
RC	si	fault	N	2	255	90	686048.5	6295040.9
RC	si	fault	N	3	160	90	686047.6	6295039
RC	si	fault	N	3	280	90	686051.9	6295036.5
RC	ss	fault	N	3	80	90	687263.1	6295087.9
RC	ss	fault	N	3	250	80	687261.4	6295077
RC	ss	fault	N	3	150	35	687258.2	6295060.5
RC	ss	fault	N	3	250	80	687253.4	6295053.1
RC	ss	fault	N	3	50	90	687250.9	6295040
RC	ss	fault	N	3	180	90	687251.1	6295045.1
RC	siturb_ss	fault_contact	R	1	165	40	686287.6	6294913
RC	ss	fault	N	2	70	90	686297	6294908.6
RC	ss	fault	R	2	235	35	686304.9	6294904.3
RC	ss	fault	R	3?	255	30	686313.7	6294908.3
RC	ss	fault	R	2	240	65	686310.5	6294905.3
RC	ss	fault	R	2	230	45	686313.5	6294903.8
RC	ss	fault	R	2	280	40	686319.7	6294901
RC	ss_siturb	fault_contact	X	1	85	90	686330.8	6294891.4
RC	siturb	fault	R	1	255	50	686334.2	6294893.2
RC	siturb	fault	R	1	250	35	686330.2	6294893.5
RC	siturb	fault	N	3	70	90	686334.2	6294889.2
RC	siturb	fault	R	3	85	85	686337.7	6294889.8
RC	siturb	fault	R	3	260	85	686338.5	6294888.8
RC	siturb	fault	N	3	75	90	686341.8	6294884.9
RC	siturb	fault	N	3	355	55	686346.3	6294884.5
RC	si	fault	N	3	5	55	686356.2	6294875.7
RC	si	fault_contact	R	2?	250	40	686365.9	6294882.3
RC	si	fault	N	3	65	90	686360.6	6294875.5
RC	si	fault	R	3	25	45	686363.4	6294875.1
RC	si	fault	R?	3?	185	20	686368.2	6294871
RC	si	fault	R?	2?	180	50	686546.5	6294764.2
RC	si	fault	N	3	220	90	686542.3	6294766.5
RC	si	fault	N	3	195	90	686538.6	6294768.1
RC	si	fault	N	3	235	90	686531.4	6294772.1

station	lithology	measurement	sense	class	strike	dip	Easting	Northing
RC	si	fault	N	3	175	90	686528.5	6294775.9
RC	si	fault	R	3	20	30	686526.5	6294776.7
RC	si	fault	R	3	20	30	686525.2	6294777.9
RC	si	fault	N	2	20	40	686519	6294778.9
RC	si	fault	R	2?	195	20	686514.9	6294782.9
RC	si	fault	N	2	30	40	686512.4	6294784.1
RC	si	fault	R	2	160	85	686511.9	6294786.7
RC	si	fault	N	3	50	60	686510.8	6294787.1
RC	ss	fault	R	3	205	70	686500.4	6294789.4
RC	ss	fault	R	3	225	90	686501.1	6294792.6
RC	ss	fault	R	3	230	90	686498.6	6294792
RC	ss	fault	R	2	215	20	686480.8	6294798.5
RC	si	fault	N	3	155	90	686702.1	6294690.6
RC	si	fault	N	3	300	60	686700.7	6294692.2
RC	si	fault	N	3	170	90	686699.1	6294692.2
RC	si	fault	R?	2	40	45	686694.7	6294695.6
RC	si	fault	N?	3	230	90	686693.8	6294696.8
RC	si_ss	fault_contact	R	2	200	45	686681.3	6294700.8
RC	si_ss	fault_contact	R	2	250	30	686678.8	6294704.3
RC	ss	fault	N	3	240	90	686673.2	6294705.5
RC	ss	fault	N	3	240	90	686664.7	6294710
RC	ss	fault	R	2	235	50	686661.7	6294711.7
RC	ss	fault	N	3	195	70	686655.7	6294714.8
RC	ssturb	fault	R	3	60	70	687648.2	6296451.4
RC	ssturb	fault	R	3	250	70	687648	6296449.6
RC	ssturb	fault	R	2	65	80	687648.7	6296447.8
RC	ssturb	fault_contact	R	2	250	85	687644.1	6296438.9
RC	ssturb	fault	R	3	90	75	687643.9	6296434.6
RC	mss	fault	R	2	275	80	687643.4	6296430
RC	mss	fault	N	2	270	50	687643.4	6296427.8
RC	mss	fault	R	3	130	30	687644.6	6296422.6
RC	mss	fault	R?	2	85	85	687646.5	6296417
RC	mss	fault	R?	1	165	45	687645.7	6296415
RC	siturb	fault	N?	3	10	90	687649.5	6296403.8
RC	siturb	fault	R?	3	35	80	687650.5	6296403.4
RC	siturb	fault	R	1?	275	75	687648.7	6296402.6
RC	siturb	fault	R?	1?	190	30	687650.7	6296402.1
RC	siturb	fault	R?	3	270	55	687652.6	6296400.6
RC	siturb	fault	N	2	100	90	687652.5	6296397.4
RC	siturb	fault	N	2	95	90	687654.6	6296394.4
RC	siturb	fault	R	2	240	10	687655.4	6296392.4
RC	siturb_ss	fault_contact	R	1	65	90	687658.7	6296383.7
EW	ord	fault_unconf	R	1	95	75	686030.3	6296111.4
EW	mss	fault	R?	1	315	75	686029	6296117.9
EW	mss	fault_contact	R	2?	10	50	686025.7	6296132
EW	mss	fault_contact	R	2?	115	75	686025.7	6296136.9
EW	mss	fault	R	2?	105	45	686021.9	6296146.2

station	lithology	measurement	sense	class	strike	dip	Easting	Northing
EW	mss	fault_contact	R	2	80	60	686019.5	6296155.1
EW	mss_ord	fault_unconf	R	1	90	75	686019.2	6296160.6
EW	ord	fault	U	0	105	50	686017	6296211.7
EW	ord	fault	U	0	95	35	686011	6296216.9
EW	ord	fault	U	0	90	75	686010	6296219
EW	ord	fault	U	0	130	70	686009.1	6296226.9
EW	ord	fault	U	0	285	75	686011.6	6296234.3
EW	ord	fault	U	0	5	80	686012.4	6296242.7
EW	ord	fault	U	0	65	60	686008	6296253.6
EW	ord	fault	U	0	110	50	686008.3	6296256.8
EW	ord	fault	U	0	270	80	686011.6	6296274.2
EW	ord	fault	U	0	80	90	686012.4	6296276.4
EW	ord	fault	U	0	85	90	686012.7	6296280.5
EW	ord	fault	U	0	110	55	686015.4	6296281.3
EW	ord	fault	U	0	65	35	685998.3	6296338.9
EW	ord	fault	U	0	285	30	686009.1	6296310.4
EW	ord	fault	U	0	65	40	686006.4	6296318.8
EW	ord	fault	U	0	355	50	686002.6	6296329.2
EW	ord	fault	U	0	265	35	686013.8	6296299.5
EW	ord	fault	U	0	355	35	685992.5	6296355.5
EW	ord	fault	U	0	125	60	685992.3	6296363.7
EW	ord	fault	U	0	110	20	685989.3	6296374.3
EW	ord	fault	U	0	160	5	685975.1	6296411.8
EW	mss_turb	fault_contact	R	1	230	50	685967.8	6296429.2
EW	mss_turb	fault_contact	R	1	225	40	685965.6	6296430
EW	mss_turb	fault	N	2?	230	85	685968.1	6296431.4
EW	mss_turb	fault_contact	R?	1	215	25	685963.7	6296431.4
EW	mss_turb	fault	R	1	210	65	685964.3	6296438.2
EW	si_ord	fault	N	3	90	90	686020.1	6296336.7
EW	si_ss	fault	R	2	280	45	686020.4	6296338.9
EW	si_ord	fault_unconf	R	1	290	35	686014.2	6296346.9
EW	si	fault	R	3	50	60	686011.6	6296360
EW	si	fault	R	3	20	75	686008.1	6296370.4
EW	si	fault	R	2	270	50	686001	6296390.6
EW	ss	fault_contact	R	2	75	75	685992.1	6296439.3
SW	si	fault	R	2	170	35	685751.3	6295493.4
SW	redsi_turb	fault_contact	R	1	240	90	685745.4	6295492
SW	siturb	fault	N?	3	145	60	685718.2	6295483.4
SW	siturb	fault	N?	3	210	75	685696	6295475.1
SW	ss	fault	N?	3	185	65	685597.3	6295449.2
SW	ss	fault	N	3	200	70	685589.9	6295447.6
SW	ss	fault	N	3	170	90	685578.5	6295442.8
SW	ss	fault	N?	3	150	85	685542.3	6295431.7
SW	siturb	fault	R	2	345	45	685557.6	6295437.1
SW	siturb	fault	R	2	320	40	685558.4	6295437.9
SW	ss	fault	N?	2	20	45	685567.9	6295440.9
SW	siturb_ss	fault	N?	2	340	40	685517.2	6295423.6

station	lithology	measurement	sense	class	strike	dip	Easting	Northing
SW	ssturb	fault	R	2	345	35	685507	6295419.1
SW	ssturb	fault	R	2	140	45	685497.8	6295413
SW	ssturb	fault	R?	1	330	80	685494.6	6295412.3
SW	ssturb	fault	R	1	140	70	685485.4	6295408.8
SW	ssturb	fault	R	1	160	45	685483	6295407.7
SW	ssturb	fault	N	3	345	70	685484.6	6295407.9
SW	si	fault	R	1	145	90	685393.2	6295449.1
SW	mss_turb	fault_contact	R	2	115	45	685439.8	6295450.3
SW	si	fault	N	3	325	50	685394.8	6295448.9
SW	si	fault_contact	R	1	140	90	685397.7	6295449.4
SW	si_mss	fault_contact	R	1	140	90	685411.5	6295450
SW	si_mss	fault_contact	R	2	125	75	685424.6	6295450.8
SW	ss_mss	fault_contact	R	2	65	30	685434	6295450.8
SW	ssturb	fault	N	3	210	85	685483.2	6295451.1
SW	ssturb	fault	R	2	75	20	685483.7	6295445.7
SW	ss	fault	N	3	195	80	685571.5	6295461.7
SW	ss	fault	N	3	185	70	685585.5	6295464.2
SW	ss	fault	R	2	205	80	685641.6	6295477.8
SW	ss	fault	R	2	200	90	685665.9	6295485.8
SW	ss	fault	R	2	230	80	685670.3	6295487.1
SW	si_cong	fault_contact	R	2	190	90	685695.5	6295497.7
SW	si_cong	fault_contact	R	2	170	45	685697.4	6295495.8
SW	si	fault	N	2	200	45	685707.2	6295502.5
SW	si	fault	R?	3	50	15	685725.3	6295509.2
SW	si	fault	N	2	220	90	685729.2	6295510
SW	si	fault	N?	2	210	90	685758.6	6295525.1
CE	siturb_si	fault	X	3	215	80	686734	6294815
CE	ss_siturb	fault	N	3	60	60	685819	6295246
CG	ss	fault?	R?	2?	205	90	687569	6296732
CG	ss	fault	R	1	100	80	687562	6296712
CG	ss	fault_bed	R	2?	40	85	687557	6296666
CG	SKARN	fault	U	0	285	80	687292	6296205
CE	ss	fault?	R	1	190	50	686526	6295309
CG	bc_sibx	fault?	R?	1	135	85	686815	6295945
CG	bc	fault?	R	1	130	85	686811	6295948
CG	bc?bx?	fault?	R?	1?	255	65	686715	6295908
CG	bc?	fault?	R?	2?	175	85	686455	6295852
CG	ord	fault	U	0	1	85	686454	6295838
CG	ord	fault	U	0	225	65	686433	6295826
CG	si	fault	R?	2?	10	90	686399	6295783
CG	siturb	fault	R	2	150	80	686307	6295725
CG	ssturb	fault?	R?	1	220	85	686241	6295796
CG	sibx	fault?	R?	1?	180	85	686708	6296072
CG	sibx?	fault	R?	1?	5	60	686730	6296100
RC	si	fault_bed	R	2	185	70	686600	6294751
RC	ssturb	fault?	R	2	15	45	686508	6294779
RC	si	fault	R	2	250	45	686511	6294808



station	lithology	measurement	sense	class	strike	dip	Easting	Northing
RC	si?turb?	fault	R	1	220	70	686424	6294872
RC	si?turb?	fault?	R	2?	95	85	686435	6294878
SR	si	fault	R	2?	265	80	686291	6296016
SR	ss?	fault?	R?	2?	20	90	686094	6296090
SR	ord	fault	U	0	275	60	686090	6296078
SR	si	fault	R	1	30	90	686253	6295798
SR	ss	fault_bed	R	1	40	90	686256	6295803
SR	bc	fault	R	1	45	90	686212	6295907
SR	ss	fault	R	2?	40	80	686109	6296333
SR	si	fault	R	1?	260	70	686193	6296156
CG	ss	fault?	R?	2?	95	80	687599	6296612
CG	ss	fault?	R	2?	80	85	687563	6296651
CG	ss	fault?	R	2?	40	65	687563	6296662
CG	ss	fault?	R	2?	50	80	687570	6296704
CG	ssbx	fault	R	1?	10	65	687574	6296713
CG	siturb?	fault_bed?	R	1?	325	75	687689	6296667
CG	ssturb?	fault?	R	1	195	75	687739	6296772
RC	si	fault	R	2	35	60	687673	6296494
RC	si	fault	R	2	30	90	687673	6296486
RC	ss?	fault	R	2	100	50	687638	6296445
RC	ss?	fault	R	2	80	75	687639	6296445
EW	ssturb	fault	R	1	205	60	685939	6296606
EW	mss	fault_bed	R	1	175	30	685866	6296587
WW	ord	fault	U	0	170	75	684760	6295938
WW	ord	fault	U	0	140	40	684730	6295968
WW	ord	fault	U	0	110	70	684750	6295971
WW	ord	fault	U	0	330	40	684763	6296016
WW	ord	fault	U	0	140	55	684762	6296011
WW	ord	fault	U	0	175	80	684771	6296051
WW	ord	fault	U	0	115	80	684760	6296137
WW	ord	fault	U	0	140	75	684764	6296145
WW	ord	fault	U	0	340	40	684764	6296153
WW	ord	fault	U	0	165	75	684763	6296160
WW	ord	fault	U	0	140	65	684737	6296203
WW	ord	fault	U	0	340	60	684746	6296227
WW	ord	fault	U	0	350	85	684748	6296234
WW	ord	fault	U	0	80	55	684756	6296257
WW	ord	fault	U	0	350	50	684764	6296277
WW	ord	fault	U	0	170	70	684765	6296295
WW	ord	fault	U	0	100	60	684799	6296393
WW	ord	fault	U	0	110	65	684808	6296409
WW	ord	fault	U	0	355	50	684827	6296443
EW	si_ord	fault_unconf	R	1	90	65	685983	6296103
EW	si	fault	R	1	110	70	686024	6296148
EW	sibx	fault	R	1	75	35	686030	6296149
EW	si	fault_bed	R	2?	80	65	686034	6296154
EW	si	fault	R	1	110	85	686023	6296164

station	lithology	measurement	sense	class	strike	dip	Easting	Northing
EW	ord	fault	U	0	95	80	686032	6296160
EW	ord	fault	U	0	100	75	686023	6296174
EW	ord	fault	U	0	95	90	686024	6296170
EW	ord	fault	U	0	115	90	686018	6296191
EW	ord	fault	U	0	95	35	686017	6296197
EW	ord	fault	U	0	170	80	686014	6296227
EW	ord	fault	U	0	100	50	686014	6296228
EW	ss_ssturb	fault_contact	R	1	180	70	685972	6296426
WW	ord	fault	U	0	145	50	684835	6296464
WW	ord	fault	U	0	195	65	684827	6296466
WW	ord	fault	U	0	15	80	684843	6296483
WW	ord	fault	U	0	90	50	684871	6296513
WW	ord	fault	U	0	55	40	684878	6296521
WW	ord	fault	U	0	160	75	684891	6296538
WW	ord	fault	U	0	175	70	684891	6296536
WW	ord	fault	U	0	165	80	684896	6296543
WW	ord	fault	U	0	185	60	684899	6296557
WW	ord	fault	U	0	135	65	684921	6296581
WW	ord	fault	U	0	20	40	684933	6296600
WW	ord	fault	U	0	250	75	684950	6296564
WW	ord	fault	U	0	210	40	684932	6296558
WW	ord	fault	U	0	130	60	684929	6296551
WW	ord	fault	U	0	160	70	684922	6296542
WW	ord	fault	U	0	195	50	684923	6296544
WW	ord	fault	U	0	160	65	684919	6296537
WW	ord	fault	U	0	65	70	684947	6296624
WW	ord	fault?	U	0	105	60	684944	6296623
WW	ord	fault	U	0	350	35	684969	6296648
WW	ord	fault	U	0	100	75	684960	6296643
WW	ord	fault?	U	0	170	70	684969	6296648
WW	ord	fault	U	0	5	60	684974	6296661
WW	ord	fault?	U	0	70	40	684989	6296677
WW	ord	fault	U	0	50	80	684996	6296721
WW	ord	fault	U	0	150	50	684995	6296759
WW	ord	fault	U	0	320	35	684995	6296782
WW	ord	fault	U	0	110	50	684985	6296832
WW	ord	fault	U	0	190	60	684973	6296854
WW	ord	fault	U	0	115	65	684942	6296898
WW	ord	fault	U	0	125	40	684928	6296916
WW	ord	fault	U	0	110	40	684925	6296918
WW	ord	fault	U	0	35	60	684911	6296935
WW	ord	fault	U	0	100	65	684907	6296941
WW	ord	fault	U	0	130	70	684906	6296950
WW	ord	fault	U	0	180	60	684881	6296977
WW	ord	fault	U	0	110	75	684880	6296977
WW	ord	fault	U	0	35	60	684873	6297007
WW	ord	fault	U	0	290	40	684867	6297025

station	lithology	measurement	sense	class	strike	dip	Easting	Northing
WW	ord	fault	U	0	15	40	684866	6297026
WW	ord	fault	U	0	290	45	684866	6297037
WW	ord	fault	U	0	40	65	684863	6297041
WW	ord	fault	U	0	290	60	684860	6297048
WW	ord	fault	U	0	270	45	684857	6297053
WW	ord	fault	U	0	350	35	684858	6297070
WW	ord	fault	U	0	315	55	684858	6297074
WW	ord	fault	U	0	60	50	684855	6297084
WW	ord	fault	U	0	120	45	684857	6297107
WW	ord	fault	U	0	135	35	684856	6297116
WW	ord	fault	U	0	40	35	684857	6297115
WW	ord	fault	U	0	310	75	684860	6297123
WW	ord	fault	U	0	285	55	684850	6297138
WW	ord	fault	U	0	115	30	684845	6297145
WW	ord	fault	U	0	70	40	684835	6297159
WW	ord	fault	U	0	60	35	684824	6297173
WW	ord	fault	U	0	340	55	684820	6297180
WW	ord	fault	U	0	305	55	684819	6297189
WW	ord	fault	U	0	15	50	684830	6297203
WW	ord	fault	U	0	90	55	684852	6297213
WW	ord	fault	U	0	195	70	684855	6297220
WW	ord	fault	U	0	165	50	684843	6297229
WW	ord	fault	U	0	180	65	684851	6297251
WW	ord	fault	U	0	355	60	684863	6297258
WW	ord	fault	U	0	25	50	684876	6297273
WW	ord	fault	U	0	155	65	684878	6297275
WW	ord	fault	U	0	20	60	684894	6297288
WW	ord	fault	U	0	110	50	684900	6297294
WW	ord	fault	U	0	140	60	684907	6297300

### **Appendix III: Drillcore Logs**

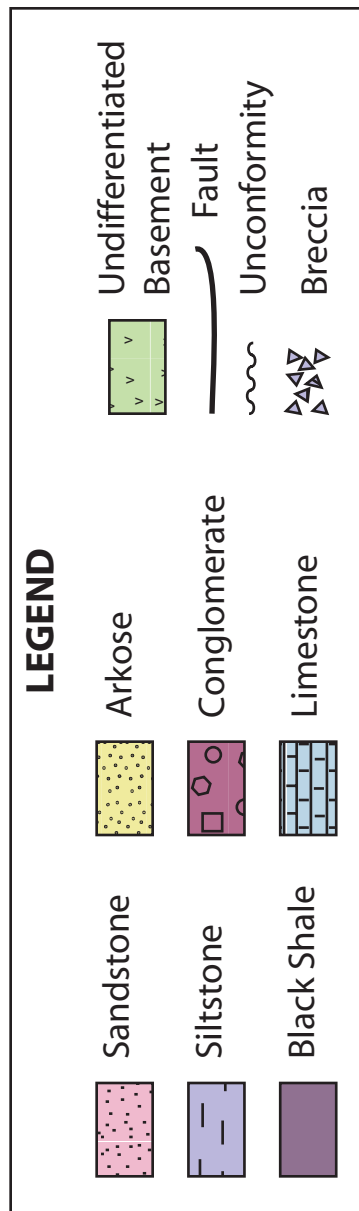
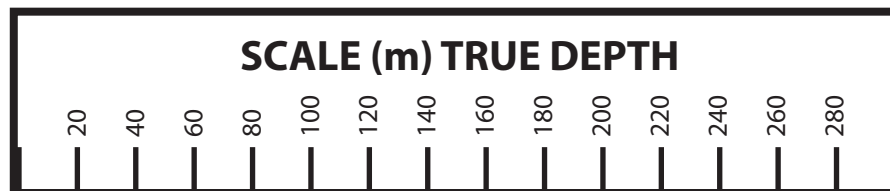
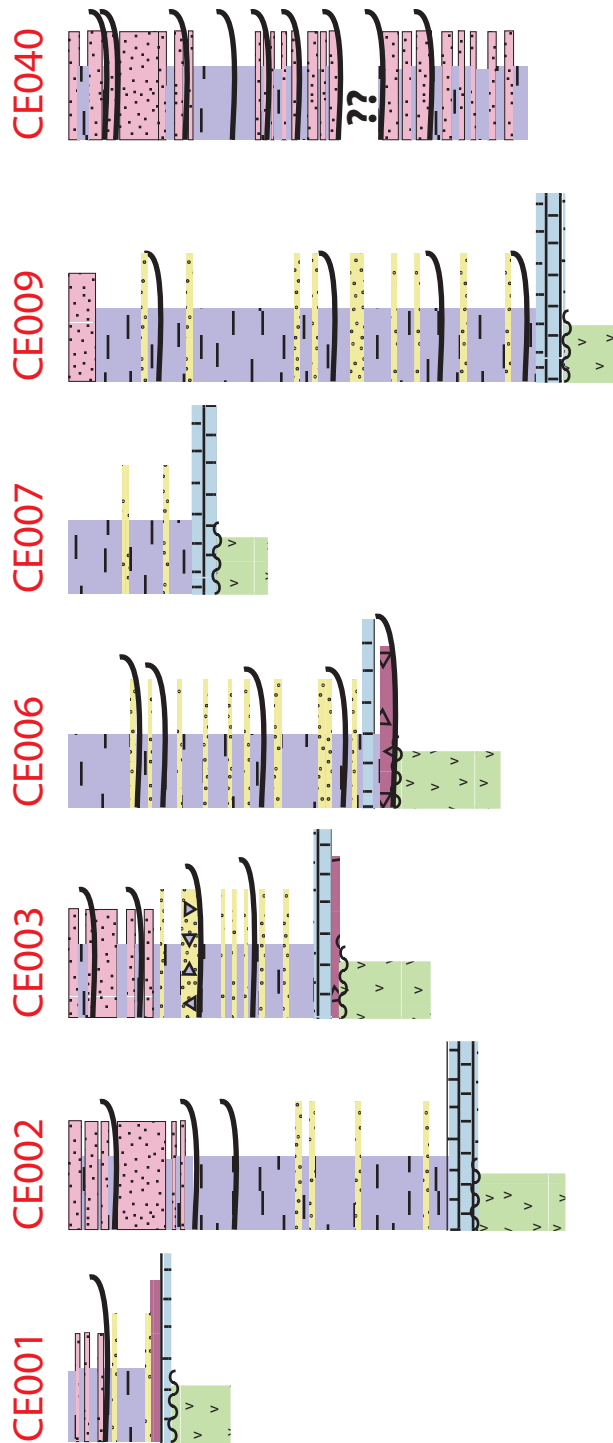
The Silurian Waugoola Group was examined in drillcore, and the following graphic core logs were produced. Drillcore was logged both on-site and from digital photographs provided by Newcrest Mining Ltd. in order to differentiate lithology and identify major structures. Detail was recorded at the 1:200 scale. These logs were used to constrain cross sections and better understand the Waugoola Group architecture, specifically at Cadia East.

A reference map is provided to show the locations of drillhole collars.

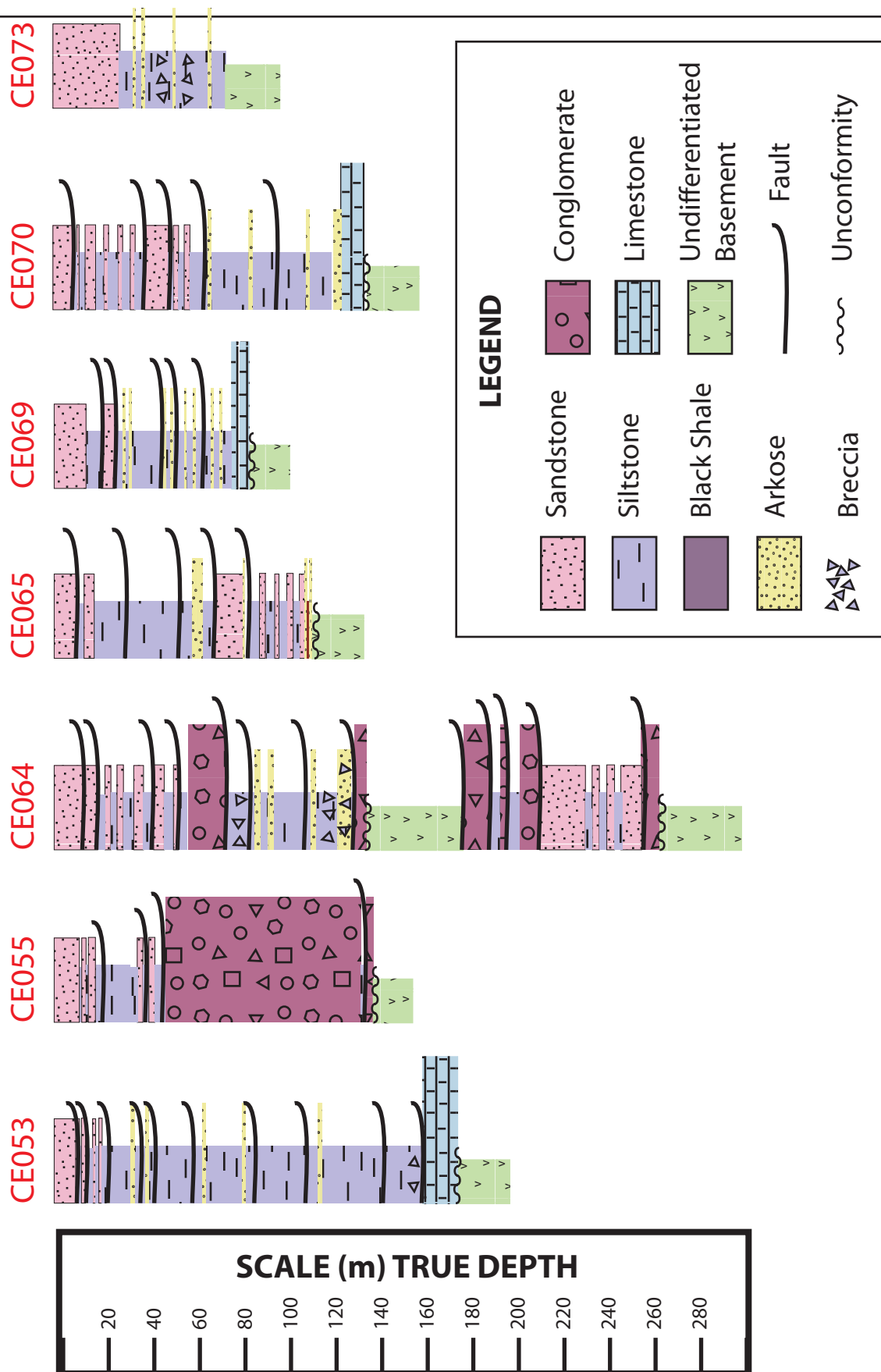
Abbreviations used are as follows: Bst = Mesozoic basalt cover; Ss = Waugoola Group sandstone; Ss-Si = Waugoola Group interbedded siltstone and sandstone; Si = Waugoola Group siltstone; Cgl = Waugoola Group conglomerate; CIC = Cadia Intrusive Complex; FRV = Forest Reefs Volcanics; Skn = magnetic skarn; Wm = Weemalla Formation.



# Drillcore Logs: CE Holes 001-040

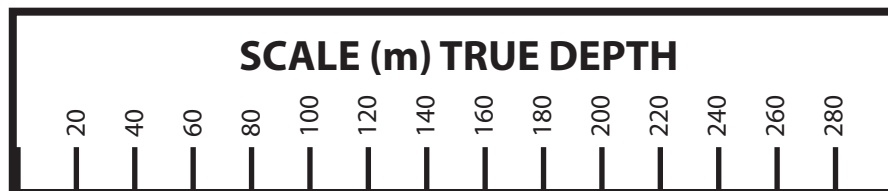
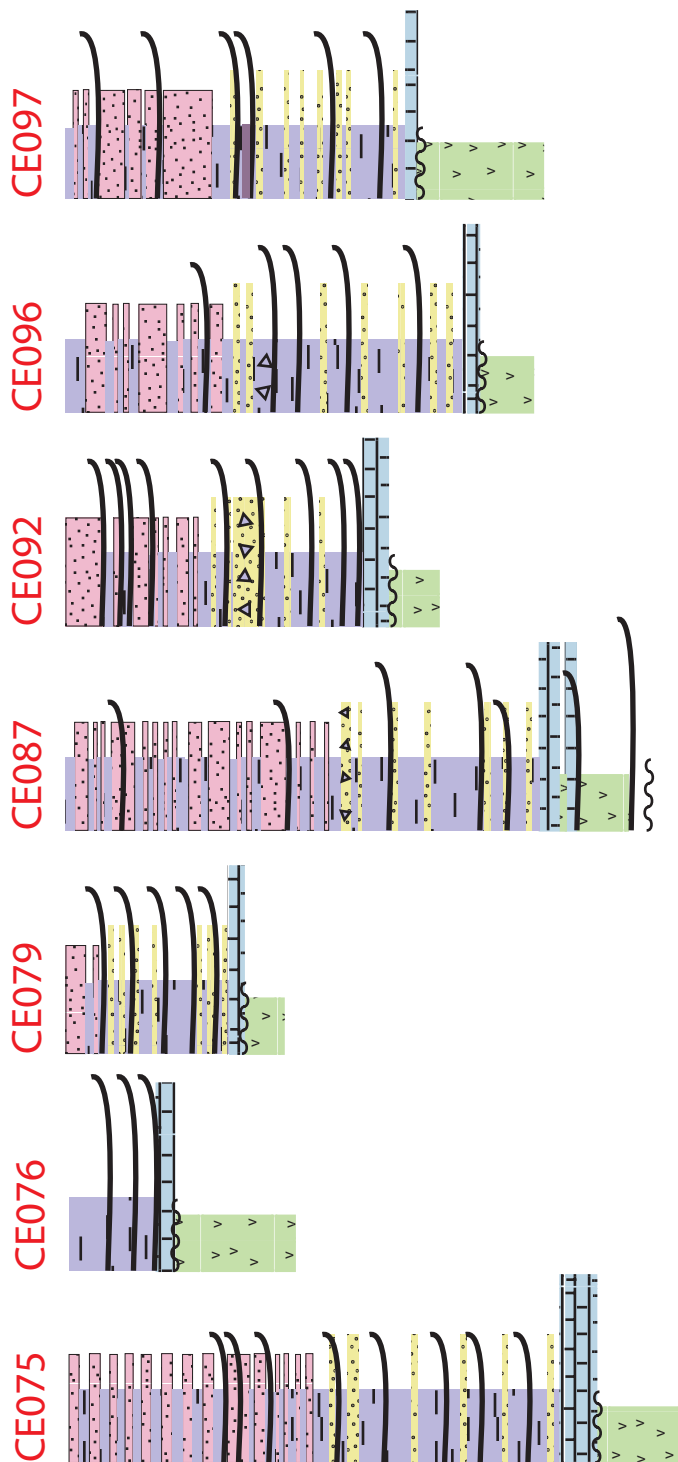


# Drillcore Logs: CE Holes 053-073

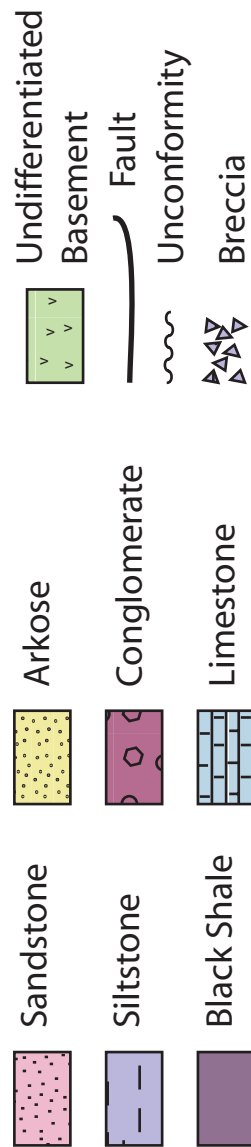




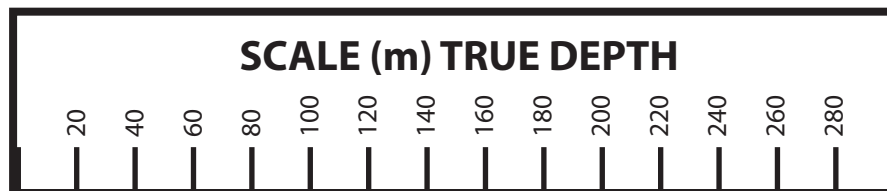
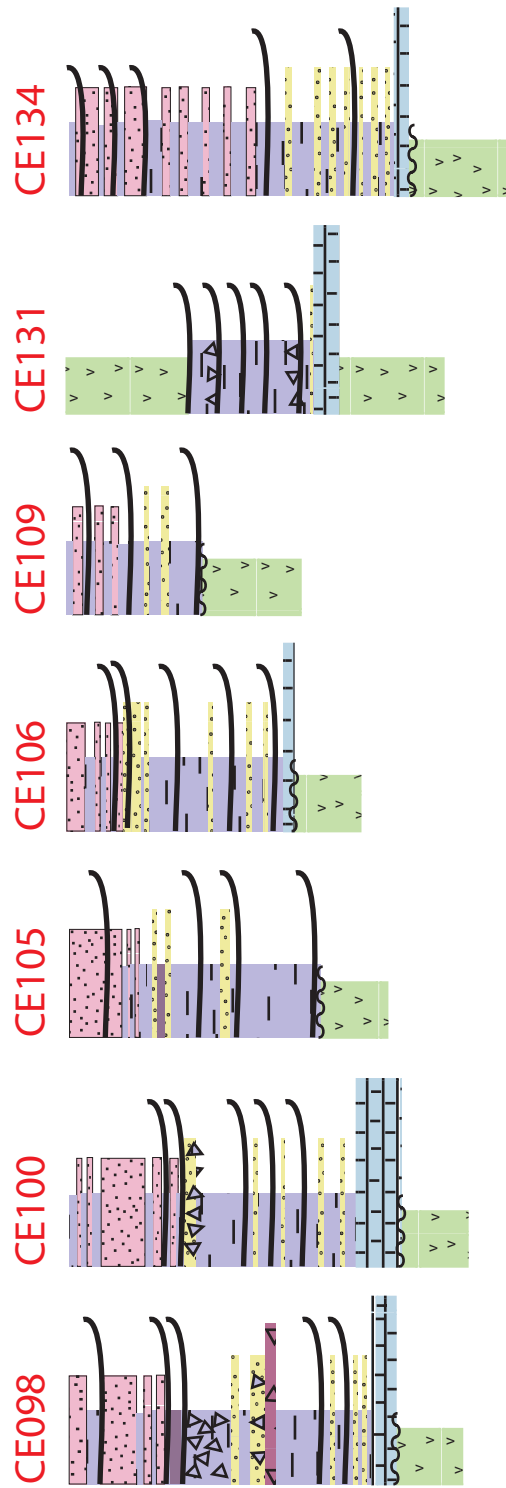
# Drillcore Logs: CE Holes 075-097



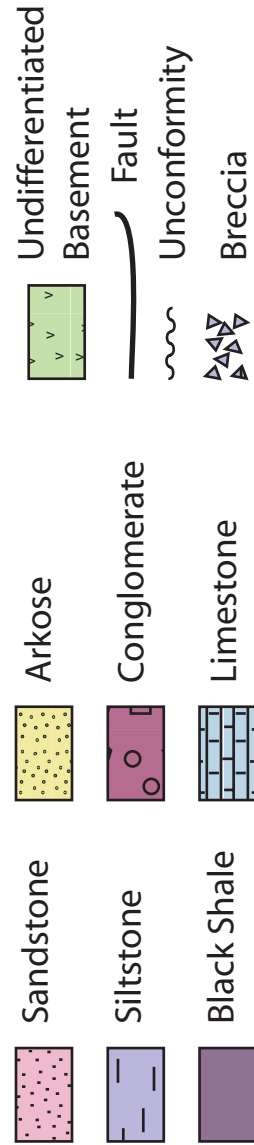
## LEGEND



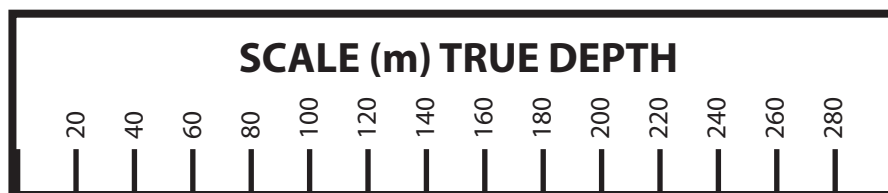
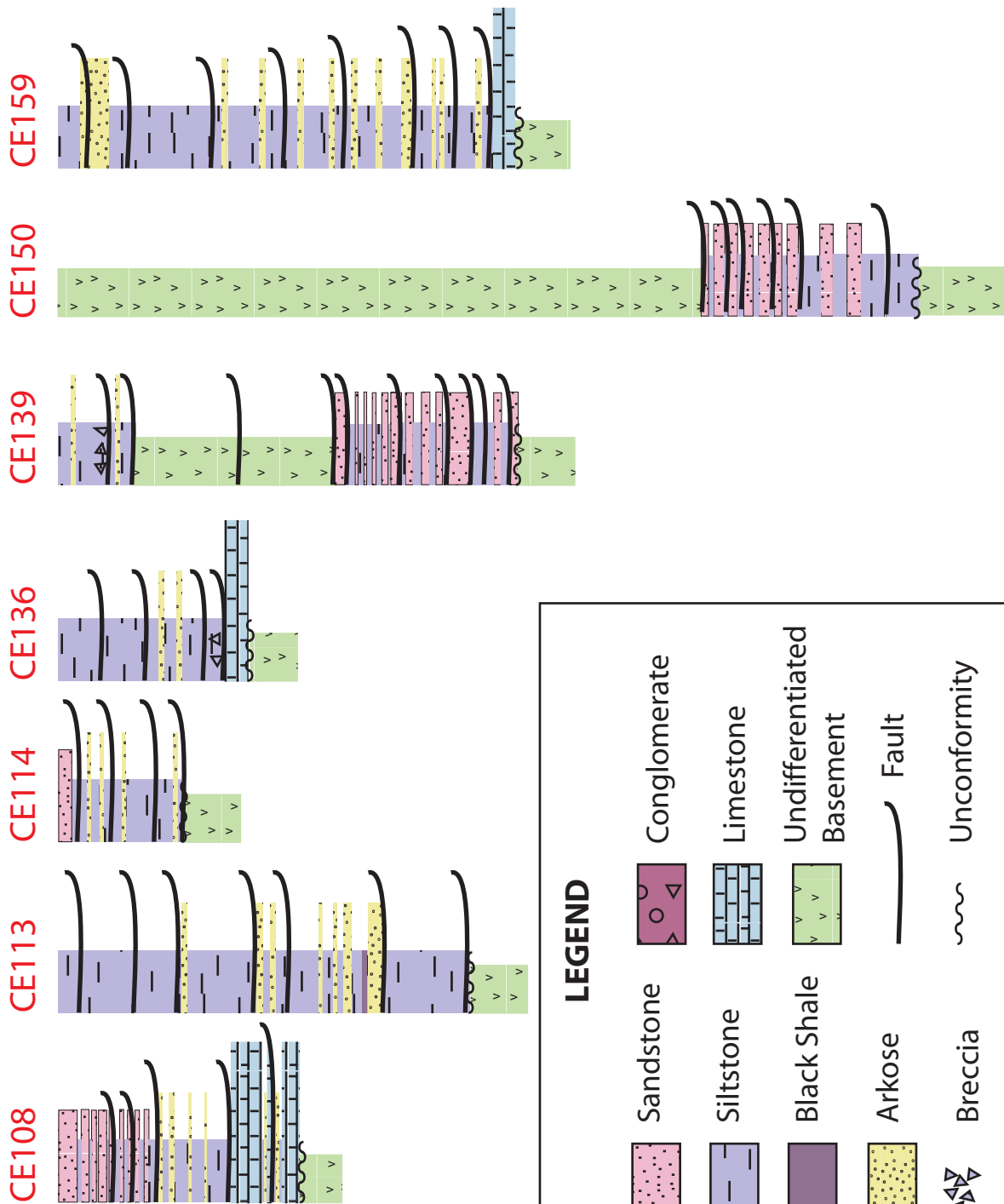
## Drillcore Logs: CE Holes 098-134



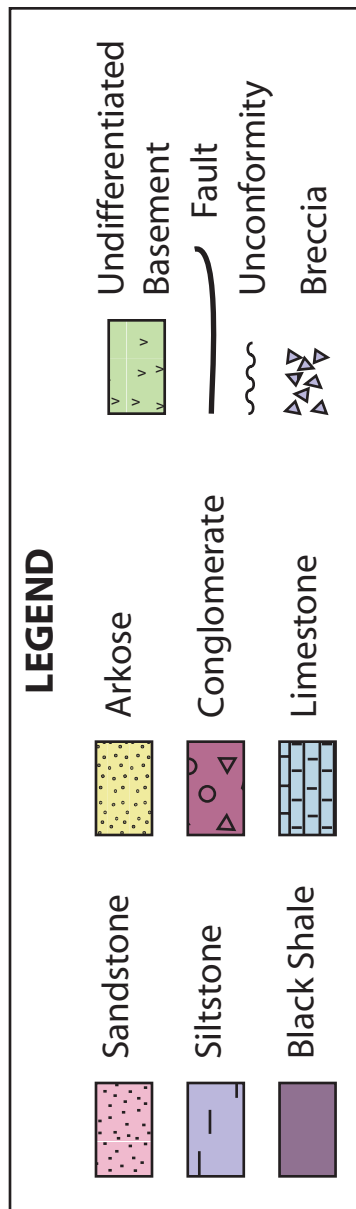
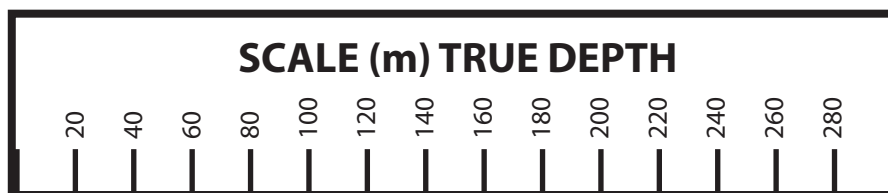
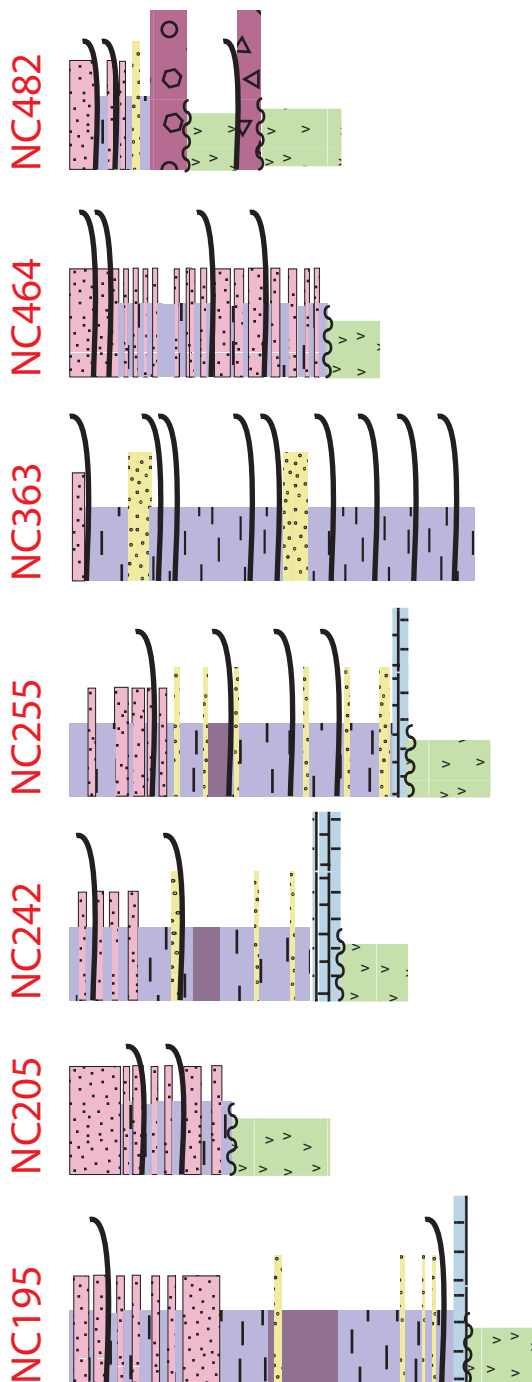
### LEGEND



# Drillcore Logs: CE Holes 108-159



# Drillcore Logs: NC Holes



## Drillcore Logs: PC Holes

